Institute of Hydrology
Albert-Ludwigs-University of Freiburg, Germany

Karin Spiegelhalter

Modeling the coupled influence of climate and glacier change on discharge

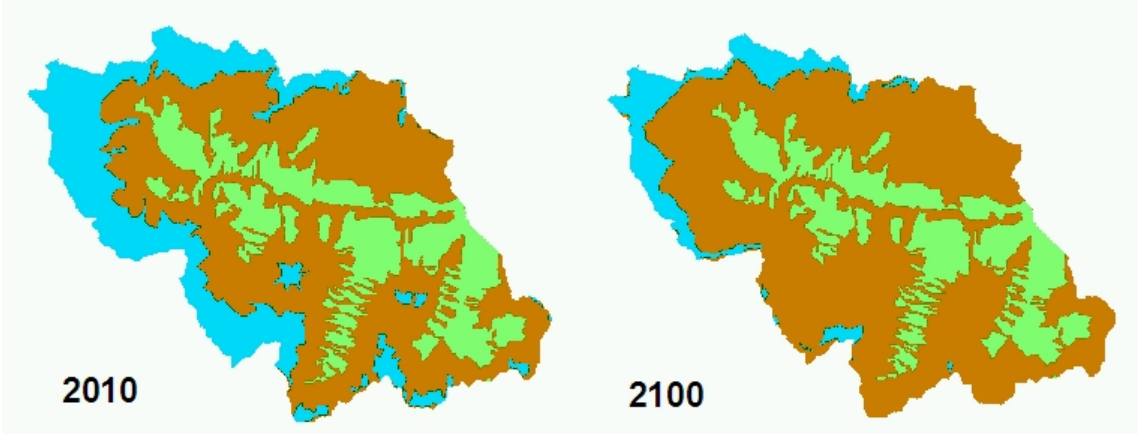

Supervisor: Prof. Dr. Markus Weiler
Co-Supervisor: Dr. Kerstin Stahl

Freiburg, December 17, 2009

Institut für Hydrologie
der Albert-Ludwigs-Universität Freiburg im Breisgau

Karin Spiegelhalter

Modellierung des gekoppelten Einflusses von Klima- und Gletscheränderungen auf den Abfluss

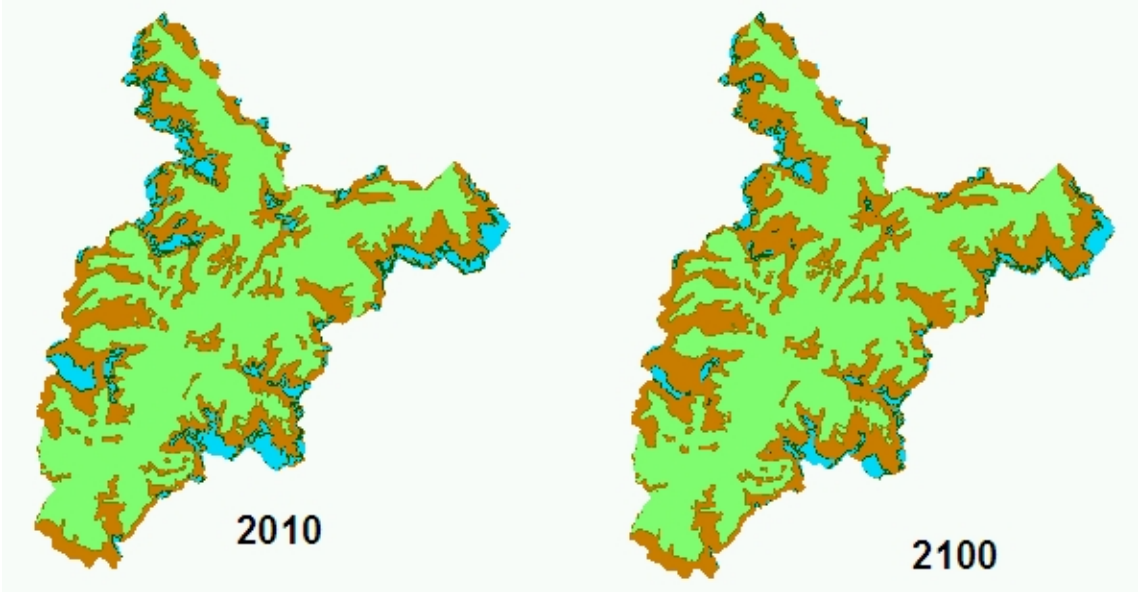

Referent: Prof. Dr. Markus Weiler

Koreferent: Dr. Kerstin Stahl

Freiburg, den 17. Dezember 2009

Acknowledgements

"Gesundheit ist die wichtigste Nebensache der Welt."
Gerhard Kocher

I would like to thank

- Prof. Dr. Markus Weiler for the direction of the thesis and the helpful discussions.
- Dr. Kerstin Stahl for supervising this study in an excellent manner.
- Alex Canon for providing future scenarios for my simulations.
- David Hutchinson for his support with the input files of the model and his reviewing ideas.
- Frank Weber for providing input and calibration data.
- Jürgen Strub for his support concerning all my small and bigger computer problems inclusive restoring my data after the crash of a hard disk.
- all the assistant professors, employees and Ph.D. students of the institute for the hydrological discussions and the good ambiance at the institute.
- my "Kernkompetenzteam", namely Katharina Dieckmann, Maria Friderich, Sandy Hack, Manuela Nied and Katharina Walter for its support to prepare me for the job interviews.
- the students of the "Diplomantenraum", the "Rheinstrasse" and the "Hebelstrasse" for their help and ideas.
- my reviewers Benjamin Gralher, Jürgen Harsch, Manuela Nied, Bastian Pöschl, Elke Spiegelhalter, Robin Weber and Deborah Zwilling. A special thank to Carsten Bierwald for his assistance with the layout of the thesis.
- Johanna Bernhard for providing me with papers and her emotional support.
- Sandy Hack and Manuela Nied for their friendship, their hydrological ideas and the great time we spent together.
- my former and recent house mates who let me feel at home in our "Heiteren Heim in Heitersheim".
- all my friends with who I had a great time in Freiburg, also thank you to my friends in Rheinstetten to stay in contact with me.
- my family for their support during the whole study time.
- my boyfriend Jürgen Harsch for his care and for all the vitamins to be able to write this thesis.

Contents

List of Figures

List of Tables

List of Abbreviations

AAR	Accumulatin Area Ratio
BC	British Columbia
BE	Benchmark Efficiency
EF	Nash-Sutcliffe Efficiency
e.g.	for example, abbr. of Latin "exempli gratia"
GCM	Global Climate Model
HRU	Hydrological Response Unit
IPCC	Intergovernmental Panel on Climate Change
MAE	Mean Absolute Error
ME	Mean Error
SC	Snow Course
SL	Snow Line
SWE	Snow Water Equivalent
UBC	University of British Columbia
WSD	Water Stewardship Division of the Ministry of Environment of the Government of British Columbia, Canada

A list of parameters can be found in table 8.1 on page 40.

Summary

The daily discharge of the two glacierized catchments Canoe and Illecillewaet in British Columbia, Canada, was simulated using the conceptual precipitation-runoff model HBV-EC. Discharge was calculated for the period 2001–2100 considering changes in climate and glacier area. The obtained results were compared with the ones of the Bridge catchment, a highly glacierized catchment in British Columbia, whose discharge was simulated by STAHL ET AL. (2008) in a similar way. The three catchments differ in size as well as in glaciation, heterogeneity in landuse and other catchment characteristics.

For calibration and validation a multi-objective approach was used. Besides discharge, snow course, snow pillow and actual snow line data were applied to evaluate model simulation. Future precipitation and temperature, input data of the model, were generated by two different Global Climate Models using two different climate scenarios as defined by the Intergovernmental Panel on Climate Change (IPCC). After each decade the glacier size was adapted via the simulated mass balance and an empirical volume-area relation.

The study showed that climate change does not influence discharge in the same way in the three considered catchments. However, total discharge, iceflow and glacier size decline until the end of the 21th century in all three catchments. Considering the high uncertainty due to different parameter sets, Global Climate Models, downscaling results and scenarios, a precise estimation of future discharge is not possible.

Keywords: discharge, climate change, glacier, precipitation-runoff simulation, HBV-EC, volume-area scaling

Zusammenfassung

Der tägliche Abfluss des Canoe- und Illecillewaet-Einzugsgebiets wurde mit Hilfe des konzeptionellen Niederschlag-Abfluss-Modells HBV-EC für den Zeitraum 2001–2100 modelliert. Beide Einzugsgebiete liegen in British Columbia, Kanada. Bei der Modellierung wurden sowohl der Klimawandel als auch die daraus entstehende Gletscherveränderung berücksichtigt. Die Ergebnisse wurden mit denen des Bridge-Einzugsgebiets verglichen. Dieses hoch vergletscherte Einzugsgebiet liegt auch in British Columbia und sein Abfluss wurde von STAHL ET AL. (2008) auf ähnliche Weise modelliert. Die drei betrachteten Einzugsgebiete unterscheiden sich nicht nur in ihrer Größe und ihrem Grad an Vergletscherung, sondern auch in der Heterogenität, ihrer Landnutzung und anderen einzugsspezifischen Eigenschaften.

Zur Kalibrierung und Validierung wurde der Multi-Objective-Ansatz verwendet. Zur Bewertung des Models wurden neben Abflussdaten Daten von Transsektmessungen des Schneeäquivalents, von Schneekissen und von Befliegungen, bei denen die aktuelle Schneelinie bestimmt wurde, verwendet. Die Eingangsgrößen Niederschlag und Temperatur wurden mit Hilfe zweier verschiedener Globaler Klimamodelle errechnet, die jeweils zwei unterschiedliche Klimaszenarien verwendet haben. Die Gletscherfläche wurde nach jedem Jahrzehnt unter Verwendung einer empirischen Volumen-Flächen-Beziehung angepasst.

Die Diplomarbeit zeigt, dass der Abfluss in den drei betrachteten Einzugsgebieten unterschiedlich auf den Klimawandel reagiert. Jedoch nehmen der Gesammtabfluss, der Gletscherwasserabfluss, sowie die Gletscherfläche in allen drei Einzugsgebieten im Laufe des 21. Jahrhunderts ab. Die hohe Unsicherheit der Ergebnisse aufgrund der verwendeten Parametersätze, der Globalen Klimamodelle, der Ergebnisse aus dem Downscaling-Verfahren und der Szenarien lässt eine eindeutige Aussage über den zukünftigen Abfluss jedoch nicht zu.

Schlüsselwörter: Abfluss, Klimwandel, Gletscher, Niederschlag-Abfluss Modellierung, HBV-EC, Volumen-Flächen Beziehung

Chapter 1

Introduction

There is no doubt about a worldwide climate change (IPCC, 2007). In the Pacific Northwest for example, the mean warming rate ranges between 0.1 and 0.6 °C per decade for the 21th century. For the time beyond 2050 the warming depends on the emissions during the next decades. Yearly precipitation is expected to be relatively stable until the end of the century, but most models simulate more precipitation in winter time and less precipitation in summer time (MOTE ET AL., 2005).

Not only BARRY (2006) characterizes glaciers as "key indicators" for climate change, also many other authors (e.g. HAGG ET AL., 2006; SIDJAK and WHEATE, 1999) see in glaciers one of the most visible signs of climate change.

Glaciers and ice sheets contain about 75 % of the available drinking water on the Earth (IPCC, 2007). 99.5 % of this freshwater is contained in the Greenland and Antarctic Ice Sheets; the remaining 0.5 % are contained in glaciers and smaller ice caps (JANSSON ET AL., 2003). In Canada there are about 200,000 km^2 of glaciers and small ice caps, containing the third largest freshwater reservoir in the world (BOON ET AL., 2009). Comparing this area with the glacier area in British Columbia in the 1980th more than 10 % of the Canadian glaciers are in British Columbia, representing about 4 % of global and 23 % of North American glacier cover, respectively (WILLIAMS AND FERRIGNO , 2002 in: SCHIEFER ET AL., 2007). The size of glaciers is influenced by latitude, elevation and the proximity to an upwind moisture source (BARRY, 2006).

Glaciers as a water storage are not only important for drinking water supply, but also for hydroelectric power and irrigation. They play an important role for flood forecasting and influence sea level rise, sediment transport and formation of landscapes (JANSSON ET AL., 2003; OERLEMANS ET AL., 1998).

As a consequence of climate change the volume and area of glaciers decrease. First the glacier thins before the retreat at the tongue is visible (HUSS ET AL., 2007). Some glaciers – especially the smaller ones – will disappear during the next decades (e.g. REES and COLLINS, 2006) while for big glaciers there is no real threat to existence at the moment (ESCHER-VETTER, 2001). The sensitivity of glaciers depends besides the glacier size on annual mean precipitation and the hypsometry (BOON ET AL., 2009). Continental glaciers e.g. are expected to be less sensitive than maritime ones (OERLEMANS ET AL., 1998). After JOHANNESSON ET AL. (1989) the adjustment of glaciers to climate change takes rather 10 to 100 years than often presumed 100 to 1000 years. Valley glaciers have a smaller response time than e.g. subpolar ice caps (OERLEMANS ET AL., 1998).

WATSON ET AL. (1996) expect that until 2050 a quarter of the global mountain glacier mass has disappeared, until 2100 half of the glacier mass.

Even representing only a small percentage of landuse glacier influence catchment hydrology (MOORE and DEMUTH, 2001). They store water in winter and release water

concentrated in the melting season (HOCK ET AL., 2005). This leads to a pronounced seasonality of discharge (JANSSON ET AL., 2003) as e.g. in the Massa catchment where 88 to 98 % of the discharge flows between 1st May and 30th September as a consequence of snow and ice melt (COLLINS, 2006). With increasing glacier cover the discharge peak shifts from early summer to late summer (FOUNTAIN and TANGBORN, 1985). Besides this seasonal cycle there is a diurnal cyclicity as a consequence of diurnal energy variations – especially long-wave heat flux variations (HOCK, 2005). The amplitude of daily discharge from a glacier depends on the short-time storage in firn, snow and ice. Storage of a few days takes place in the firn cover whereas there is a relatively fast through flow through the glacier itself;the snow cover of a glacier is an intermediate short-time storage (JANSSON ET AL., 2003). After MEIER AND TANGBORN (1961) in: FOUNTAIN and TANGBORN (1985) glaciers moderate interannual flow variability in discharge by storing water as snow and ice in cold and wet years and by melting snow and ice in dry and warm years. Depending on the study the minimum of the year-to-year variability is at 20 to 44 % glacierisation in the Alps and in the North Cascade Mountains (CHEN and OHMURA, 1990a; COLLINS and TAYLOR, 1990; FOUNTAIN and TANGBORN, 1985).

Discharge of glacierized catchments can be more, less or equal to total precipitation depending on the storage or release of water (COLLINS and TAYLOR, 1990). Whereas discharge of glacier free catchment is mainly influenced by precipitation, in glacierized catchments energy dominates the production of runoff (CHEN and OHMURA, 1990a).

The following simplified and generalized chronology can be expected for the discharge when glaciers decrease: For some decades there is an increase of discharge because the equilibrium line rises and so ice can melt also in higher elevation zones. The reason for the rising is the increased energy input. Additionally, ones the snow over a glacier has melted, there is a higher melting rate as ice has a slower albedo than snow. Hence the ablation zone stays stable or even increases (HAGG ET AL., 2006; REES and COLLINS, 2006). If the icemelt from additional exposed ice cannot compensate the decrease in ice area and volume at the glacier terminus – even with higher melt rates – discharge decreases (HUSS ET AL., 2007; REES and COLLINS, 2006; MOORE and DEMUTH, 2001). The peak discharge is expected to shift from late summer to early summer and spring whereas in summer water deficiency will prevail (HAGG ET AL., 2006; BRAUN ET AL., 2000). In British Columbia SCHIEFER ET AL. (2007) assessed already a strongly negative mass balance and glacier thinning in the late 20th century. Also STAHL and MOORE (2006) brought to light that most glaciers in British Columbia are already in the phase of decreasing discharge.

The consequences of the decrease of glaciers depend on the degree of glaciation in a catchment, the glacier mass balance, the hypsometry and vertical extent of the glacier, the rate of energy input enhancement and the precipitation change (COLLINS, 2006; HAGG ET AL., 2006).

DYURGEROV and MEIER (1997) calculated that glacier melt has a percentage on global sea level rise of about 14 to 18 % during the 20th century and until 50 % at the end of the 20th century. Other consequences are less freshwater availability for agriculture, consumption and hydropower – especially in summer when rivers will be fed only by groundwater and rainfall (BARRY, 2006; HAGG ET AL., 2006; BARNETT ET AL., 2005), threatening of ecosystems during the low flow in summer (STAHL and MOORE, 2006), migration of plants and animals as a consequence of landuse change and exposure of

new mineral resources (BARRY, 2006), but also rock-ice avalanches as e.g. 2002 in Russia (KOTLYAKOV ET AL., 2004). Also tourism will be affected of glacier decrease (BARRY, 2006). In summary HAGG ET AL. (2006) suspect not only social, but also economic, hygienic and ecological consequences because of the decrease of water resources in glacier-fed catchments.

Chapter 2

Review

2.1 Discharge simulation in glacierized catchments

The aim of many studies was to simulate glacier retreat and advance as a consequence of climate change. Some of these studies simulated glacier change of the past (e.g. OERLEMANS, 1988), but there are also studies where future glacier change was simulated (e.g. HUSS ET AL., 2007; OERLEMANS ET AL., 1998). In other studies not only the retreat and advance of glaciers in future was simulated, but also the resulting discharge. Different approaches were used:

In some hydrological models there is no specific routine for runoff generation from glacierized areas; runoff from glacierized and glacier-free areas is generated in the same way. BRAUN and AELLEN (1990) used e.g. the HBV-3 version to simulate discharge of the highly glaciated Massa catchment in Switzerland. 66 % of the catchment is covered by glacier (Großer Aletsch glacier), but there is no specific glacier routine in the used HBV-3 model to take the specific behavior of glaciated landuse into account. The importance of a specific glacier modul in a model showed ZAPPA ET AL. (2000). They simulated discharge in a catchment in the Swiss Alps with the spatially distributed hydrological model PREVAH – one time with a glacier modul, the other time without the glacier modul. Without the glacier modul there was a highly underestimation of discharge, especially in summer. The Nash-Sutcliffe coefficient (see NASH and SUTCLIFFE, 1970) decreased from 0.9 to 0.3.

Even taking the specific behavior of the glacier landuse into account, many hydrological models simulate discharge keeping glacier area and volume constant over time.

BRAUN ET AL. (1993) used the HBV3-ETH version to simulate discharge in the Langtang Khola Basin in Nepal. This model bases on the HBV-3 model, but has an integrated glacier routine. Also the conceptual SNOWMOD model has a glacier routine. SINGH and BENGTSSON (2005) used it to simulate discharge in different catchments in the Himalayan region. As a third example SCHAEFLI ET AL. (2005) developed a semi-lumped conceptual glaciohydrological model, namely GSM-SOCONT, where glacier covered and non glacier covered parts of the catchment are separated. They tested this model which was developed for climate studies in three catchments in the Swiss Alps.

In all three studies however, the reduction of glacier area as a consequence of climate change is not taken into account.

Modeling discharge in glacierized catchments without considering ice area and volume changes leads however to wrong results: STAHL ET AL. (2008) showed that discharge is highly overestimated, especially in summer when a great part of the discharge comes from glacier melt. HUSS ET AL. (2008) could confirm this effect and calculated an overestimation of about 3 % in 2027, of between 7 and 72 % in 2050 depending on the scenario used and an overestimation of more than 100 % in 2100. VAN DE WAL and WILD (2001)

calculated an overestimation of 19 % of sea level rise without adaption of the glacier area. Thus keeping the size of glaciers constant is only acceptable in the next decades; longtime applications of these models into the future is precluded.

Some studies consider the adaption of glaciers, but not in a transient way:

HAGG ET AL. (2006) analyzed the effect of glacier change on discharge. They simulated discharge in different catchments in Central Asia with the HBV-ETH model. They assumed first a reduction of glacier size of 50 % and then a total disappearance of the glacier. In this study the reduction of glacier size is considered, but there is no transient response on climate change and no reference to time at all.

Two studies which consider glacier change, but only for the years 2070 to 2099 are the one of HORTON ET AL. (2006) and and the one of SCHAEFLI and GUPTA (2007). Using the accumulation-area ration (AAR) method they simulated discharge in different catchments in the Swiss Alps with the GSM-SOCONT model. This method assumes that the recent AAR (the percentage of the accumulation area to the entire glacier area) is constant, also in the future. Simulating the size of the accumulation zone on the future climate conditions and using a constant AAR, the area of the entire glacier can be calculated. HUSS ET AL. (2008) criticized the AAR method as it does not conserve mass and is not capable to simulate glaciers in a transient way.

There are only little studies which consider future climate change, transient glacier response and the resulting discharge. Some of these are physically based while some use a conceptual approach.

As an example for the first group the study of FLOWERS ET AL. (2005) should be shortly presented. Combining a thermomechanical ice sheet model and a distributed hydrological model they simulated the sensitivity of Vatnajokull ice cap to climate change. The simulation is based on the continuity equation of mass, momentum and energy. The model was preconditioned during 400 years (1600 to 2000); the reference climate period was from 1961 to 1990. Under the assumption of a temperature increase of 0 to 4 °C per century and a precipitation increase of 0 to 10 % per century they simulated discharge, the geometry of the ice cap, mass balance, velocity structures and subglacial water pressures and fluxes for the years from 2001 to 2100.

One of the main problems of the physically based hydrological models are their enormous demand of input data. Mountain catchments are often data sparse catchments and so not all the required data are available. Another problem is the huge computational capacity. All in all it is difficult to apply physically based models in complex catchments.

In data sparse and often complex mountainous catchments discharge is often simulated using conceptual precipitation-runoff models. Three studies could be found which use such a conceptual precipitation-runoff model to simulate future discharge:

REES and COLLINS (2006) simulated discharge in two hypothetical catchments, one in the eastern, the other in the western part of the Himalaya. They used a temperature-index-based hydro-glaciological model to simulate discharge from 1990 on during the next 150 years. They assumed first climate conditions as during the period 1961–1990, then a temperature increase of 0.6 °C per year. The ice depth varied by melting or by

adding ice at the end of the year if there is accumulated snow left. This snow is distributed as ice over all icebands. The adaption of glacier size is realized by removing icebands in the case of an ice depth of zero after ice melt.

HUSS ET AL. (2008) used the glacio-hydrological model GERM to simulate discharge and mass balance in three catchments in the Swiss Alps. They calibrated and validated the model between 1962 and 2006 with observed discharge data and ice volume data from digital elevation models. The simulation period was 2007 to 2100. To simulate into the future HUSS ET AL. (2008) used two extreme and a median climate scenario obtained from regional climate models. The glacier size was adapted annually by distributing the mass balance change as an ice thickness change over the glacier area. A used pattern considers elevation for the ice thickness change.

STAHL ET AL. (2008) simulated discharge in the Bridge River Basin in British Columbia (Canada). They used the HBV-EC model, which bases on the HBV model. Additionally, a glacier scaling module was integrated in the HBV-EC model to consider advance and retreat of glaciers via an empirical volume-area scaling approach (see below). Mass balance and discharge data were used for calibration and validation during the period 1986–2004. The simulation period was between 2001 and 2100. To simulate into future three different scenarios where used: One assumes that the observed climate of the period 1986–2004 continues, the other scenarios were downscaled from a Canadian Climate Model and based on two different scenarios as defined in the special report about emission scenarios by the Intergovernmental Panel on Climate Change (IPCC)(see IPCC, 2000).

As in this study likewise to the study of STAHL ET AL. (2008) the volume-area scaling method was used to consider the transient retreat and advance of glaciers, a short review about this approach follows.

2.2 Volume-area scaling

To consider the reduction or growth of the glacier, a volume-area scaling module has been added to the HBV-EC model by STAHL ET AL. (2008). The scaling method is based on the empirical formula of CHEN and OHMURA (1990b). Comparing volume measurements of 63 mountain glaciers in different countries by radio-echo and seismic sounding they set up the following equation:

$$V = C_0 * A^{C_1} \tag{2.1}$$

with the volume V [10^6 m^3], the glacier area A [10^6 m^2], the scaling constant C_0 and the exponent C_1. CHEN and OHMURA (1990b) calculated different values for C_0 and C_1 considering different types of glaciers and different volume measurements. The range for C_0 is between 17 and 30, the one for C_1 between 1.15 and 1.52. Glacier slope and the basal shear stress are not considered in the V-A relationship.

CHEN and OHMURA (1990b) concluded that their empirical relation between volume and area by a power relationship agrees well with measured data, especially for longer time periods.

BAHR ET AL. (1997) showed the physical basis of the power relationship between glacier volume and glacier area. By respecting mass and momentum conservation they

calculated C_1 as a function of the width, slope, side drag and mass balance of the glacier. Climate change alters especially the mass balance. For valley glaciers C_1 gets the value 1.375 which agrees well with the empirically derived exponents. As most glaciers have a similar flow regime BAHR (1997) expected that the value of C_0 do not vary much .

RADIC ET AL. (2007) agreed with the theory of BAHR ET AL. (1997) for any glacier in a steady state. But they wondered if the power law is still valid in a non-steady state as it is the case by employing the volume-area scaling for climate change studies. In their study they investigated the theory of BAHR ET AL. (1997) under steady state and non-steady state conditions and they compared the volume-area approach with a 1-D ice-flow model. For their study they used synthetic glaciers.

As a first result they got under steady state conditions a C_1 of 1.56. They suggested that this value differs from the value obtained by BAHR ET AL. (1997) because of the simple geometry of the synthetic glaciers.

Under non-steady state conditions C_1 ranges between 1.80 and 2.90 with larger values for decreasing initial glacier size and warming scenarios. As a reason for the difference of 21 to 86 % between the exponent at steady state and non-steady state condition they assumed the problem that they did not scale the width with the length.

VAN DE WAL and WILD (2001) reported a difference of less than 20 % between steady state and non-steady state conditions.

RADIC ET AL. (2007) conducted also some sensitivity analysis: They compared different C_1 values and different scaling methods with the results of a ice flow model. They found out that the choice of the scaling method is much more important than the C_1 value: While the difference of volume calculated with various C_1 values to the ice flow model was at most 6 % after 100 years, using different scaling methods caused differences of up to 23 % under steady state conditions and up to 74 % under non-steady state conditions. Assuming at first 100 years of non-steady state conditions and then 200 years of steady state conditions only the method which considers area changes and implies them in the mass balance calculation gave acceptable results. Also for steady and non-steady state conditions this scaling method gave the best results.

One year later RADIC ET AL. (2008) compared the volume-area, a similar volume-length and a volume-area-length method with the mentioned ice flow model at six real glaciers in different countries. They got the best results using the volume-length method. As it is easier to gather glacier area data than to measure the length of glaciers along the snowline, they recognized that it might be more practical to use the volume-area method. Again they could confirm that results are relatively insensitive to the value of the scaling exponent. The scaling constant however affect the initial volumes and volumes after 100 years. After normalizing volume by the initial volume it is relatively insensitive to the value of the scaling constant. RADIC ET AL. (2008) propose to compare the different approaches with 2-D or 3-D ice flow models to confirm their results.

BAHR ET AL. (1997) described the empirical volume-area method as "a practical and physical based method for estimating glacier volumes." This method is useful especially if there are not enough data available to use a physical model. Additionally, it is cheaper

to gather glacier area data from satellite images or aerial photographs than to do measurements of ice volume (BAHR ET AL., 1997).

For this study C_0 has the value 28.5 and the exponent C_1 the value 1.357 as in the study of CHEN and OHMURA (1990b).

Chapter 3

Aim of the thesis

Glaciers are retreating as a consequence of climate change. As about a sixth of the Earth population rely on melt water (IPCC, 2007) it is important to predict changes in discharge. HAGG ET AL. (2006) declare that the relation between climate, glaciers and discharge are not entirely understood. This thesis should help to get new information about this relation and/or to confirm results of former studies. In comparison to many other studies the transient landuse change should be considered. Only three studies could be found which simulate future discharge considering climate change as well as the transient glacier response with a conceptual precipitation-runoff model.

The aim of this thesis is to simulate discharge in the Canoe and in the Illecillewaet catchment in British Columbia (Canada) for the time period 2001–2100. The retreat or advance of glaciers is simulated via an empirical volume-area scaling. The results should be compared with the simulation of the future discharge in the Bridge catchment. The future discharge of this catchment was simulated by STAHL ET AL. (2008) in the almost same way. The three catchments differ not only in size, but also in glacier cover, heterogeneity of landuse and other physiographical characteristics.

To achieve the aim of the thesis the following steps should be done:

- First the input data time series of the Canoe catchment must be completed.
- In a second step the model must be calibrated and validated in the Canoe as well as in the Illecillewaet catchment.
- Using the parameter sets of the calibration and downscaled climate scenarios the future discharge should be simulated.
- An analysis of the simulated discharge and glacier area uncertainty should be done.
- Finally the simulation results of the discharge in the Canoe and Illecillewaet catchment should be compared with the ones of the Bridge catchment.

Chapter 4

Study areas

The Canoe, Illecillewaet and Bridge catchment are located in the southern part of British Columbia (BC) in Canada (see figure 4.1).

In this section the main characteristics of the three considered catchments concerning geography, geology, surficial materials, soils, landuse, climate and hydrology are described.

If not otherwise mentioned the geographic and landuse information is from the base thematic map (BTM) of Canada, which is based on Landsat data from the early 1990s and is released by Environment Canada. Elevation information is derived from the National Research Council – Canadian Hydraulics Centre (NRC-CHC). The hypsographic curves are based on this data.

The geological information is based on the digital geological map of the British Columbia Project operated by the Government of British Columbia.

Information about soils and soil moisture are derived by maps of the Ministry of Environment (MOE, 2007a,b). The surficial material map is edited by Natural Resources Canada (NRCAN, 2008).

General information about the climate is from the Ministry of Environment (MOE, 2007c); climate data of the different climate stations are from the operator of the climate stations, BC Hydro.

Discharge data are from HYDAT, the database of the Water Survey of Canada.

4.1 The Canoe catchment

4.1.1 Geography

The Canoe catchment extends over an area of about 306 km^2. It is situated in the south-east of British Columbia in the Cariboo Mountains, which is a part of the Columbia Mountains, west of Valemount. It has an elevation range of 965 to 3335 m.a.s.l. with a mean elevation of 1935 m.a.s.l. Figure 4.2 shows the hypsographic curve.

4.1.2 Geology

The geology in the Canoe catchment consists of sedimentary rocks of the Upper Proterozoic. The main rocks are fine clastic sedimentary rocks: mudstone, siltstone and shale. From the south-east part to the north-west part of the catchment there are two parallel stripes of quartzite and quartz arenite which are about 3 km wide each. In the western part of the catchment there are coarse clastic sedimentary rocks. In the western part of these sedimentary rocks there is an about 500 m wide stripe in north-south direction of limestone, marble and calcareous sedimentary rocks. This small stripe is the most permeable part of the catchment.

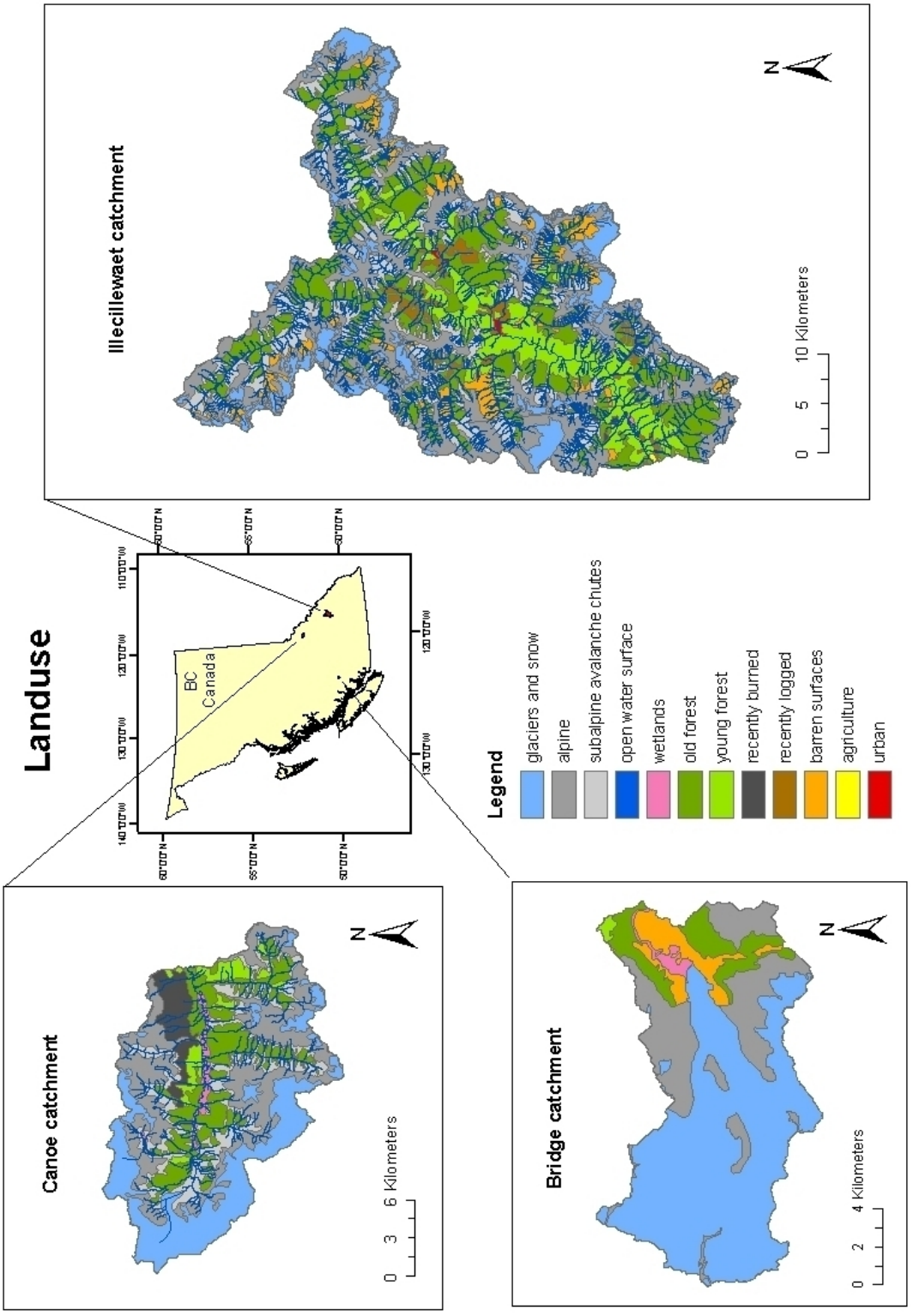

Figure 4.1: Map of British Columbia illustrating the situation of the three considered catchments and their landuse.

4.1.3 Surficial Materials and Soils

More than 75 % of the surface of the Canoe catchment consists of rocks. Besides of rocks Quaternary deposits prevail. The catchment is characterized by alpine and glacial landforms.

At higher elevations there are ice fields. At lower elevations Lithic soils dominate which include rocks and pre-stages to a Humo-Ferric Podzol. Humo-Ferric Podzols are soils which have typically an organic litter layer (LFH), a bleached horizon (Ae) and a Bf horizon where iron, aluminum and a little bit of organic matters accumulate. The horizon sequence ends with the transitional horizon BC and the rock horizon C. If there are no Lithic soils at lower elevations Humo-Ferric Podzols prevail.

The catchment lies in a humid area with a possible very slight water deficit.

4.1.4 Landuse

As illustrated in figure 4.1 about 26.1 % of the Canoe catchment (79.8 km^2) is covered by ice and snow. About 23.4 % (71.6 km^2) is forest and the remaining 50.5 % of the catchment (154.8 km^2) are wetlands, recently burned areas or subalpine avalanche chutes. These areas are combined and called "open" areas in this study.

4.1.5 Climate

The Pacific plays an important role determining the climate of BC – differently for winter and summer time.

Winter storms are generated in the North Pacific Ocean, a source of heat and moisture. Normally the storms coming from the Aleutian Low move to the Gulf of Alaska where they die. If there are outliers of the storms these air masses meet a large scale barrier – the perpendicularly lying Coast Mountains. The Coast Mountains build a first barrier, the further inland lying Columbia Mountains a second, but smaller one. The air masses are forced to raise and condense when reaching the condensation level. This is the reason why at the western mountain slopes the climate is wetter than at the eastern slopes. In general the mountains determine if at a considered location Pacific air masses or Continental air masses dominate and the daily specific location of the Aleutian Low determines if this location is affected by more or less heavy rains. Moving from east to west and from north to south the protection against Arctic air masses increases because of the north-south extending mountain chains with higher elevation in the south.

In summer time the westerlies weaken and so the frequency and intensity of Pacific storms and coastal rainfalls. Showers and thundershowers from convective air masses dominate. Until mid-summer so-called "cold low" storms path through on the way to the Great Plains.

As the Columbia Mountains are an area of great vertical relief there are strong climate gradients. The mean temperature at the climate station "Cariboo Lodge", 1128 m.a.s.l., is about 2.7 °C (1976–2004). The mean yearly precipitation constitutes 1041 mm (1976–2004).

4.1.6 Hydrology

The Canoe River is one of the most northern tributaries to the Columbia River. It has a glacial regime (PARDE, 1947) with an annual discharge of about 1390 mm (1976–2004) at the gauging station "Canoe River below Kimmel Creek". Peaks in May and June result from snowmelt, peaks in July to September from glacier melt. Rain or rain-on-snow events can produce floods during fall (EATON and MOORE, 2007). The MQ for the period 1971–2007 constitutes 14.6 m^3/s.

4.2 The Illecillewaet catchment

4.2.1 Geography

The Illecillewaet catchment has an area of about 1149 km^2 and is located south of the Canoe catchment at the west slopes of the Selkirk Mountains, a part of the Columbia Mountains (LOUKAS and QUICK, 1996). The catchment extends between the towns Golden in the east and Revelstoke in the west. The elevation range is between 505 and 3230 m.a.s.l. with a mean elevation of about 1715 m.a.s.l. Figure 4.2 illustrates the elevation distribution of the catchment.

4.2.2 Geology

All the geological structures in the catchment run in south-east direction. In the northern parts of the catchment there are sedimentary rocks consisting of quartzite and quartz arenite of the Upper Proterozoic to the Lower Cambrian. At the other parts of the catchment there are younger sedimentary rocks of the Cambrian to Devonian: mudstone, siltstone, clastic shale and undivided sedimentary rocks. In the north, in the middle and in the south of the catchment there are about 1 km wide stripes of limestone and other permeable sedimentary rocks. At the western part there are metamorphic rocks of the Devonian composed of orthogneiss. In the catchment there are "islands" of intrusive rocks (granodiorites) of the Jurassic in the north and of the Cretaceous in the south. On the whole the geology of the catchment is very heterogeneous. The small limestone stripes and potentially the metamorphic rocks are the areas where water can drain.

4.2.3 Surficial Materials and Soils

At the upper parts of the catchment there are mainly rocks and Quaternay deposits as in the Canoe catchment. At the lower part there are mainly colluvial deposits.

Beside ice fields the catchment is dominated by Humo-Ferri Podzols which are described above.

The Illecillewaet catchment lies in a transition zone between humid and subhumid soil moisture regimes. Very slight to significant water deficits are possible.

4.2.4 Landuse

In the Illecillewaet catchment about 9.8 % (112.3 km^2) of the area is covered by glaciers and snow. 38.9 % of the catchment (446.9 km^2) are forest. The "open" area (51.3 % and

569.8 km^2,respectively) is very heterogenous (vgl. figure 4.1) with wetlands, recently burned, logged and barren surfaces, alpine areas and subalpine avalanche chutes. There is agricultural land, a small lake and it is the only catchment with an aggregation of some houses.

4.2.5 Climate

As described above there are strong climate gradients in the Columbia Mountains. The mean temperature at the "Glacier NP Rogers Pass" climate station (1323 m.a.s.l.) is 1.8 °C (1976–2004), the mean yearly precipitation 1511 mm (1976–2004). In contrast at the Revelstoke climate station (443 m.a.s.l) the mean temperature is about 8.6 °C (1976–2004) and the mean yearly precipitation 710 mm (1990/1 + 2001–04). LOUKAS and QUICK (1996) describe the climate in the catchment as continental, with cold winters and warm summers with numerous hot days. In winter time the whole catchment is covered by snow. At late spring the snow melts at the deeper and middle elevation zones. This is a main influence on the hydrological regime.

4.2.6 Hydrology

At Revelstoke the Illecillewaet River flows into the Columbia River and so in the Arrow Lakes reservoir, which is used for hydroelectric power generation, water supply and flood protection (LOUKAS and QUICK, 1996). The mean annual discharge (1976–2004) at the gauging station "Illecillewaet River at Greeley" is about 1450 mm; the MQ (1963–2008) is 53.1 m^3/s. In contrast to the other two catchments the hydrological regime of the Illecilewaet catchment is mainly influenced by snow melting and can so be classified as a nival regime with the main peak in June (PARDE, 1947).

CHAMPOUX86A and CHAMPOUX86B in SIDJAK and WHEATE (1999) made an inventory and monitoring of the Illecillewaet Icefield area which is situated in the most northeastern part of the catchment. They showed from historical records that the terminus of the Illecillewaet Glacier retreated more than 1 km between 1887 and 1962. From 1962 to 1984 it advanced about 100 m and since 1984 it is retreating again.

4.3 The Bridge catchment

4.3.1 Geography

The Bridge catchment with about 153 km^2 is the smallest of the three catchments. It is situated in the south-west of BC in the Southern Chilcotin Mountains about 180 km north of Vancouver. The elevation range of the catchment extends between 1375 and 2930 m.a.s.l. with a mean of 2032 m.a.s.l. The hypsographic curve is illustrated in figure 4.2 .

4.3.2 Geology

In the south-eastern part there are intrusive rocks consisting of quartz and diorites of the Late Cretaceous. The northern part of the catchment is built up by intrusive rocks, granodiorites, of the Late Crataceous to Paleogene. At the south-western part there are metamorphic rocks consisting of orthogneiss where the age is unknown. At the north east

part there are younger rocks of the Miocene, mainly undivided volcanic rocks overlying the intrusive rocks. No permeable units can be found in this catchment.

4.3.3 Surficial Materials and Soils

At the surface of the catchment rocks and Quaternary deposits dominate as in the other two catchments. On the parts where there are no glaciers Lithic soils prevail which are characterized by bar rocks and significant inclusions of Ferro-Humic Podzols and well drained Folisols. Ferro-Humic Podzols are comparable with the above mentioned Humo-Ferric Podzols, but with a higher fraction of organic matter. Folisols belong to the Organic order and are composed mainly of organic matter. They are rarely saturated and are made up of forest debris over a thin mineral layer or rock.

The soil moisture regime is characterized by no or only slight water deficits. Therefore the soils belong to the perhumid or humid types.

4.3.4 Landuse

Most of the Bridge catchment is covered by glacier and snow (60.1 % or 91,7 km^2). There are about 9.4 % (14.3 km^2) of forest and the remaining 30.5 % (46.6 km^2) are wetlands, alpine or barren surface and will be called "open" areas as well. In figure 4.1 the landuse is illustrated.

4.3.5 Climate

In contrast to the other two catchments the Bridge catchment lays in the Coast Mountains, the wettest part of Canada. The observed mean annual precipitation at the climate station "Upper la Joie" (1829 m.a.s.l.) are 1067 mm (1986–2004). It is problematic to define precipitation and temperature in the Bridge catchment. The catchment is situated at the east of the highest mountains in the region. There are high elevation gradients and as a consequence also high temperature and precipitation gradients. The climate station "Upper la Joie" is situated east of the catchment in a much drier region than the catchment and can not be seen as a representative station for the catchment (personal information by STAHL 2009). Heavy rains fall in winter time. The mean temperature at the climate station is 1.0 °C (1976–2004). At higher elevations summers are cool and short. Snowpacks can stay until mid-summer.

4.3.6 Hydrology

The Bridge River flows into the Downton Lake which is located west of the town Gold Bridge. The average annual discharge at the gauging station "Bridge River below Bridge Glacier" is 2600 mm and the MQ (1978–2008) constitutes 12.7 m^3/s, respectively. The Bridge River has a glacial regime (PARDE, 1947). As the third largest hydropower development the Bridge River Complex plays an important role in the energy supply (STAHL ET AL., 2008).

4.4 Glacier fluctuations in British Columbia

After the end of the last Ice Age, the Wisconsin glaciation, at about 10 ka BP glaciers in British Columbia had more or less the same limits as today. Between the Wisconsin glaciation and the Little Ice Age, which began at about 900 BP and ended during the 18th or 19th century, there have been some expansions of glaciers: e.g. during the Garibaldi phase at about 5–6 ka BP or the Tiedeman Advance at about 3,3–2,3 ka BP.

In the last century the following recession and advance periods took place: Between 1850 and 1920 the limits of the glacier remained close to the limits of the Little Ice Age whilst during 1920 and 1960 rapid recessions occurred. In the following ten years there were slight glacier recessions or even advances. In consequence of increased winter precipitations and slow summer air temperatures glaciers advanced between 1970 and 1980. This was rather a lateral than a frontal advance. Since 1980 glaciers retreat (OSBORN and LUCKMAN, 1988). SCHIEFER ET AL. (2007) confirm and quantify the retreat of glaciers in British Columbia at the end of the 20th century.

4.5 Summary

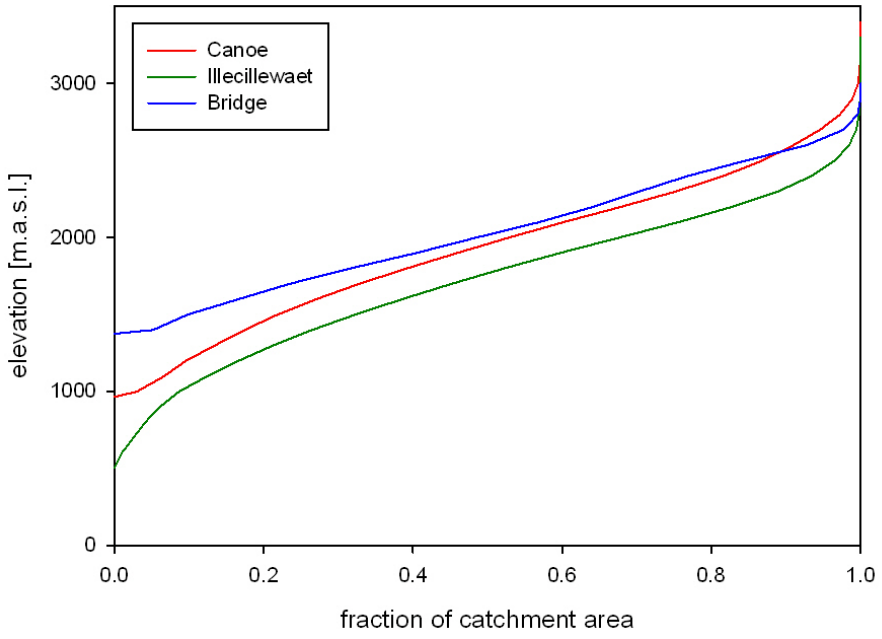

Figure 4.2: Hypsographic curves of the three catchments.

Comparing the three catchments one can see that they are very different. Although the Canoe and Illecillewaet catchments are both situated in the Columbia Mountains and have got similar climatic influences not only their geology differs, but also soils, landuse and hydrology.

The form of the hypsographic curve of the Illecillewaet and the Canoe catchment are similar, but the Canoe catchment extends over higher elevations than the Illecillewaet

catchment. Both catchments are characterized by very low fraction of the highest elevation zones. They differ at lower elevations where the Illecillewaet catchment raises rapidly until a certain elevation whereas the hydromatic station of the Canoe catchment is situated at a relatively high level. The Bridge catchment is the highest situated catchment of the three considered catchments. There the elevation zones are more or less uniformly distributed.

The Illecillewaet catchment is the largest catchment, but with the smallest percentage of ice cover. It is characterized by a very heterogeneous geology and landuse. In contrast the Bridge catchment is the smallest catchment with the greatest percentage of glacierized area. The Canoe catchment has a middle position concerning size of catchment and percentage of glaciers. It is characterized by glaciers surrounding the catchment. In summary the catchments have more or less the same size of glacierized areas despite different sizes of the catchments.

Whereas no studies could be found about the Canoe catchment there are even climate change studies carried out in the Illecillewaet catchment (LOUKAS and QUICK, 1996; MARTINEC and RANGO, 1989). The Illecillewaet Icefield situated at the most northeastern part of the catchment was a study area for mapping glacier using Landsat Thematic Mapper satellite imagery combined with digital elevation data (SIDJAK and WHEATE, 1999) and for estimating lichenometric ages (MCCARTHY, 2003). In the Bridge catchment there is one study besides the study of STAHL ET AL. (2008) about the glaciation prior to the late Neoglacial maximum (RYDER and THOMSON, 1986). SCHIEFER ET AL. (2007) calculated glacier volume changes in different regions of British Columbia during the period 1985–1999 using radar data and digital terrain models from aerial photography.

Chapter 5

Model description

5.1 Development and application

In this thesis the Hydrologiska Byrans Vattenbalansavdelning – Environment Canada (HBV-EC) model is applied. It is based on the HBV model, which Bergström developed in the 1970s (e.g. BERGSTRÖM, 1995). LINDSTRÖM ET AL. (1997) describe the HBV model as "a model of high performance" and characterize its structure as "very robust and surprisingly general, in spite of its relative simplicity".

Many modelers modified the originally Swedish HBV model, e.g. LINDSTRÖM ET AL. (1997), who introduced an automatic weighting of precipitation and temperature stations and a new calibration scheme (HBV-96), or SEIBERT (2005), who changed the HBV-6 version in a Windows version, which can be easy used for research and education. LINDSTRÖM ET AL. (1997) re-evaluated the standard HBV model which was used by the Swedish Meteorological and Hydrological Institute (SMHI). They expect no further improvements of the model if only the standard inputs are used and the performance of the model is evaluated only by analyzing discharge.

Since the mid 1980s MOORE has adjusted the HBV model to involve snow and glacier processes and developed the semi-distributed HBV-EC model (RODENHUIS ET AL., 2007; MOORE, 1993). Since 2000 MOORE, Environment Canada and the University of British Columbia (UBC) have collaborated to simulate watershed responses (CHC, 2007).

Besides the UBC Watershed Model and the Distributed Hydrology Soil Vegetation Model the HBV-EC model is one of the main watershed models applied in British Columbia (RODENHUIS ET AL., 2007).

Selected applications of the HBV-EC model are listed in table 5.1.

Table 5.1: Selected applications of the HBV-EC model

Catchment	Location	Size [km^2]	Glacier cover	Reference
Lillooet River	British Columbia, CA	2,160	17%	MOORE (1993)
M'Clintock River	Yukon, CA	1,700		HAMILTON ET AL. (2000)
Bridge River	British Columbia, CA	152	62 %	STAHL ET AL. (2008)

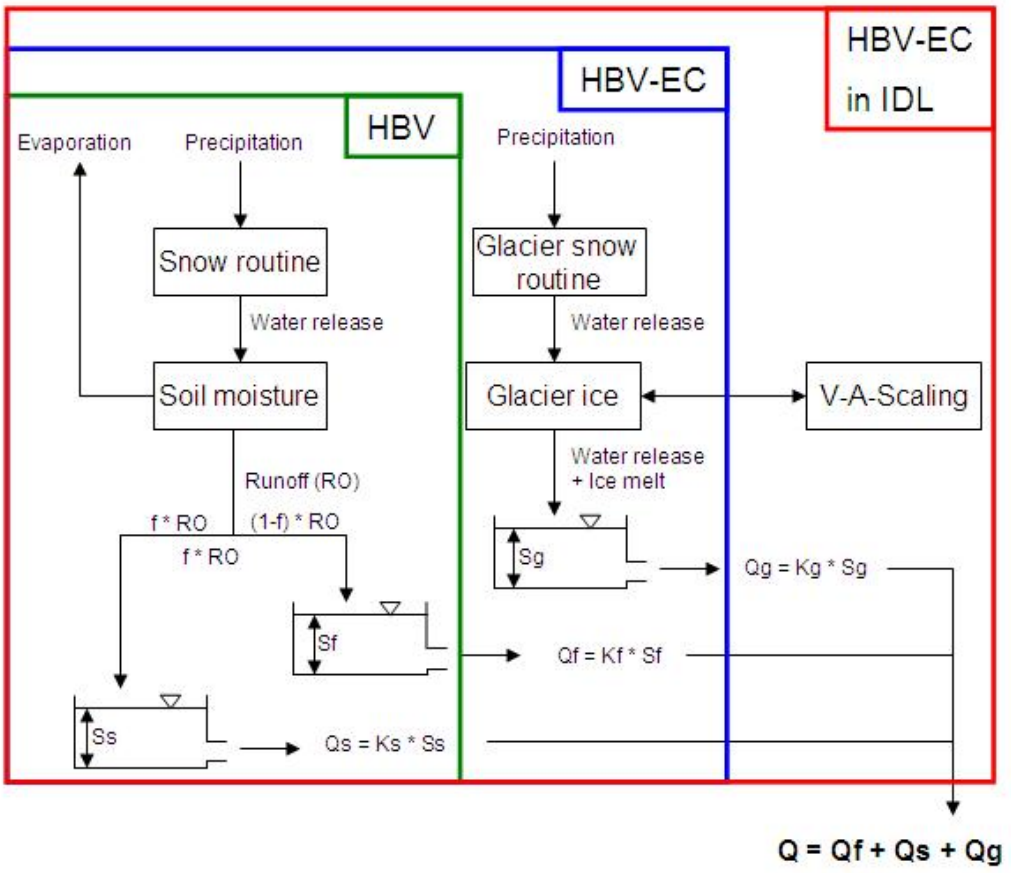

Figure 5.1: Principal structure of the HBV model, the HBV-EC model and the HBV-EC model written in IDL (modified after HAMILTON ET AL., 2000).

5.2 Structure and input

The principal structure of the HBV-EC model is shown in figure 5.1. Originally, the HBV-EC model is written in a C-language and has been rewritten in IDL (Interactive Data Language) to involve the mass balance and volume-area scaling module. For this thesis some modifications of the IDL version have been done. These modifications and the different modules are explained in the following sections. If not mentioned otherwise, the model description is based on STAHL ET AL. (2008), HAMILTON ET AL. (2000) and MOORE (1993).

The HBV-EC model uses Hydrological Response Units (HRUs) to simulate the hydrology efficiently in a semi-distributed manner. Land cover, elevation, slope and aspect divide the watershed in various HRUs. Additionally, in the HBV-EC model written in a C-language climate zones account for climate gradients which can occur in large basins. This novelty – in comparison with the HBV model – has not been transferred into the IDL version.

Inputs for the HBV-EC model are the daily values for mean Temperature (T [°C]), total rainfall (RF [mm]) and total snowfall (SF [mm]). Additionally, in the C-language version the mean monthly potential evaporation (EP [mm]) is necessary.

To calculate rainfall and snowfall from the precipitation time series of the climate stations, there is a threshold temperature TT [°C] and a parameter TTI [°C], which is used to create an interval TT $\pm$ TTI. In this interval it is supposed that there is a mixture of rain and snow falling. Above the interval there is only rain and below the interval there is only snow.

The rainfall and snowfall records are corrected by the rainfall correction factor RFCF [-] and the snowfall correction factor SFCF [-] respectively. That way systematic measurement errors and the representativity of the climate station for the basin are taken into account. Additionally, the snow fall correction factor adjusts for the missing evaporation and sublimation from the snow pack (SEIBERT, 1997). To calculate values for each elevation band the following equations are used:

$$T(z) = Ts + (Zs - Z) * (Tlapse + 0.002 * \cos(\frac{2 * \pi * (DOY + 190)}{365}) \tag{5.1}$$

$$P(z) = Ps * [1 + Pgrad * (Z - Zs)] \tag{5.2}$$

$$EP(z) = EPs * [1 - EPgrad * (Z - Zs)] \tag{5.3}$$

Temperature, precipitation and potential evaporation at each elevation z [m] are calculated using measured values (Ts [°C]], Ps [mm],EPs [mm]) and gradients (Tlapse [°C /m], Pgrad [1/m], EPgrad [1/m]). Zs is the elevation of the climate station, DOY is the considered day of the year. As the temperature gradient varies during the year (see appendix A.1), a gradient, which varies in a cosinusoidal way over the year, has been programmed for this thesis. The two other gradients are assumed to be constant over the year.

There are two gradients for precipitation. PGRADL [-] is the precipitation gradient below and PGRADH [-] is the one above a threshold elevation EMID [m.a.s.l.]. If the calculated potential evaporation or precipitation is negative, the calculated value is replaced by the value zero. At temperatures below 0 °C the evaporation values are also zero.

The interception is taken into consideration by a fixed percentage of precipitation, but only in forested areas. There are different percentage values for rain (TFRAIN [-]) and snow (TFSNOW [-]).

5.3 Modules

5.3.1 Snow- and icemelt

To calculate the snowmelt M [mm/d], the HBV-EC model uses – like the HBV model – the temperature index method (see equation 5.4) which includes a threshold temperature for melt TM [°C] and a melt factor CM [mm/°C]. This melt factor varies from a minimum during the winter solstice (CMIN [mm/°C]) to a maximum during the summer solstice in a sinusoidally way. The difference between these two values is the calibration parameter DC [mm/°C]. The actual value for the melt factor can be calculated by using equation 5.5, where t are the days counted from the winter solstice. CM is only valid for open, flat areas. Equation 5.6 considers additionally aspect a [-] and slope [s] – a further novelty of the HBV-EC model; AM [-] is a calibration parameter.

$$M = CM * (T - TM) \tag{5.4}$$

$$CM(t) = CMIN + 0.5 * (CMAX - CMIN) * (\cos(\frac{2 * \pi * t}{365})) \tag{5.5}$$

$$CM'(t) = CM(t) * (1 - AM * \sin(s) * \cos(a)) \tag{5.6}$$

Additionally, in forested areas the melt factor is reduced by the reduction factor MRF [-] to consider the shading effects and the consequential reduced energy input for the snow melt. On the other side, the melt factor is enhanced by the factor MRG [-] in glacierized areas when the new snow has melted. This takes into account the reduced albedo of firn and ice in comparison with the one of snow.

However, there is only snowmelt, if the water retention capacity CWR [mm] is exceeded. This retention capacity is a fixed fraction WHC [-] of the snowpack storage SWE [mm]. The upper limit LWR [mm] of the retention capacity assumes that there is an upper limit above which the water cannot refreeze again.

The refreezing of melt water occurs if the air temperature is under the threshold temperature for melt and can be calculated by the following equation:

$$F = CRFR * (TM - T) \tag{5.7}$$

F [mm] is the amount of refrozen water and is added to the snowpack storage; CRFR [mm/(d * ^{o}C] is a refreezing coefficient. If the calculated amount of refrozen water is more than the liquid water available, F gets the value of the actual water storage.

The water release WR [mm] to the soil moisture storage or glacial ice surface is calculated by adding rain, snowmelt and liquid water in the snowpack, deducting afterward the refrozen water, and comparing this amount of water with the retention capacity. The excess becomes the water release.

5.3.2 Soil moisture

The soil moisture is calculated differently for forested/open and glaciated areas. To calculate the runoff RO [mm] from a certain forested or open HRU the following equation is used:

$$RO = \begin{cases} WR * (\frac{SM}{FC})^b, & SM < FC, \\ WR, & SM > FC. \end{cases} \tag{5.8}$$

SM stand for the soil moisture storage [mm]. FC is the field capacity of the soil [mm] and has to be calibrated as well as the parameter b [-]. The difference between water release and runoff is added to the soil moisture storage. If the soil moisture exceeds the field capacity, all the water release becomes runoff.

5.3.3 Potential and actual evaporation

Previous applications of the HBV-EC model required direct input of typical monthly reference values for the potential evaporation. For this thesis HAMON 's empirical method (HAMON, 1961) was implemented. HAMON 's aim to calculate average potential evapotranspiration PET [mm/day] as a function of air temperature resulted in equation 5.9. HPD [-] considers the possible hours of sunshine per day as a percentage of 12 hours, SVP [g/m^3] is the saturated water vapor density at the daily mean temperature and c is an empirical correlation coefficient, which has the value of 0.55 (HAMON, 1961).

$$PET = c * HPD^2 * SVP \tag{5.9}$$

HAMON takes into account that the average potential evaporation depends on the relative humidity by calculating the potential evaporation as a percentage of the saturated water vapor density at the daily mean temperature. Referring to empirical studies (PENMAN , 1956; YAMAOKA , 1958) HAMON regards the influence of wind as insignificant and uses a constant value for this estimation. As main heat source for the evaporation process he regards the net radiation. Daily averages of the net radiation can be estimated by using the daily mean temperature and the average duration of day-time hours as a percentage of 12 hours.

In conclusion HAMON 's method to estimate potential evapotanspiration needs as input air temperature, the latitudinal position of the climate station and the time as day of the year. HORNBERGER and WIBERG (2005) wrote a R-code for this estimation referring to the adaptation of HAITH and SHOEMAKER (1987). A new programmed procedure is based upon this R-code (see appendix A.2). The daily values have been smoothed by calculating the mean of the five days before and after the considered date. That way the influence of the variability of the air temperature was reduced.

When all snow has melt, the actual evaporation EP [mm] from the soil moisture storage can be computed (cp. equation 5.10). Inputs are the potential evaporation, the soil moisture storage and the soil moisture content (LP [-] * FC) below which the actual evaporation is less than the potential evaporation.

$$EP = \begin{cases} PE * (\frac{SM}{LP * FC})^b, & SM < LP * FC, \\ PE, & SM > LP * FC. \end{cases} \tag{5.10}$$

If the calculated value for the actual evaporation is greater than the water available in the soil moisture storage, the value of actual evaporation is the actual value of this storage. If there is snow in the HRU, the actual evaporation is equal to the potential evaporation.

5.3.4 Outflow

Outflow from glacierized and non-glacierized HRUs is calculated separately.

The runoff from all non-glacierized HRUs and all elevation bands is summed and afterward split by a factor FRAC [-] into two lumped reservoirs: a fast reservoir SF [mm] and a slow reservoir SS [mm]. In contrast to HAMILTON ET AL. (2000) and MOORE (1993), there is no percolation from the fast reservoir to the slow reservoir in the HBV-EC model.

The outflow from the fast reservoir QF [mm/d] is controlled by the parameter KF [d^{-1}].

$$QF = KF * SF \tag{5.11}$$

The outflow from the slow reservoir QS [mm/d] is calculated in a similar way, where KS [d^{-1}] describes the outflow parameter.

$$QS = KS * SS \tag{5.12}$$

To determine the outflow from glacierized HRUs, the sum of water release over glaciers and of icemelt over all elevation bands is calculated and added to the glacial storage reservoir. Equation 5.13 calculates the outflow QG [mm/d]; SG [mm] is the liquid water storage for a certain HRU and KG [d^{-1}] is an outflow parameter.

$$QG(t,g) = KG(t,g) * SG(t,g) \tag{5.13}$$

The outflow parameter KG is time variable and accounts for the development of the glacier (cp. equation 5.14). KGMIN [d^{-1}] represents the situation where the drainage system of the glacier is not well developed and deep snow lies over the glacier. DKG [d^{-1}] is the difference between KGMIN and KGMAX, the latter representing the late summer situation with bare ice on the surface of the glacier and a well developed drainage system. AG [mm^{-1}] is a calibration parameter and SWE [mm] is the snow water equivalent for a certain glacier g at a certain time t.

$$KG'(t,g) = KGMIN + DKG * e^{-AG*SWE(g,t)} \tag{5.14}$$

Before using the calculated parameter KG'(t,g) in equation 5.13, a certain delay of the parameter is taken into consideration (cp. equation 5.15). Therefore a calibration factor KGRC [d^{-1}] is introduced.

$$KG(t,g) = KG'(t,g) - KGRC * KG'(t,g) + KGRC * KG'(t-1,g) \tag{5.15}$$

The time variable modeling of the glacier drainage system is one of the big differences between the HBV and the HBV-EC model. That way seasonal and annual variations in the englacial and subglacial drainage system can be taken into account.

The total outflow of the catchment is the sum of the fast outflow QF, the slow outflow QS and the outflow from glacierized HRUs QG. Unlike in the HBV model no parameter MAXBAS [d] is used to convert the outflow into discharge.

5.4 Mass balance calculation

Using the glacier module the HBV-EC model computes the annual mass balance for each HRU. The net mass balance (bn [m]) is composed of the winter mass balance (bw [m]) and the summer mass balance bs [m].

If the summer balance of the previous year was negative, the winter mass balance of the present year (y) consists of the maximal daily value of the snow water equivalent of the present year (SWEmax(y)). However, if the summer balance of the previous year

was positive, the winter balance can be calculated by equation 5.16, where SWEmin(y-1) stands for the minimal daily value of the snow water equivalent of the previous year.

$$bw(HRU, y) = SWEmax(y) - SWEmin(y-1) \tag{5.16}$$

To calculate the summer mass balance, there is a distinction depending on the minimal daily value of the snow water equivalent of the present year (SWEmin(y)). In case of a positive value of SWEmin(y) the summer mass balance is computed by determining the difference between the minimal and the maximal daily value of the snow water equivalent of the present year. In case of a negative value of SWEmin(y) the summer mass balance is the negative sum of SWEmax(y) and the glacier melt of the present year.

The mass balance (MB [m^3]) for the entire glacier is calculated by the following equation, where A stands for area [m^2].

$$MB = \sum A(HRU) * bn(HRU) \tag{5.17}$$

The mass balance module can also calculate the mass balance for a specific elevation band over all years, the mass balance for a specific year over all elevation bands and the equilibrium line altitude.

5.5 Volume-area scaling

To consider the shrinking or growing size of the glacier, the volume-area scaling method after CHEN and OHMURA (1990b) was used in this thesis (see equation 2.1 in section 2.2). BAHR (1997) confirmed the physical basis of the empirical equation and RADIC ET AL. (2008) noted that without better input data neither ice-flow models, nor a non-steady state method with changing exponents can be used for future volume projections.

The landuse of 1995 constituted the initial landuse and so the initial glacier area. Using equation 2.1 the initial volume was calculated. Calculating the mass balance over the next 10 years first the new glacier volume and then a new glacier area could be calculated by converting equation 2.1. That way the area and volume of the glacier for the year 2005 and afterward for every 10 years could be computed.

The way how the glacier shrinks or grows follows a common method in digital image processing. First, the glacier size change is converted into a certain number of pixel, which has to be removed or added to the existing "glacier pixels". Then, the glacier between its minimum elevation and the equilibrium line is divided into eight glacier zones. If the glacier shrinks a certain number of pixels forming a certain shape are removed beginning at the deepest glacier zone. If there are pixels left, the same number of pixels are removed again at the deepest glacier zone. This can be repeated 10 times. If there are pixels left, pixels are removed from the second deepest glacier zone, then from the third deepest and so on until the equilibrium line is arrived. If there are pixels left at the equilibrium line, the erosion continues at the deepest glacier zone. The new glacier-free area has the landuse "open". If the glacier grows, it expands to the previous extension of the glacier.

Chapter 6

Data

The HBV-EC model needs daily precipitation and temperature data as input. To calibrate the model, data of discharge, snow course, snow pillow and snow line were used.

Figure 6.1 shows the location of the measurement stations in the three different catchments. Further information about the stations can be found in the appendix (A.1 and A.2).

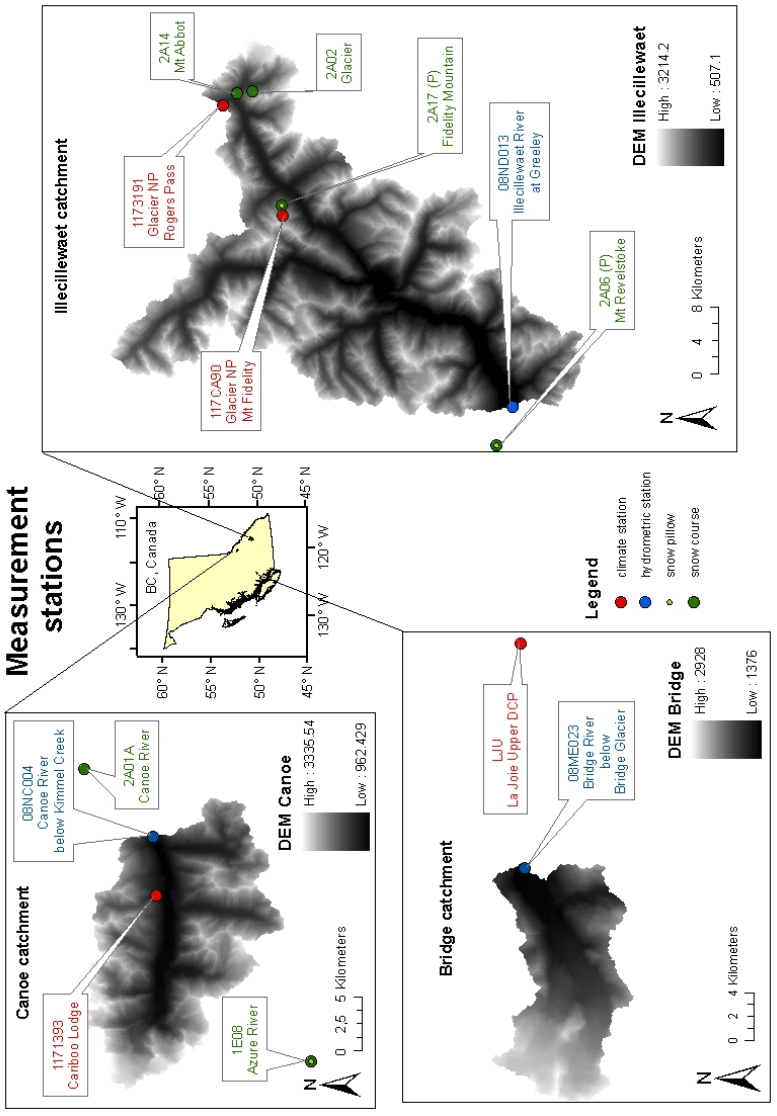

Figure 6.1: Map of the measurement stations in the three considered catchments.

6.1 Input data

6.1.1 Canoe catchment

The "Cariboo Lodge" station (♯ 1171393) situated at 1128 m.a.s.l. is the climate reference station in the Canoe catchment.

As there are data gaps of about 13.5 months in the precipitation and about 15 months in the temperature time series during the calibration and validation period of 1976–2004, a regression analysis was done to fill the gaps. Climate stations in a distance of about 100 km to the reference station were chosen for a possible regression. Figure 6.2 shows the 11 resulting stations.

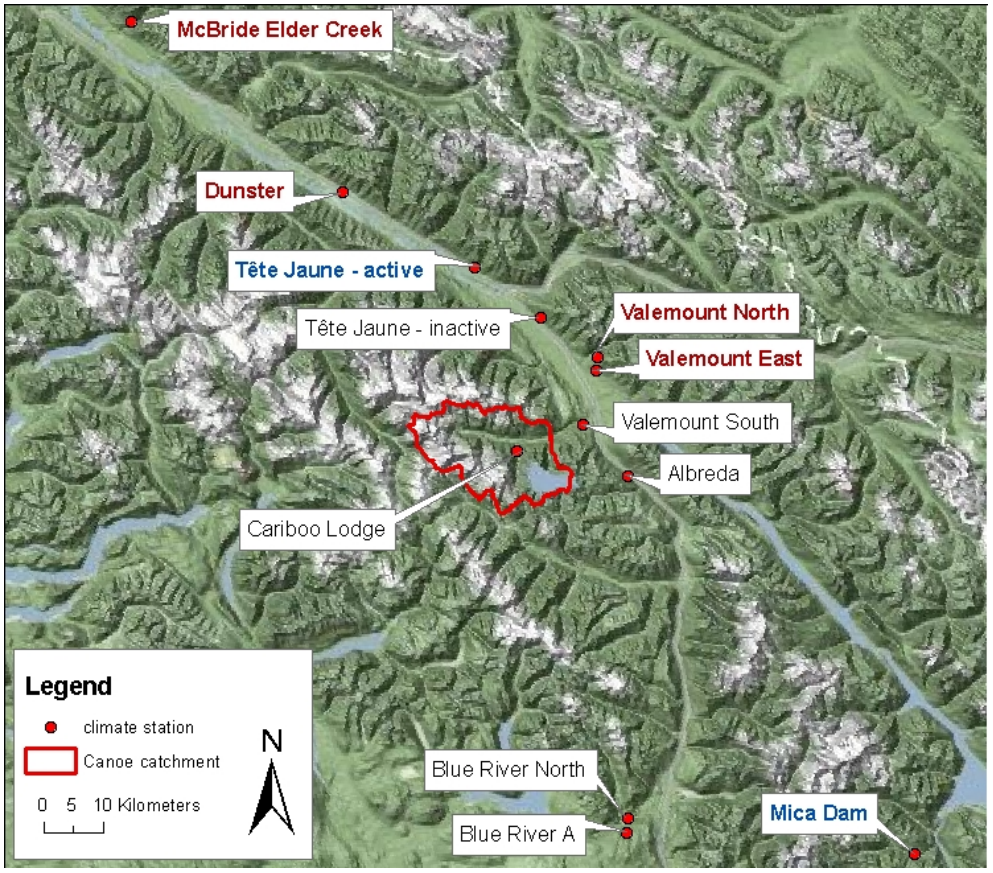

Figure 6.2: Map of climate stations to fill the gaps at the "Cariboo Lodge" climate station. Blue colored stations to fill the gaps in the precipitation time series, red colored stations to fill the gaps in the temperature time series.

Taking a shifting of precipitation events into consideration the precipitation data were smoothed: At the reference station and at each of the selected 11 climate stations the moving average of the precipitation time series was build with means of $\pm$ 6 days. The temperature time series were calculated by averaging the given minimum and maximum temperatures. With these smoothed and averaged time series regression equations between the reference station and each of the 11 stations were made. To fill the gaps the stations with the best coefficient of determination (R^2) were chosen considering additionally the length of the time series and their gaps. Information about the coefficient of

determination and the position of all 11 climate stations can be found in the appendix, A.3.

To fill the gaps in the precipitation time series the climate station "Mica Dam" (♯ 1175122) was used. The coefficient of determination between the reference station and this climate station is 0.59. As there is a data gap in the precipitation time series at the "Mica Dam" station in July 2004, a further station was necessary to complete the time series. The station with the next highest coefficient of determination with data in July 2004 is the climate station "Tête jaune" (♯ 109QJ36) with R^2 = 0.40.

To complete the temperature time series of the reference station four proximate climate stations were necessary. The names, the used time periods and the coefficient of determination of the four stations can be seen in table 6.1.

Table 6.1: Information about the four climate stations which were used to complete the temperature time series of the reference station.

Name of station	Number	Used time series	R^2
Valemount North	♯1178CL9	Jan 1st ,1976 – June 30th, 1989	0.97
Dunster	♯1092578	July 1st, 1989 – Apr 30th, 1995	0.96
McBride Elder Creek	♯1094948	Mai 1st, 1995 – Apr 6th, 1998	0.95
Valemount South	♯11783L9	Apr 7th, 1998 – Sept 30th, 2004	0.96

6.1.2 Illecillewaet catchment

To model the Illecillewaet catchment a complete temperature and precipitation time series for the time period 1976–2004 was available at the climate station "Glacier NP Rogers Pass" (♯ 1173191), situated at 1323 m.a.s.l. There is a second climate station in the catchment ,"Glacier NP Mt Fidelity" ,whose data however were not used for this study because of its shorter time series.

6.2 Calibration and validation data

6.2.1 Discharge data

HYDAT, the database of the Water Survey of Canada, delivered discharge data to calibrate and validate the model. Discharge as the output of the hydrological system can be seen as the integration of all the processes in the catchment (DINGMAN, 2002) and is therefore a very important parameter for calibration and validation. The calibration and validation time together at the Canoe and Illecillewaet catchment spans the years 1976–2004. Data during this time period from the hydrometric station "Canoe River below Kimmel Creek" ♯ (08NC004) were used to calibrate and validate the HBV-EC model at the Canoe catchment. The calculated discharge at the Illecillewaet catchment was calibrated and validated with data from the "Illecillewaet River at Greeley" (♯ 08ND013) hydrometric station. "Bridge River below Bridge Glacier" (♯ 08ME023), the hydrometric station of the Bridge catchment, delivered calibration and validation data for the years 1985–2004 in the Bridge catchment.

How the outflow is calculated by the HBV-EC model was explained in the section "Model description"', subsection 5.3.4.

6.2.2 Snow course and snow pillow data

Snow course and snow pillow data were collected by the Water Stewardship Division of the Ministry of Environment of the Government of British Columbia (WSD). Snow course data result from averaging measured snow water equivalents at specific points at a cross section. Snow pillows are installed at a specific place and measure the snow water equivalent based on the hydrostatic pressure of the overlying snow (DINGMAN, 2002). While snow course data deliver information about the spatial distribution of snow, snow pillow data measure the snow equivalent at one place, but with a high temporal resolution.

In the Canoe catchment there are no snow courses or pillows. To calibrate and validate two measurement stations outside the catchment were used: North-east of the catchment downstream of the hydrometric station there is the snow course measurement station "Canoe River" (♯ 2A01A) and south-west of the catchment there is a snow course and a snow pillow measurement station called "Azure River" (♯ 1E08). The latter belongs to the Thompson River basin.

In the Illecillewaet catchment there are three snow course and one snow pillow measurement stations: The "Glacier" (♯ 2A02) snow course station at 1250 m.a.s.l., the snow course station "Mount Abbot" (♯ 2A14) at 1980 m.a.s.l. and the snow course and snow pillow station "Fidelity Mountain" (♯ 2A17) at 1870 m.a.s.l. Additionally, there is the snow pillow and snow course station "Mount Revelstoke" (♯ 2A06) outside the catchment, downstream of the hydrometric station at 1830 m.a.s.l.

To calibrate and validate a procedure has been written to find the snow water equivalent of a certain HRU which has the same elevation as the snow pillow or snow course station, the landuse "open", the smallest existing slope and the same aspect as the station. The latter criterion results from creating an aspect layer out of the digital elevation model with ArcGIS.

6.2.3 Snowline data

Snow line data from BC Hydro as a fourth criterion were used to calibrate the model. Small planes took readings of the sporadic snowline elevation almost each year between 1994 and 2000 at specific locations. Elevations between certain locations were averaged and the results have a precision of about $\pm$ 100 m (personal information by WEBER, 2009).

The averaged snow line elevation for the Canoe catchments results from six measurements between Donald and the Canoe Reach some kilometers north of the Kinbasket Lake. For the Illecillewaet catchment readings along the Illecillewaet River valley at four specific locations have been taken and averaged.

To calibrate the model a procedure has been written. It averages the elevation of the highest open HRU without snow and the lowest HRU with snow. Using two different slopes and aspects four possible elevations result. Comparing these calculated elevations with the measured snow lines the highest snow lines seemed to be the most realistic ones and were used for calibration.

Chapter 7

Methodology

7.1 Parameter sensitivity and calibration

Parameters in a precipitation-runoff model can often not be measured, instead they have to be calibrated (SEIBERT, 1999). To calibrate a model means to obtain one or more parameter sets which are conceptually realistic and which produce an output as similar as possible to measured data (e.g. MADSEN, 2000; HARLIN, 1991). As proposed by e.g. SEIBERT (1999) a multi objective calibration was used in this study. After MADSEN (2003) a multi-objective calibration is based on

- Multi variable measurements: Several parameters are measured at the same side. For example BERGSTRÖM ET AL. (2002) used snow data, groundwater levels, stable isotopes and nitrogen concentrations besides discharge for calibration.

- Multi site measurements: The same variable is measured at different sites in the catchment.

- Multi response modes: Various objective functions are used to evaluate different responses of the processes at one measurement site, e.g. the peak flow and the low flow of a hydrograph (e.g. MADSEN, 2000; GUPTA ET AL., 1998; YAPO ET AL., 1998).

Applying this framework, the simulation of various characteristics of a system can be evaluated (MADSEN, 2003). The compensation of wrong precipitation values by errors in ice melting values and vice versa (see e.g. BRAUN and AELLEN, 1990) can be minimized (HAGG ET AL., 2006). In this thesis besides discharge measurements snow pillow, snow course and snow line measurements were used to evaluate the simulated values.

Applying the split-sample calibration-validation method (see e.g. KLEMES, 1986) the calibration period expanded between January 1st, 1985 and December 31th, 2004. This calibration period was chosen because all data for the multi objective multi step calibration were available during this period. The calendar year and not the hydrological year was chosen, because the end of the calendar year agrees approximately with the end of the recession.

To evaluate the goodness of the simulated values different objective functions were used:

For the discharge a modified Nash-Sutcliffe performance measure (NASH and SUTCLIFFE, 1970) was used. This normalized benchmark efficiency (BE), which was introduced by SCHAEFLI and GUPTA (2007), is computed as

$$BE = 1 - \frac{\sum_{t=1}^{N} (Qobs(t) - Qsim(t))^2}{\sum_{t=1}^{N} (Qobs(t) - Qbe(t))^2} \tag{7.1}$$

Qobs are the observed discharge data, Qsim are the simulated discharge values. Qbe is the benchmark discharge at time t. It is the mean of all discharge values for a certain day. A BE value of one indicates a perfect simulation, a BE value of zero means that the mean day-of-the-year values are an estimator as good as the model itself, a BE value smaller than zero puts the model into question. SCHAEFLI and GUPTA (2007) showed some examples, where this benchmark efficiency gives better results in catchments with high and constant seasonality in discharge than the commonly applied efficiency (EF); BE is equivalent to EF, where the seasonality has been eliminated. Values of BE are in general lower than efficiency values, because the BE is a more rigorous objective function than the efficiency. The difference between Qobs and Qbe is very small in a catchment with highly seasonal discharge. Therefore, the whole fraction gets a higher value and BE a smaller value.

Concerning the discharge measurements the winter measurements are highly inexact as icing raises the water level without increasing discharge (JONSDOTTIR ET AL., 2006). Therefore, the efficiencies are only calculated between March 1st and November 30th, where discharge is not influenced by icing. In general, discharge time series start in the year 1986, because the model is initialized during the year 1985.

To evaluate the goodness of the simulated snow courses (SC) and snow lines (SL) the Mean Error (ME) was calculated. A value of ME as close as possible to zero indicates a good simulation.

$$ME_{SC} = \frac{\sum_{t=1}^{N} SWE_{obs}(t) - SWE_{sim}(t)}{N}$$

$$ME_{SL} = \frac{\sum_{t=1}^{N} SL_{obs}(t) - SL_{sim}(t)}{N} \tag{7.2}$$

For the snow pillows the Mean Absolute Error (MAE) has been used, because the error using the Mean Error would be very small as negative and positive errors would even out. The closer the MAE value to zero the better the simulation.

$$MAE = \frac{\sum_{t=1}^{N} |SWEobs(t) - SWEsim(t)|}{N} \tag{7.3}$$

In this study ranges of the objective functions are indicated, which refer to the 5% and 95% quantile. That way the uncertainty of the simulation results can be seen, outliers however are excluded.

The following procedure was carried out to obtain the best parameter sets.

First, a literature research was done to receive an estimation about the possible parameter ranges of the HBV-EC or HBV model. The following authors indicated values for means or ranges of the used paramters: STAHL ET AL. (2008), HAMILTON ET AL. (2000), SEIBERT ET AL. (2000), SEIBERT (1999), UHLENBROOK ET AL. (1999), SEIBERT (1997), MOORE (1993), HARLIN and KUNG (1992). That way minimal and maximal parameter values for each parameter was obtained.

To receive an impression about the sensitivity of the parameters one parameter after the other was varied within its range by keeping the other parameters constant at their mean value. As this method does not account for interpendences between parameters it allows only a limited sensitivity analysis.

Therefore, in the next step only the most sensitive parameters of the Bridge catchment as referenced by STAHL ET AL. (2008) were varied by keeping the other parameters constant at their mean values. After analyzing these results and after same trial-and-error runnings – keeping the hydrological meaning of the parameters in mind – some ranges were adapted until a good conformance between measured and simulated values was possible.

Finally, a Monte-Carlo simulation over 2500 runs was done. The use of the Monte-Carlo method for calibration has the advantage that this method is not limited in relation to the complexity and non-linearity of the model (HARLIN and KUNG, 1992). To obtain the 20 best parameter sets a multi objective multi step approach was used. First, the 10 % of the parameter sets, which simulate discharge best were chosen. Out of this 250 parameter sets the best 40 % concerning the snow courses were taken. From those 100 parameter sets left the best 40 % regarding snow pillows were chosen. In the last step, the best 50 % of the 40 remaining parameter sets concerning snow lines were selected. In that way discharge as a very important calibration value has nearly the same influence on the choice of the best parameter sets as snow courses, snow pillows and snow lines together (10 : 8). The importance of discharge as a calibration value is strengthened by the high accuracy of discharge measurement in comparison to the low accuracy in snow measurement due to a high spatial variability of snow. Additionally, long time series of discharge are available. The snow courses consider the spatial distribution of snow, while snow pillow data show a temporally high solution. Snow lines have the least influence on choosing the best parameter sets, because they are with $\pm$ 100 m the most inexact measured data (personal information by WEBER, 2009).

7.2 Validation

To valuate the ability to simulate well also for periods beyonds the calibration period, the model was run for the period between January 1st, 1976 and December 31th, 1984. Therefor, the 20 best parameter sets of the calibration were used. As proposed and realized by AMBROISE ET AL. (1995) the model in this thesis is validated not only with discharge data. Additionally, snow course data were used for validation. Snow pillow and snow line data were not available in the two considered catchments during the validation period.

The validation with discharge data starts in the year 1977, because during 1976 the model is initialized and does not produce credible outputs. In order to show the uncertainty of the simulations, ranges of the objectives functions are indicated; the ranges are

the 5 % quantile and the 95 % quantile to exclude outliers.

7.3 Projection into future

After calibration and validation the model simulated future discharge between 2001 and 2100 with the 20 best parameter sets. Therefor, generated daily precipitation and temperature time series of two different Global Climate Models were used as input. Global Climate Models simulate energy fluxes between the sun, the atmosphere and the surface. The two Global Climate Models used are the CGCM3 and the CM2.1 model.

The CGCM3 model is the third version of the Canadian Centre for Climate Modelling and Analysis Coupled Global Climate Model. In comparison with other models it predicts rather more precipitation; it ranges concerning air temperature increase in the middle of the prediction of other commonly used GCMs (see MOTE ET AL., 2005). Further information about the model can be found in FLATO ET AL. (2000) or in CCCMA (2008).

The CM2.1 is an US Americain Global Climate Model. Information about the model can be found in DELWORTH ET AL. (2006).

The results of the two Global Climate Models have been downscaled as the output of GCMs are on a larger scale than on the required catchment scale. That way input data for a specific climate station can be obtained. This was done by the TreeGen statistical downscaling model. This model creates a relation between observed synoptic-scale atmospheric predictor fields and observed surface weather elements. Using this relationship weather elements for a specific station are created by using the atmospheric fields of the Global Glimate Models. As their is a stochastic part during the downscaling process the result of ten downscaling runs were used in this thesis. More information about the downscaling approach can be found in the appendix of STAHL ET AL. (2008).

Each input data series is additionally based on a specific scenario defined by the Intergovernmental Panel on Climate Change (IPCC, 2000). The chosen scenarios A2 and B1 represent the upper and lower limit of greenhouse gas changes in the future, especially at the end of the 21th century.

The A2 scenario predicts a large population growth with up to 15 billion people by 2100. Low mobility of ideas, persons and capital leads to high heterogeneity concerning income per person, technological change and social and political structures. The average income is low in comparison with other scenarios and there is no approximation between industrialized and non-industrialized countries. The CO_2 emission is predicted to be 2100 almost four times higher than at 1990 (IPCC, 2000).

In contrast the B1 scenario is based on a high level of environmental and social consciousness. The population raises up to nine billion people by 2050, but declines to seven billion people by 2100. Sustainability plays an important role. To use natural resources in an efficient way and to protect the environment there are big technological changes predicted. Fast changes will take place. There is the aim to obtain equitable income distribution. The CO_2 emission is predicted to be in 2100 about 60 % less than in the year 1990 (IPCC, 2000).

Using the two different Global Climate Models, the 10 different downscaling results and the two different scenarios 40 different input time series were created. Combining

these input series with the 20 different parameter sets 800 different discharge predictions for each decade for each catchment could be obtained. Glaciers have been scaled up after each decade using the mass balance of the former decade and the V-A method. That way also 800 predictions in glacier area and volume could be obtained. As in the study of LOUKAS and QUICK (1996) a mean thinning rate over a certain time period was calculated by dividing the volume change over the considered time by glacier area.

Finally, the simulation results of the Canoe and the Illecillewaet catchment were compared with the ones of the Bridge catchment. Therefor, the mean values of total discharge as well as icemelt were compared. In the Canoe and Illecillewaet catchment, these mean values were calculated as means out of 800 different simulations, which consider different parameter sets, GCMs, downscaling results and scenarios. In contrast in the Bridge catchment, only the best parameter set was used to calculate mean values.

Chapter 8

Results

8.1 Parameter sensitivity

A literature research as mentioned in section 7.1 has resulted in a parameter range for each of the 30 parameters. After some adaptions the parameter ranges in table 8.1 were used for calibration. As the parameter ranges are relatively wide and the Canoe and the Illecillewaet catchment are situated close to each other, these parameter ranges were the basis for the calibration of both catchments.

Using the parameter ranges in table 8.1, a Monte-Carlo simulation was done. Figure 8.1 illustrates the normalized parameter ranges of the 20 best simulations for all 30 used parameters.

In the Canoe catchment most of the parameters are insensitive; that means that good simulation results can be received by using a parameter value out of the whole parameter range (e.g. UHLENBROOK ET AL., 1999). Contrarily, there are some sensitive parameters which deliver good results only at a certain part of their parameter range. Defining very sensitive parameters as parameters which vary at most between 0.6 of their whole parameter range, there are three very sensitive parameters in the Canoe catchment: RFCF, TM and DC. They vary only between 0.56, 0.51 and 0.47, respectively, of their whole parameter range. Sensitive parameters, defined as parameters varying between 0.6 and at most 0.8 of their whole parameter range, are PGRADL, PGRADH, TLAPSE, TT, CRFR and KF.

Also in the Illecillewaet catchment most of the parameters are not sensitive. There are three very sensitive parameters as defined above: The parameter RFCF shows a variation of 0.58, TT a variation of 0.57 and KF a variation of 0.56 of the particular parameter range. Only one parameter (MRF), which varies about 0.67 of its parameter range, can be defined as a sensitive parameter.

Comparing the catchments it can be seen that there are more insensitive parameters in the Illecillewaet catchment than in the Canoe catchment. Analyzing the sensitive and very sensitive parameters they are not the same in the two catchments – with the exeption of RFCF, KF and TT. RFCF is a very sensitive parameter in both catchments, KF and TT are more sensitive in the Illecillewaet catchment than in the Canoe catchment.

Referring to STAHL ET AL. (2008) the following parameters were the most sensitive ones at the Bridge catchment: PFCF, PGRADL, PGRADH, EMID, TLAPSE, AM, TM, CMIN, DC and MRG. As there was another calibration scheme used, no exact comparison can be done. But it can be seen that none of these parameters is common with the (very) sensitive parameters of the Illecillewaet catchment. Comparing the Bridge and the Canoe catchment, there are five parameters which are sensitive in both catchments: DC, TM, PGRADL, PGRADH and TLAPSE. RFCF, a very sensitive parameter in the Illecillewaet as

Table 8.1: Overview about all parameters and their ranges for calibration.

Parameter name	Unit	Parameter description	Parameter range from	to
RFCF	–	rainfall correction factor	1.1	1.4
SFCF	–	snowfall correction factor	1.2	1.7
PGRADL	1 / m	increase of precipitation per meter below EMID	0	0.0001
PGRADH	1 / m	increase of precipitation per meter above EMID	0	0.00001
EMID	m.a.s.l.	mid point elevation separating precipitation gradients	1500	3000
TLAPSE	°C / m	temperature lapse rate	0.0055	0.0065
TT	°C	threshold air temperature separating rain and snow	-3	3
TTI	°C	interval for mixed rain and snowfall	0	2
EPGRAD	1 / m	fraction decrease of potential ET	0.0002	0.0006
TFRAIN	–	fraction of rainfall reaching ground below canopy	0.7	0.9
TFSNOW	–	fraction of snowfall reaching ground below canopy	0.6	0.9
AM	–	influence of aspect on melt factor	0.2	0.3
TM	°C	threshold temperature for snowmelt	-2	1
CMIN	mm / °C	melt factor for winter solstice in open areas	1	2
DC	mm / °C	increase of melt factor on summer	1	3
MRF	–	ratio melt forest to melt open	0.5	0.9
CRFR	mm / (°C * d)	rate of liquid water refreeze in snowpack	0.5	2.5
WHC	–	liquid water holding capacity in snowpack as fraction of SWE	0.05	0.2
LWR	mm	max of liquid water in snow pack	100	2500
FC	mm	field capacity of soil	50	300
BETA	–	relation between soil infiltration and soil-water release	1	4
LP	–	soil moisture content below ET is less than pot ET (fraction of FC)	0.6	1
MRG	–	ratio of melt of glacier ice to snow	1.2	1.6
AG	1 / mm	relation between SWE on glacier and runoff coefficient	0.01	0.1
DKG	1 / d	difference between maximum out and minimum outflow coefficients	0.1	0.2
KGMIN	1 / d	minimum outflow coefficient	0.01	0.1
KGRC	1 / d	coefficient for the delay in recession coefficient change	0.4	0.6
KF	1 / d	recession coefficient fast reservoir	0.01	0.5
KS	1 / d	recession coefficient slow reservoir	0.001	0.1
FRAC	–	fraction of fast reservoir	0.3	0.8

in the Canoe catchment, is none of the most sensitive parameters in the Bridge catchment.

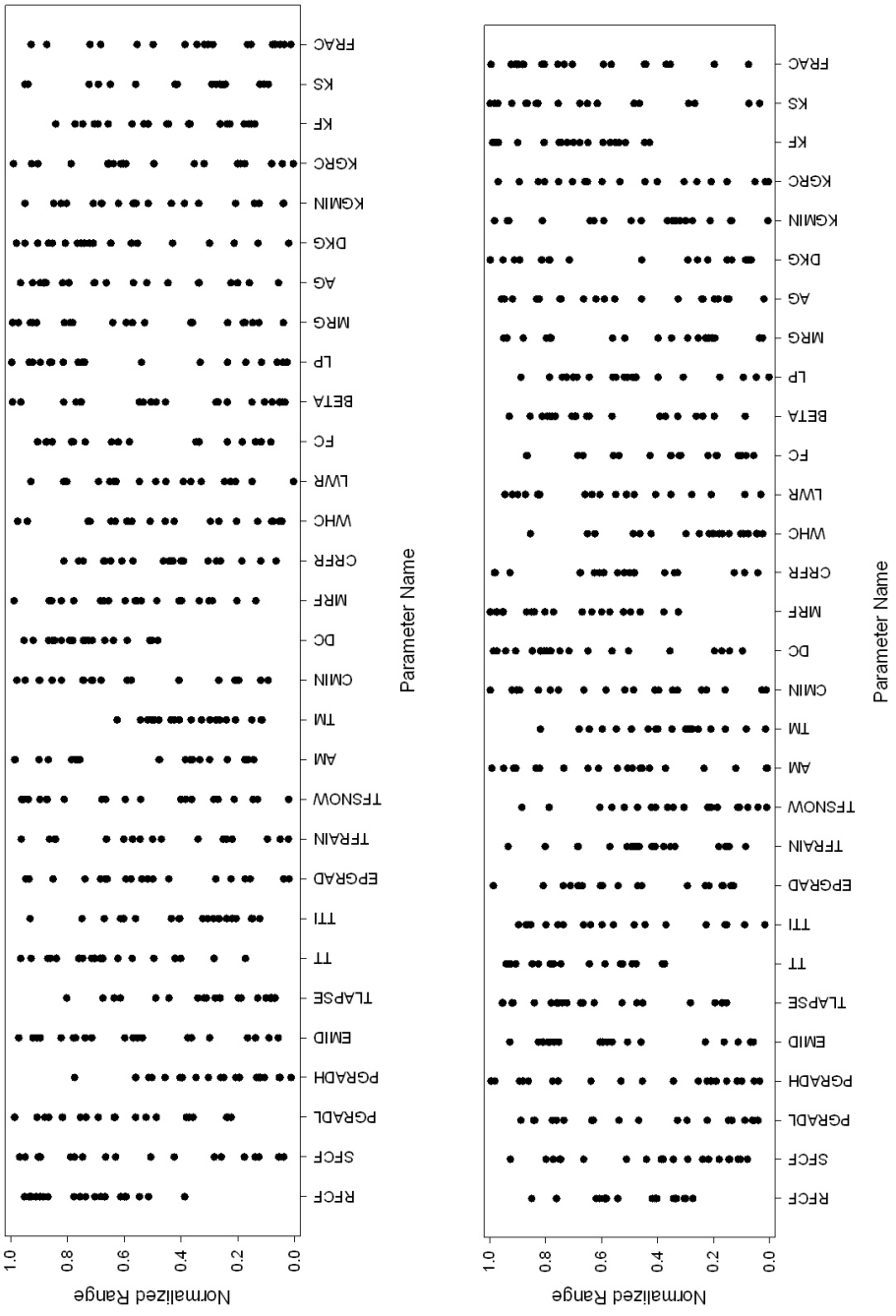

Figure 8.1: Normalized parameter ranges of all parameters in the Canoe catchment (left) and in the Illecillewaet catchment (right).

8.2 Calibration

8.2.1 Goodness of simulation in the Canoe catchment

Figure 8.2 exemplifies the simulation of discharge for three years. The time period between January 1st, 2000 and December 31th, 2002 has been chosen to be able to compare these results with the results of the Bridge catchment. The 20 best simulations are able to model the main characteristics of the discharge curve in a good way. This confirms an efficiency range between 0.83 and 0.87 and a smoothed benchmark efficiency range between 0.42 and 0.55, respectively.

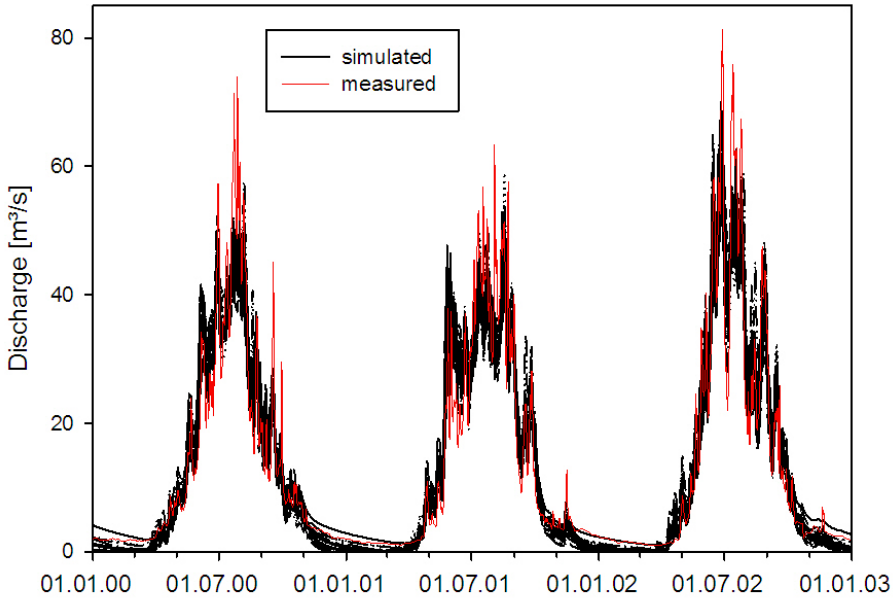

Figure 8.2: Simulated and observed discharge between January 1st, 2000 and December 31th, 2002 at the Canoe catchment.

Figure 8.3 shows on the left side the mean monthly discharge values of the 20 best simulations and of the measurements during the 20 calibration years. While during wintertime (November – March) as well as during the high flow month July discharge is rather underestimated, it is rather overestimated at the raising and decreasing part of the curve during the months May and September.

Analyzing the sum of annual runoff (see figure 8.3, right part) the model simulates runoff quite well – comparing the observed value with the mean of the simulated values. Only in the year 1986 and especially in the year 2003 all simulations underestimate runoff highly. As the time series in 1995, 1996 and 1997 are incomplete, no mean values have been calculated.

Besides comparing measured and simulated discharge data, it is interesting to know, if the model is able to simulate the snow cover well. Therefor, the snow water equivalent – measured at snow pillow stations as well as at snow course stations – is compared with

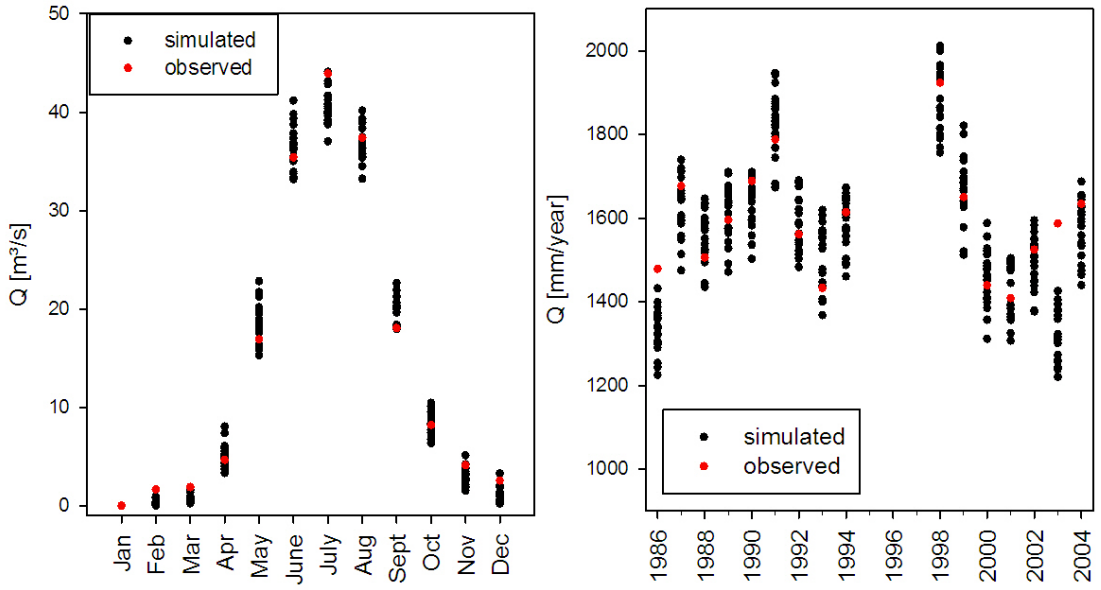

Figure 8.3: Left: Simulated and observed mean monthly discharge values. Right: Simulated and observed sum of annual runoff values. Both calculated for the Canoe catchment during the calibration time period.

the simulated snow water equivalent for the specific HRU.

Figure 8.4 illustrates the result for the snow pillow station 1E08 south of the Canoe catchment. During the first two snow accumulation periods the timing of snow accumulation and melting is well simulated. However, the amount of snow water equivalent during the snow period is about 40 % too little. At the following six years snow accumulating as well as snow melting is simulated too late. The quantity of snow water equivalent during the snow period is about 33 % up to 56 % at the period 2002–2003 too little. Comparing the dynamic, the simulated values show the same dynamic as the observed values – this means that in years with much snow (e.g. period 1998–1999) the model simulates much snow, whereas in years with less snow accumulation (e.g. period 2000–2001) also the model calculates less snow accumulation. However, the MAE at the station ranges between 315 and 333 mm.

To use the snow water equivalent (SWE) measurements at snow course stations is another possibility to evaluate the simulation of snow. Figure 8.5 shows the results comparing the SWE at different snow course stations with the simulated SWE values separately for the months April, Mai and June. One point signifies the mean of the 20 best simulations compared with the observed value at a certain date. The "uncertainty bars" result from the minimum and maximum simulated value from the 20 simulations. While the mean value shows the tendency of the simulations, the range shows the uncertainty of the 20 best model runs. The bisecting line represents the best possible result where the simulated values would correspond the observed values.

Analyzing the results of April, the simulation underestimates the SWE at the snow

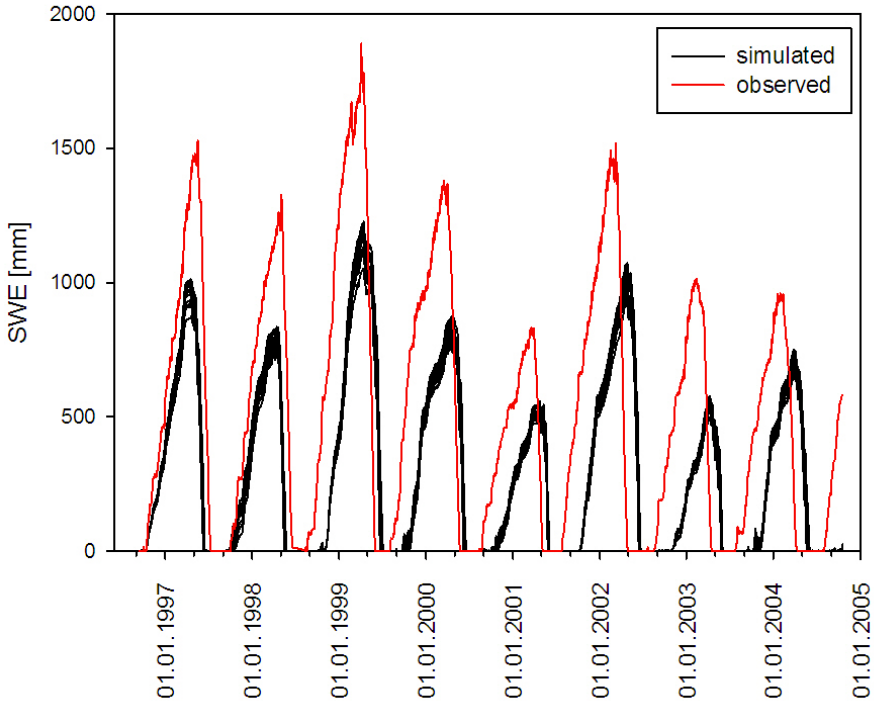

Figure 8.4: Simulated and measured values of the snow pillow station 1E08.

course station 1E08 (situated at 1620 m.a.s.l.). The ME ranges between 228 and 312 mm. In contrast, the model overestimates the SWE at the station 2A01A situated at 910 m.a.s.l.; the ME range is between -451 and -338 mm.

In May ME values between 403 and 487 mm indicate an inferior simulation at the 1E08 station to the simulation in April. At the 2A01A station there is no snow accumulation anymore, but the model calculates up to 660 mm. Having a closer look at the data all 20 simulation variants show high snow accumulation during the years 1989, 1999 and 2002, while no snow could be measured at the 2nd April in these years. In the other years the simulated and observed data agree well. A ME range between -138 and -37 mm indicate a better simulation than in April.

In June only observed data are available at the higher situated station 1E08. With a ME range of between 620 and 728 mm the model underestimates highly the SWE. While in certain years there is still snow at the snow course station, the model simulates no snow anymore.

The model in general overestimates the SWE at the lower situated snow course station 2A01A, whereas it underestimates the SWE at the higher situated station 1E08. At this station the model simulates worse from April to June.

The last possibility to evaluate the model is to compare snow lines (see figure 8.5, bottom right). With a ME ranging between -51 and 85 m and with a measurement uncertainty of $\pm$ 100 m the model is able to simulate the snow line well depending on the chosen parameter combination. However, there is a high uncertainty due due to the

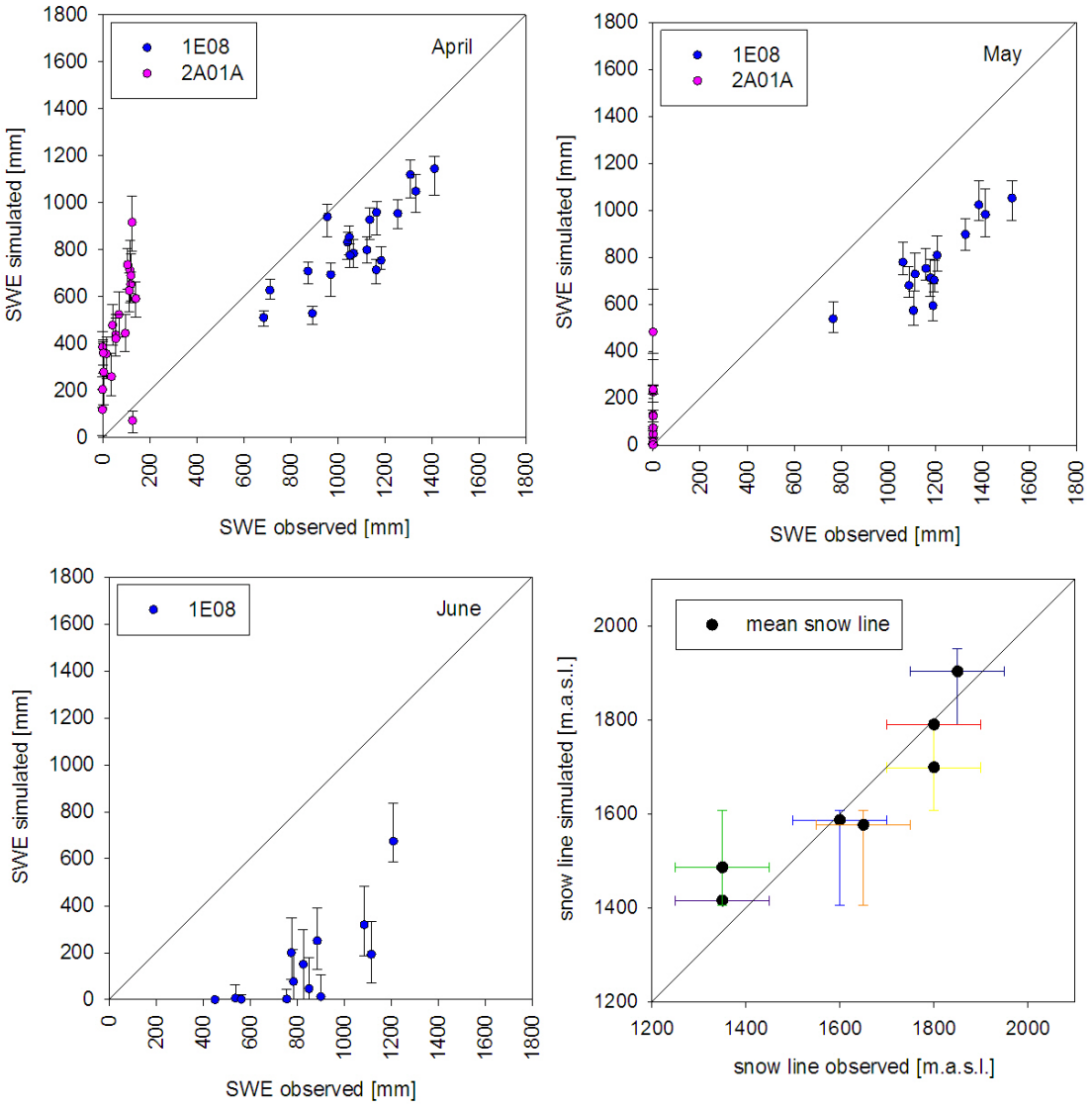

Figure 8.5: Comparison between measured and simulated SWE values at snow course stations in the Canoe catchment during April, May and June. Bottom right: Comparison between measured and simulated snow line values.

measurements.

8.2.2 Goodness of simulation in the Illecillewaet catchment

Figure 8.6 shows an example of simulated and observed discharge during three years. With an efficiency range between 0.80 and 0.84 and a mean smoothed benchmark efficiency range between 0.31 and 0.47 the model simulates discharge well. Most of the peaks are recognized, however, the amount of the peak does not always agree.

Figure 8.7 shows on the left side the mean monthly discharge values of the 20 best simulations and of the measurements during the 20 calibration years. In wintertime

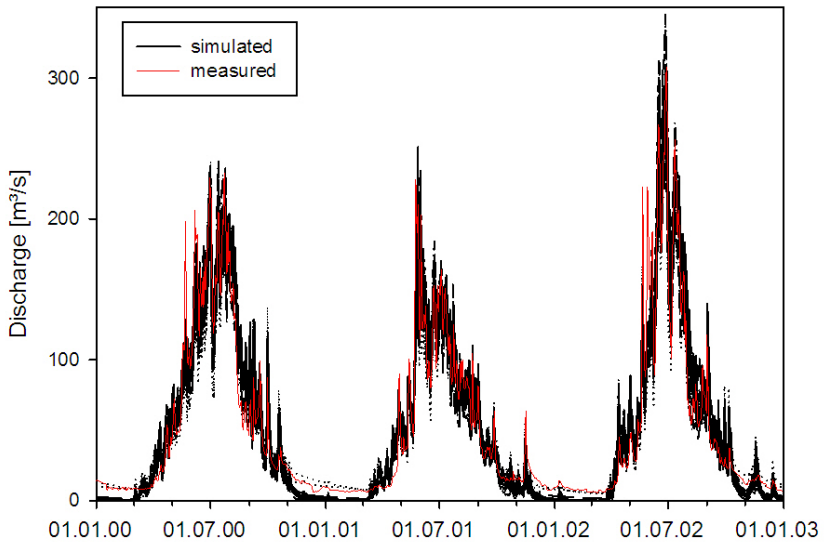

Figure 8.6: Simulated and observed discharge between January 1st, 2000 and December 31th, 2002 at the Illecillewaet catchment.

(November – February) the model rather underestimates discharge. Discharge during October and March is quite well simulated, however it is rather overestimated at the ascending part of the curve. While discharge is well simulated in June and July, it is rather overestimated in August and September.

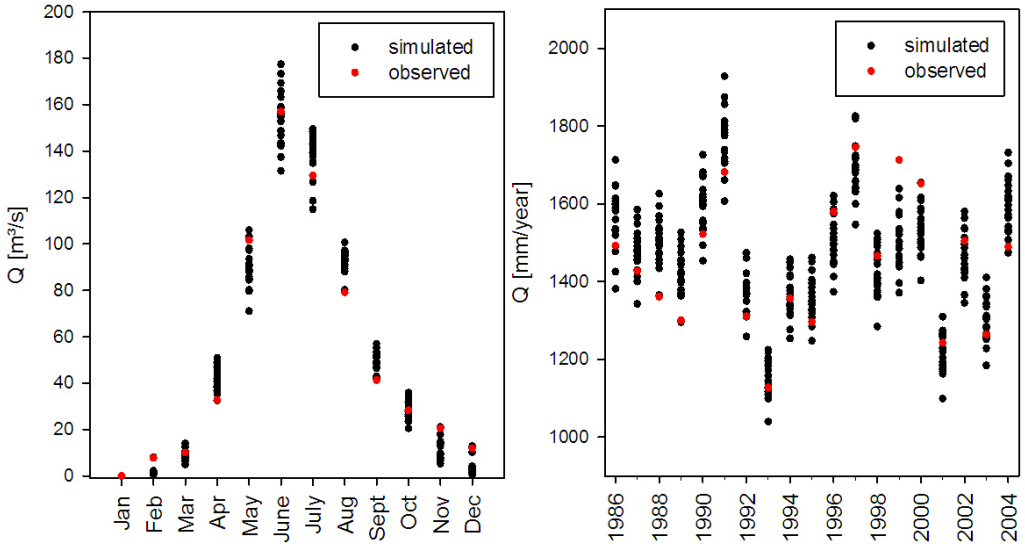

Figure 8.7: Left: Simulated and observed mean monthly discharge values. Right: Simulated and observed sum of annual discharge. Both calculated for the Illecillewaet catchment during the calibration time period.

Analyzing the annual sums (see figure 8.7, on the right) the simulated values follows the dynamic of the observed runoff in most of the years. There are years (1988, 1989) where the model rather overestimates runoff and there are years (1999, 2000) where the model rather underestimates runoff. Only in 2000 the observed value is out of the range of the simulation.

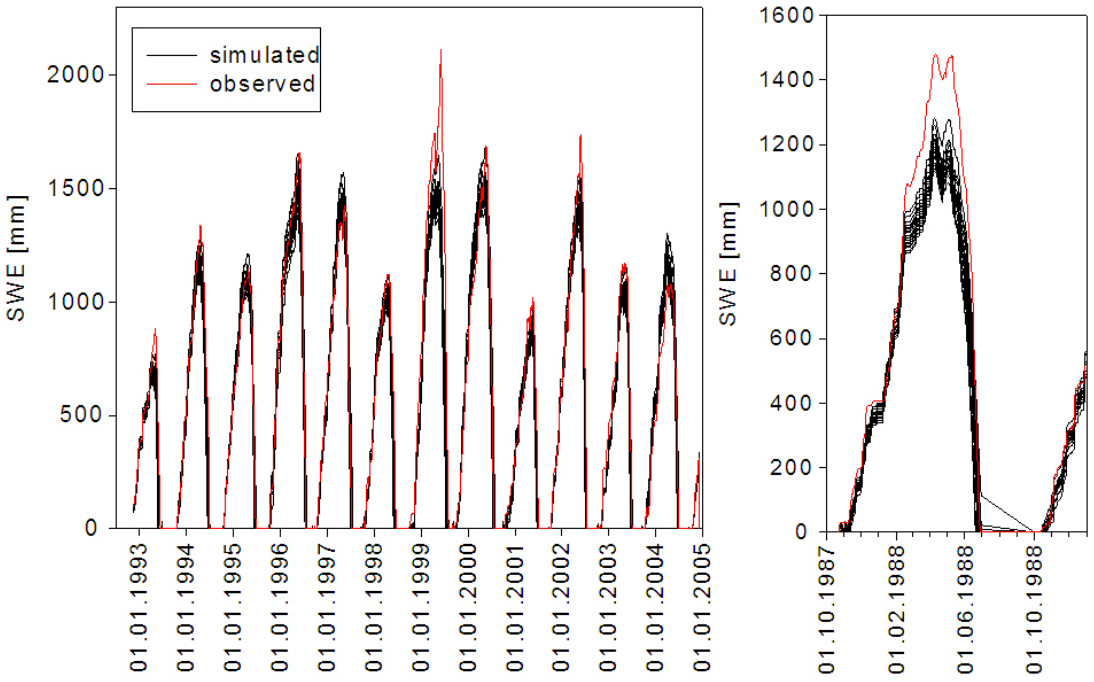

Figure 8.8: Simulated (in black) and measured (in red) values of the snow pillow station 2A17P (left) and 2A06P (right).

There are two snow pillow stations in the Illecillewaet catchment to analyze the temporal simulation of the SWE. Figure 8.8 illustrates the simulated and observed SWE values at the station 2A06P (left) and the station 2A17P (right), both situated between 1800 and 1900 m.a.s.l.. As can be seen at the 2A06P station the model simulates the dynamic of the snow accumulation and melting well, just the peaks are rather underestimated (e.g. 1999), but sometimes also overestimated (e.g. 1997, 2004). At the 2A17P station the rapidly rising and decreasing part of the snow water equivalent curve is well simulated. During March and June the model rather underestimates the SWE. The ME at the 2A06P station ranges between 69 and 94 mm SWE, the one at the 2A17P station between 84 and 140 mm SWE.

For evaluating the simulation of snow in a higher spatial resolution the modeled and observed SWE at four snow course stations in and next to the Illecillewaet catchment were compared. Figure 8.9 illustrates the results. One point represents the comparison between an observed value and the mean of the 20 best simulations. The "uncertainty bars" result from the minimum and maximum value out of the 20 best simulations. While

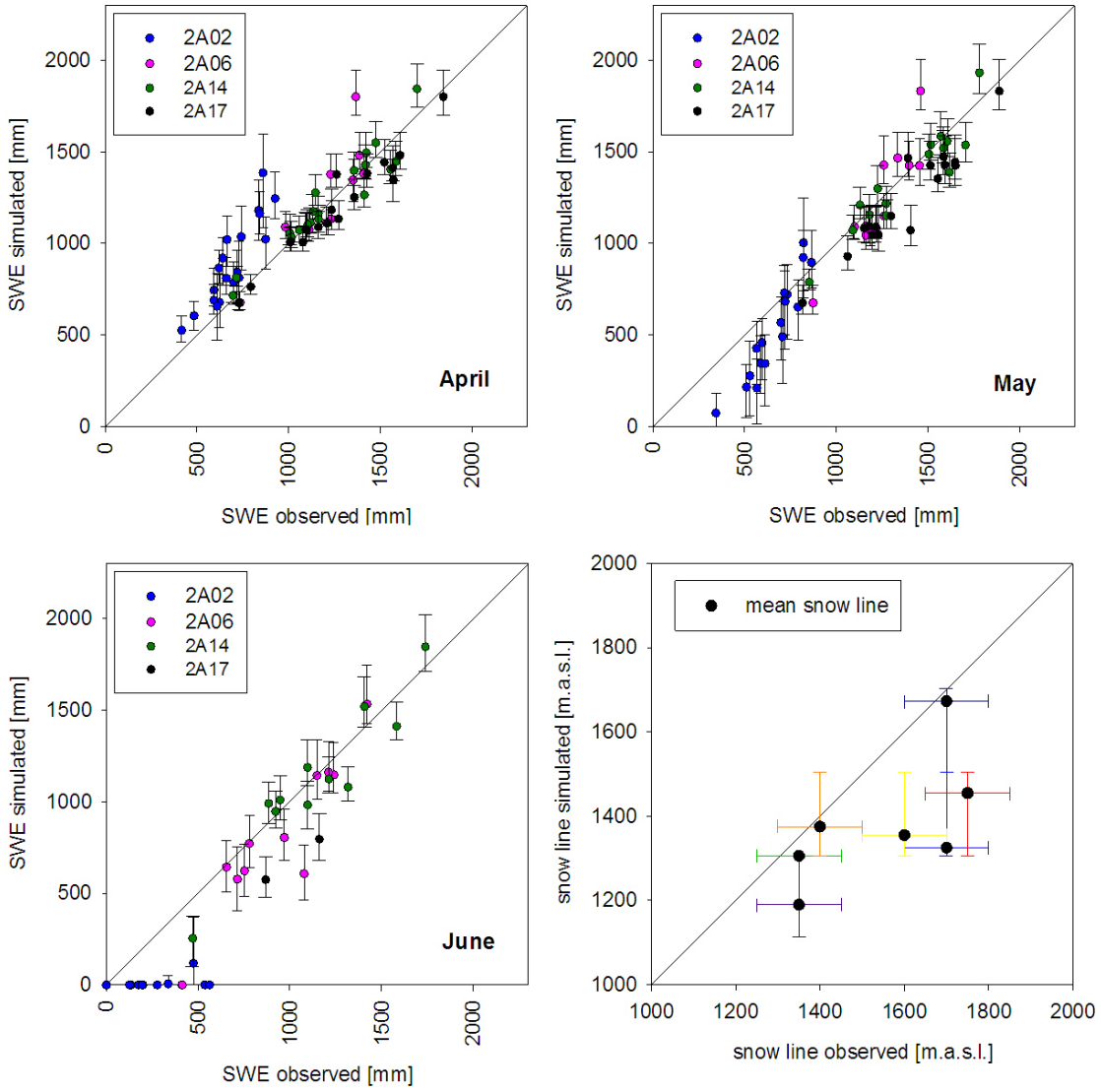

Figure 8.9: Comparison between measured and simulated SWE values in the Illecillewaet catchment during April, May and June. Bottom right: Comparison between measured and simulated snow line values.

the mean indicates the direction of the simulation, the range shows the uncertainty of the simulated values. The bisecting line represents the best possible result, where the mean simulated value would match the observed value.

In April most of the points of the higher located stations (2A06, 2A14 and 2A17) are around the bisecting line. The ME values range between -15 and 106 mm at the station 2A06, between -54 and 79 mm at the station 2A14 and between 26 and 148 mm at the station 2A17. The range between negative and positive values indicate that the model over- and underestimates depending on the parameter set; at the station 2A14 there is rather an underestimation. In contrast the model overestimates the SWE of the lowest located station 2A02 (1250 m.a.s.l.). The 20 best simulations show there a higher uncertainty and the ME ranging between -280 and -64 mm confirms the strong overestimation.

Comparing the results of April and May there are big differences especially for the lower located station 2A02. While the model rather overestimated the SWE in April, it rather underestimates the SWE in May at this station. The ME for the 2A02 snow course station ranges between 46 and 236 mm, the one for the 2A06 station between 18 and 124 mm, the one for the 2A14 station between 17 and 144 mm and the one for the 2A17 station between 137 and 240 mm. The latter objective function indicates rather an underestimation at the 2A17 station.

In June only points of the highest located snow course 2A14 are around the bisecting line. The model rather underestimates the SWE at the 2A06 station; at the 2A17 station there are only two measurements whose simulated values are too small. There is still snow at the lowest situated station 2A02, but the model simulates no snow any more – except for one point. The ME values range between 231 and 288 mm at the station 2A02, between 88 and 280 mm at the station 2A06, between -36 and 116 mm at the station 2A14 and between 302 and 490 mm at the station 2A17. The station 2A02 and 2A17 show a high underestimation of the model.

Comparing the simulations of April, May and June there is a tendency visible to underestimate the SWE over the months. Concerning the uncertainty of the simulated values, the station 2A02 shows a higher uncertainty during April and May than the other stations, but a smaller uncertainty in June – where no snow is simulated anymore.

A further possibility to compare the goodness of the simulations are snow lines (cp. figure 8.9, bottom right). The model rather underestimates the snow lines. But with a high uncertainty between the 20 best simulations and a high uncertainty of measurement, which constitutes $\pm$ 100 m, some simulated snow lines – depending on the parameter set – can reach the value of the observed snow lines. The ME of between 74 and 244 m confirms the high underestimation and uncertainty.

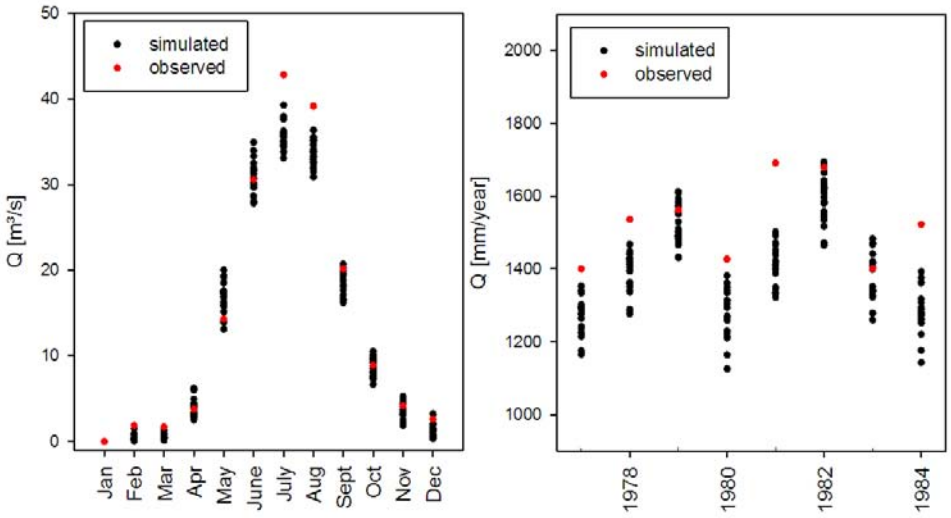

Figure 8.10: Left: Simulated and observed mean monthly discharge values. Right: Simulated and observed annual runoff values. Both calculated for the Canoe catchment during the validation time period.

8.3 Validation

8.3.1 Canoe catchment

While the efficiencies of discharge during the validation time period are almost as good as during the calibration time period (0.79–0.85 versus 0.83–0.87), the smoothed benchmark efficiencies declined from 0.42–0.55 to 0.18–0.40; the uncertainty of both objective functions has increased. An example over three simulated years can be seen in the appendix, figure A.3.

Figure 8.10 illustrates mean monthly discharge values on the left side and annual runoff data on the right side during the validation period.

Comparing the mean monthly discharge values of the calibration and validation time period there are differences, especially at the high flow months July and August. During the validation time period discharge is highly underestimated during these months and also during September there is rather an underestimation of discharge. During the other months there are no big differences between calibration and validation: The observed

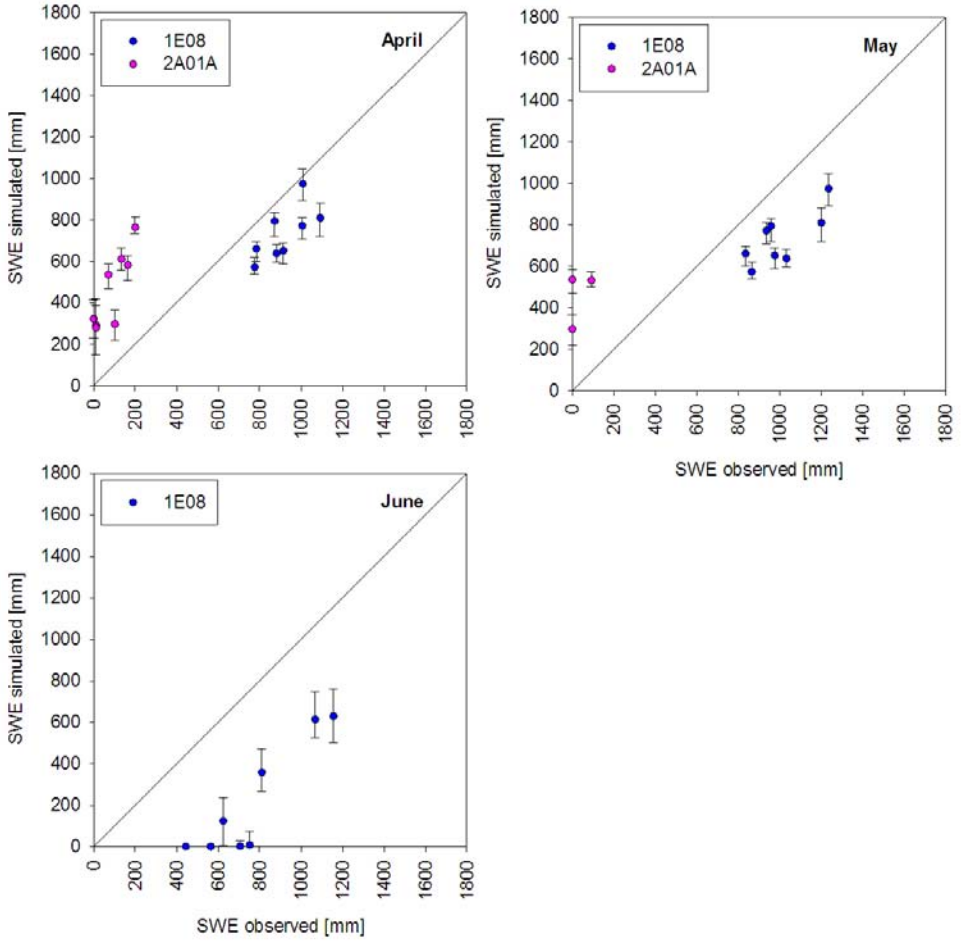

Figure 8.11: Comparison between measured and simulated SWE values at the snow course stations in the Canoe catchment during April, May and June of the validation period.

values are in the range of the simulated values with the exception of the winter months where there is rather an underestimation. During all months there is less discharge during the validation than during the calibration period.

Analyzing the results of the annual runoff data, there are often underestimations. In five of nine years there is a highly underestimation – until more than 250 mm difference between the mean simulated and the observed runoff value. During the calibration period the observed values are more often in the range of the simulation values.

Evaluating the model with snow course data (see figure 8.11) during the validation period there is the same tendency as during the calibration period: The model rather underestimates the snow water equivalent at the 1E08 station and rather overestimates the snow water equivalent at the 2A01A. The simulations at the 1E08 station are best during April and worst during June (ME_{April}= 216–294 mm, ME_{May}= 377–453 mm, ME_{June}= 578–657 mm). During the calibration period the simulations at the 2A01A station are better in May (ME between -142 and -205 mm) than in April (ME between -319 and -416 mm).

8.3.2 Illecillewaet catchment

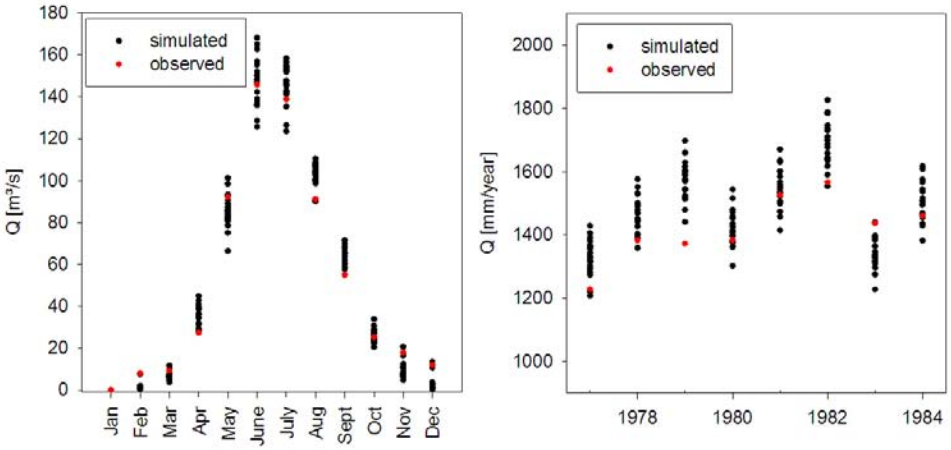

Figure 8.12: Left: Simulated and observed mean monthly discharge values. Right: Simulated and observed sum of yearly discharge values. Both calculated for the Illecillewaet catchment during the validation time period.

Comparing measured and simulated discharge in the Illecillewaet catchment during the validation period the efficiency ranges between 0.77 and 0.85; the smoothed benchmark efficiency ranges between 0.14 and 0.45. Whilst the efficiency has an even better best value than during the calibration period ($ME_{calibration}$ = 0.80–0.84), the value of the smoothed benchmark efficiency has diminished, the uncertainty has increased (for comparsion: $ME_{calibration}$ = 0.31–0.47). In the annex there is an example of discharge curves (see figure A.3).

Figure 8.12 shows on the left side mean monthly discharge values. There is virtually no difference between the calibration and validation period looking at the overestimation

and underestimation of the simulations. The only difference is the quantity of discharge with higher values during the validation period.

Looking at the annual runoff values on the left side of figure 8.12 rather an overestimation of discharge is visible, especially in the year 1979 where the observed value is outside of the range of simulation. Only during the year 1983 there is an underestimation of discharge.

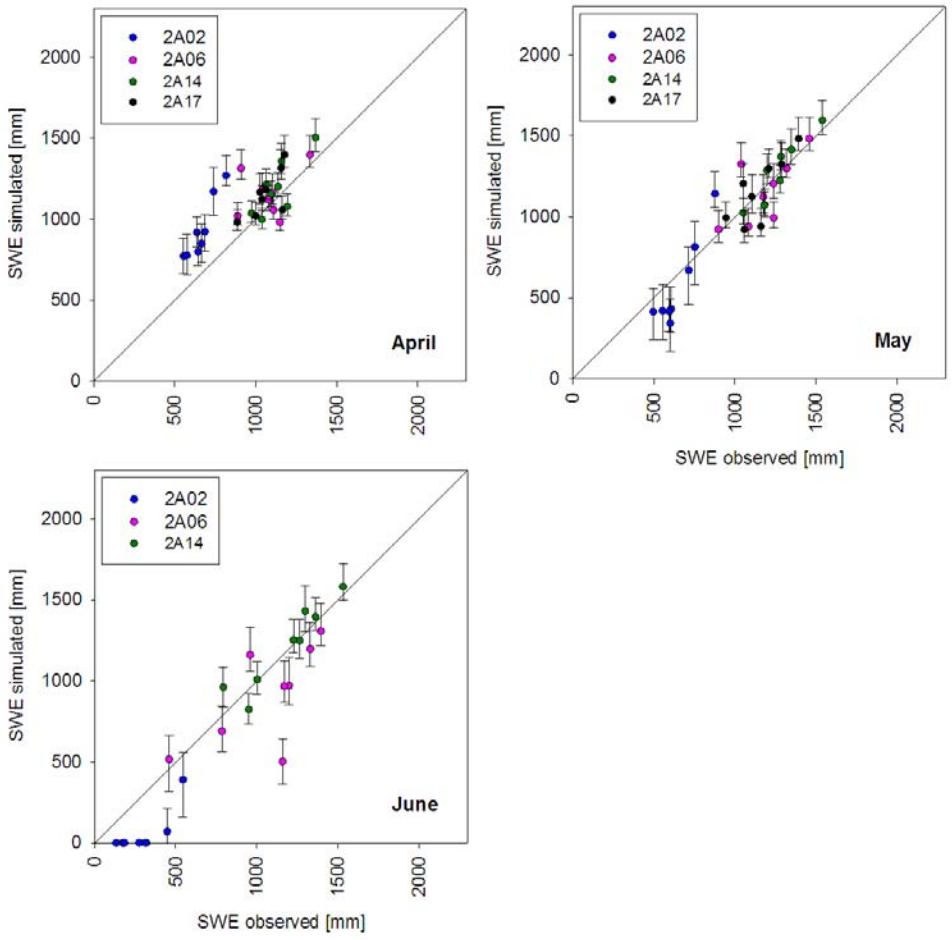

Figure 8.13: Comparison between measured and simulated SWE values at the snow course stations in the Illecillewaet catchment during April, May and June of the validation period.

To quantify the goodness of snow simulation during the validation period, the measured and simulated SWE values at snow course stations were compared (see figure 8.13). As during the calibration period there is the following tendency: In April the model simulates well at the higher situated stations, at the lower situated 2A02 station there is an overestimation of SWE. During May there is rather an underestimation at all stations. In June there is still snow at the 2A02 station, but the model calculates no snow any more. At the 2A06 station there is a bigger underestimation than in May. In contrast, the overestimation at the station 2A14 is smaller in May than in June. At the station 2A17 there are no observed data. Values for the Mean Errors can be found in table A.4 in the appendix.

8.4 Projection into future

8.4.1 Uncertainty of the future discharge

Canoe catchment

After modeling the discharge in the Canoe catchment with two different Global Climate Models, 10 different downscaling results, two different scenarios and 20 different parameter combinations, the results for the last decade of the century can be seen in figure 8.14. The red line illustrates the median, the green lines the 5 % and 95 % quantil of the resulting 800 simulations. There is a big uncertainty in discharge with a minimum interquantil range in February (1.l m^3/s) and a maximum interquantil range in June (11.5 m^3/s). The uncertainty increases with raising discharge, especially between March and April, and decreases with declining discharge.

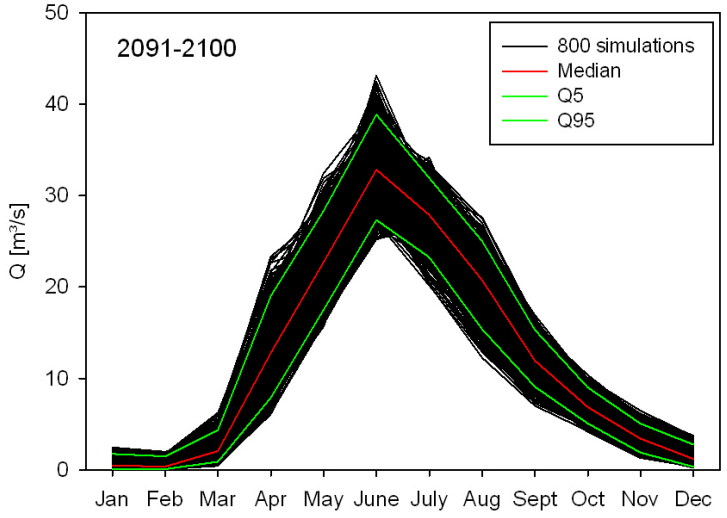

Figure 8.14: Simulated discharge in the Canoe catchment for 2091–2100.

Figure 8.14 shows the uncertainty of discharge depending on different parameter sets and on different input combinations. Figure a and c show the uncertainty of discharge as the consequence of parameter combinations for the decades 2041–2050 and 2091–2100. The box plots show the uncertainty of the input combinations resulting from different Global Climate Models, downscaling results and scenarios. Figure b and d illustrate the uncertainty of discharge as a consequence of input combinations for the decades 2041–2050 and 2091–2100. The box plots show the uncertainty of the parameter combinations. In each case the first 20 box plots are the results of the CGCM3 model, the following 20 box plots were simulated with the CM2.1 climate model. The first 10 box plots of each GCM were simulated under the assumption of the A2 scenario, the following 10 box plots under the assumption of the B1 scenario.

In table 8.2 there are the results of the calculated mean values of discharge for the two different decades. In the second column the variance is calculated as consequence of the uncertainty in the used parameter sets, in the third column the variance results out of the uncertainty in the input data.

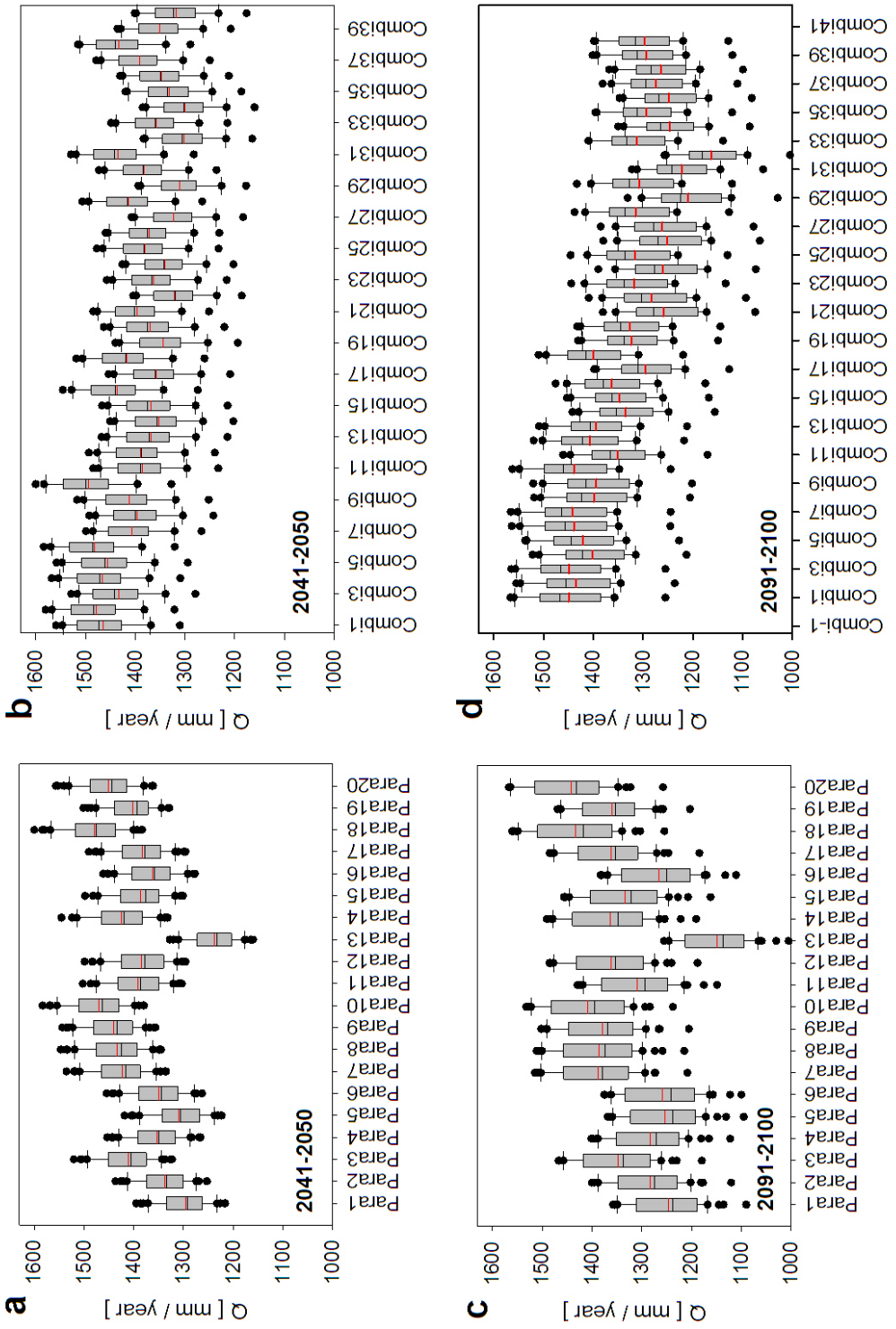

Figure 8.15: a+c: Uncertainty of discharge as a consequence of parameter combinations for the decades 2041–2050 and 2091–2100. The box plots show the uncertainty of the input combinations. b+d: Uncertainty of discharge as a consequence of input combinations for the decades 2041–2050 and 2091–2100. The box plots show the uncertainty of the parameter combinations.

Table 8.2: Analysis of the uncertainty in discharge in the Canoe catchment.

Decade	Uncertainty due to parameters	Uncertainty due to input
2041-2050	1386 ± 59 m^3/s	1386 ± 51 m^3/s
2091-2100	1330 ± 71 m^3/s	1330 ± 74 m^3/s

Comparing the variances in table 8.2, in the middle of the century there is a higher variance due to the different parameter sets while at the end of the century the different input data combinations have a slightly greater influence on the uncertainty of discharge than the parameter sets.

The uncertainty increases with time indicated by a coefficient of variation which increases from 4.3 and 3.7 % during the period 2041-2050 to 5.4 % and 5.6 % during the period 2091-2100 considering the variabilty due to parameters and due to the input combinations.

There is an increasing difference with time comparing the mean discharge values of the CGCM3 model with the ones of the CM2.1 model: During the decade 2041–2050 the mean value of the CGCM3 model is 1414 ± 46 m^3/s, the one of the CM2.1 model is 1358 $\pm$ 40 m^3/s. The mean difference is 56 m^3/s. During the decade 2091–2100 however, the difference is about 120 m^3/s, resulting from a mean discharge value of the CGCM3 model of 1391 ± 46 m^3/s and a mean discharge value of the CM2.1 model of 1270 ± 39 m^3/s. The CGCM3 model simulates in both decades higher discharge values. The resulting coefficient of variation indicates a slightly higher uncertainty with time and comparing the two models a slightly higher uncertainty of the CGCM3 model.

Comparing the two different scenarios, in the decade 2041–2050 there is a bigger difference in the mean discharge values using the CGCM3 model (70 m^3/s) than in the CM2.1 model (4 m^3/s). In the decade 2091–2100 the difference increases slightly in the CGCM3 model (72 m^3/s); using the CM2.1 model there is a high increase from 4 to 17 m^3/s in the difference between the A2 and B1 scenario. There are always higher discharge values for the A2 scenario.

Illecillewaet catchment

Like in the Canoe catchment there is a high uncertainty in simulated discharge in the Illecillewaet catchment e.g. during the decade 2091–2100 (see figure 8.16). The red line illustrates the median, the green lines the 5 % and 95 % quantile of the 800 simulations, a result of the 2 different Global Climate Models, the 10 different downscaling results, the 2 different scenarios and the 20 different parameter sets. The biggest interquantil range is in July (71.9 m^3/s), the smallest in February (8.0 m^3/s). The interquantile range increases with increasing discharge, reaches a particular high value in July, and decreases afterwards.

Figure 8.17 illustrates the results of an analysis about the sources of the uncertainty in discharge. Figure a and c show the uncertainty of discharge due to parameter combinations for the decades 2041–2050 and 2091–2100. The box plots result from the uncertainty of the input combinations due to different Global Climate Models, downscaling results and scenarios. Figure b and d show the uncertainty of discharge due to input variations

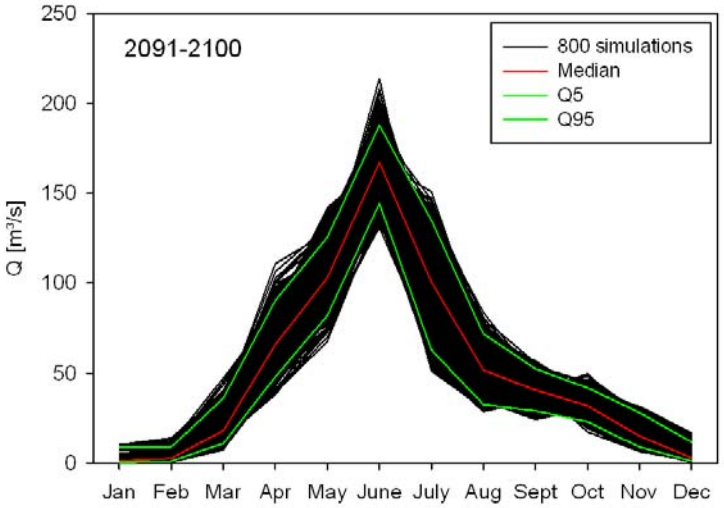

Figure 8.16: Simulated discharge in the Illecillewaet catchment for 2091–2100.

for the decades 2041–2050 and 2091–2100. The box plots show the uncertainty of the parameter combinations. The first 20 box plots were calculated with the CGCM3 model while the other 20 box plots are simulation results from the CM2.1 model. At each model the first 10 box plots are based on the A2 scenario and then there are 10 box plots assuming the B1 scenario.

In table 8.3 the mean discharge values and their variance are listed for the time period 2041–2050 and 2091–2100, respectively. The variances result either from the different parameter sets (second column) or from the different input combinations (third column).

Table 8.3: Analysis of the uncertainty in discharge in the Illecillewaet catchment.

Decade	Uncertainty due to parameters	Uncertainty due to input
2041-2050	1451 ± 51 m^3/s	1451 ± 64 m^3/s
2091-2100	1454 ± 58 m^3/s	1454 ± 75 m^3/s

In the Illecillewaet catchment the variance of the mean discharge values, which are based on different input combinations, are for both time periods higher than the variances, which are based on different parameter sets.

As in the Canoe catchment the coefficient of variation increases during time in the Illecillewaet. It increases from 3.5 % and 4.4 % in the period 2041-2050 to 4.0 % and 5.2 % in the period 2091-2100 considering the variablity due to parameters and due to the input.

Comparing the two different global climate models the difference of simulated discharge increases with time. During the period 2041–2050 the CGCM3 model simulates a mean discharge of 1501 ± 33 m^3/s whereas the CM2.1 model predicts only 1401 ± 45 m^3/s. The mean difference is 100 m^3/s. During the period 2091–2100 the difference increases to 128 m^3/s. The simulated mean discharge of the CGCM3 model is 1518 ± 32 m^3/s, the one of the CM2.1 model is 1390 ± 46 m^3/s. The CGCM3 model simulates

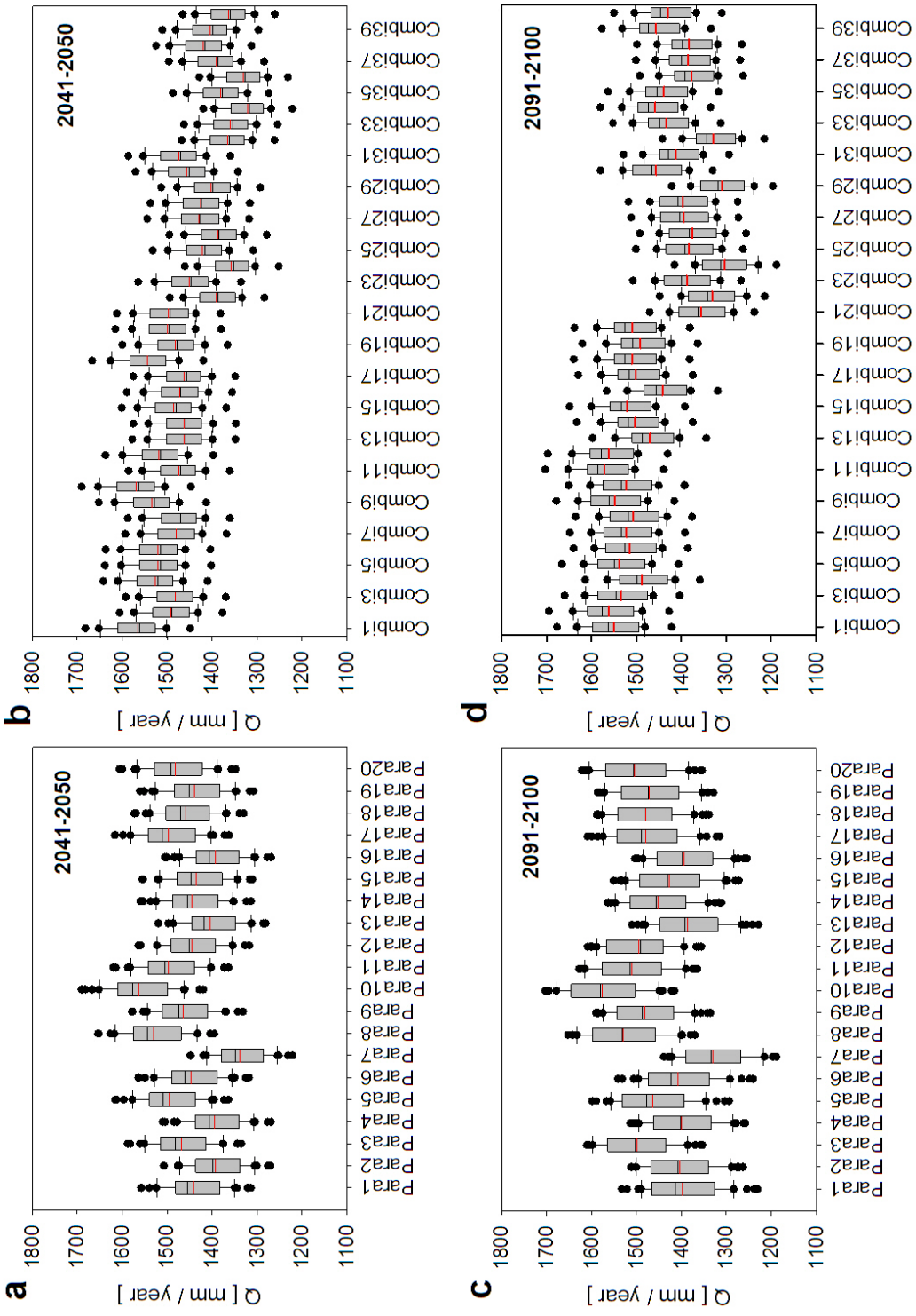

Figure 8.17: a+c: Uncertainty of discharge as parameter combinations for the decades 2041–2050 and 2091–2100. The box plots show the uncertainty of the input combinations. b+d: Uncertainty of discharge as a consequence of input combinations for the decades 2041–2050 and 2091–2100. The box plots show the uncertainty of the parameter combinations.

higher discharge values in both time periods. The coefficient of variance indicates a slight increase in uncertainty over time using the CM2.1 model, but a slight decrease in uncertainty over time for the CGCM3 model. Comparing the coefficient of variance between the two models in both periods there is a higher uncertainty at the CM2.1 model than at the CGCM3 model.

Examining the differences between the A2 and B1 scenario for the period 2041–2050 the simulated discharge differs in 31 m^3/s using the CGCM3 model and in 41 m^3/s using the CM2.1 model. During the period 2091–2100 there is a smaller difference (21 m^3/s) between the scenarios using the CGCM3 model than during the period 2041–2050. For all three cases the model simulates higher discharge values using the A2 scenario than using the B1 scenario. In contrast, the CM2.1 model simulates smaller discharge values using the A2 scenario than using the B1 scenario during the period 2091–2100. The difference between the two scenarios stays constant with a value of 41 m^3/s.

8.4.2 Future discharge

Canoe catchment

Figure 8.18 shows the development of simulated total discharge and discharge resulting from icemelt over time. The hydrographs illustrate mean values of the 800 simulations to show the mean tendency in discharge.

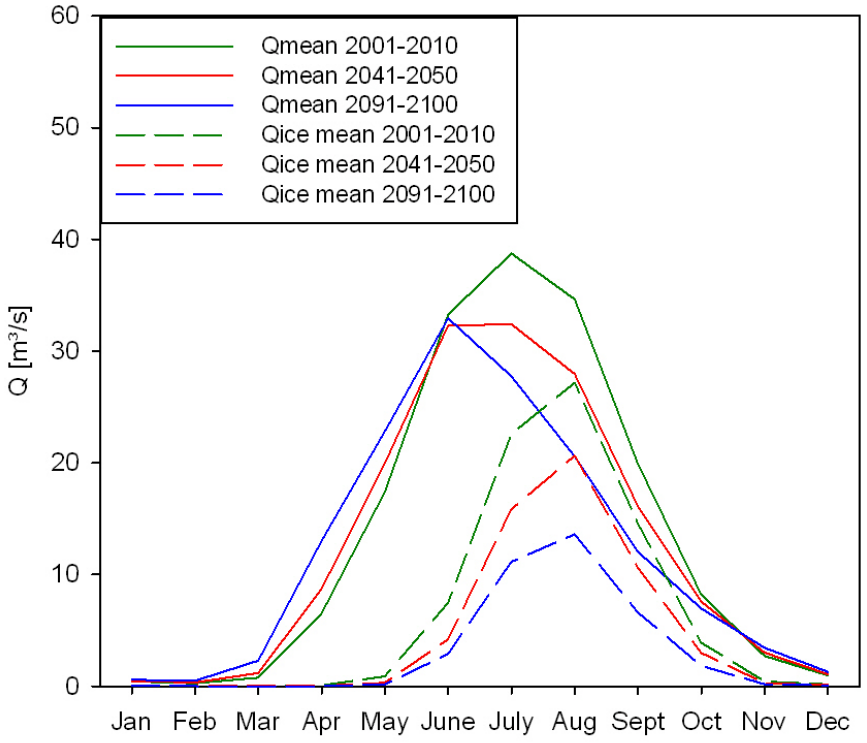

Figure 8.18: Development of simulated total discharge and discharge resulting from icemelt over time in the Canoe catchment.

As can be seen in the figure the discharge resulting from icemelt decreases over time. During the period 2001–2010 there are about 670 mm/a icemelt. This value decreases to about 480 mm/a during the period 2041–2010 and finally to about 320 mm/a during the period 2091–2100. This means that there is a decrease of icemelt volume of about 53 % during the periods 2001-2010 and 2091-2100. The discharge peak of the icemelt occurs in the month August in the three considered decades.

Analyzing the hypsographs of total discharge, there is also a decrease in volume over the years. During the period 2001–2010 the reduction is about 1390 mm/a, during the period 2041-2050 1280 mm/a and during the period 2091-2100 about 1220 mm/a. This signifies a reduction of about 13 % between the period 2001–2010 and the period 2091-2100. The shift of the peak discharge is clearly visible. During the period 2001–2010 there is a pronounced peak in July. During the period 2041–2050 there is rather a plateau during the high flow month June and July. During the period 2091–2100 there is again a pronounced peak, but in the month June. Also the shifting of the discharge volume is clearly visible: There is a decrease in discharge during the month June to October, whereas there is an increase in discharge volume from March until June.

In the appendix there is an illustration of the development of the input data over time (see figure A.4). Summarized there are the following tendencies between the input data during the period 2001-2010 and the period 2091-2100:

There is less rainfall during the summer months, especially during the months June till September. In contrast, there is more snowfall in winter time, especially between November and April. Comparing the snowfall there is a decrease over time, rather uniformly distributed over the year. Altogether, there is a decrease in precipitation. Only during the months March to May there are no big changes.

Analyzing the development of temperature over time, there is a continuous increase. During the period 2001–2010 the mean air temperature is predicted to be 3.5 ± 0.3 °C. Until the period 2091–2100 the mean air temperature increases to 5.3 ± 0.7 °C. The Global Climate Model CGCM3 predicts in general about 0.2 °C higher air temperature values than the CM2.1 model.

As already shown, the simulation of discharge in future is highly variable. An example of the uncertainty of total discharge and discharge resulting from icemelt over time for the decades 2041–2050 and 2091–2100 is illustrated in figure 8.19. For each decade a parameter and input combination has been chosen which is expected – resulting from the figure 8.15 – to simulate a minimum and a maximum discharge. The settings can be seen in table 8.4.

Taking the total discharge of the period 2041–2050 into consideration, there is a difference of 390 mm/a between the minimum and maximum hydrograph. There is no coincident peak: Whereas the peak at the mimimum hydrograph is in July, the peak is at the maximum hydrograph already in June. During the decade 2091–2100 there is a difference of about 510 mm/a between the minimum and maximum hydrograph. Both hydrographs have their peaks in June, but there is a difference of more than 11 m^3/s concerning the value of the peak. Comparing the two periods, the difference between the annual discharge of the minimum and maximum hydrographs increases over time whilst the total volume decreases.

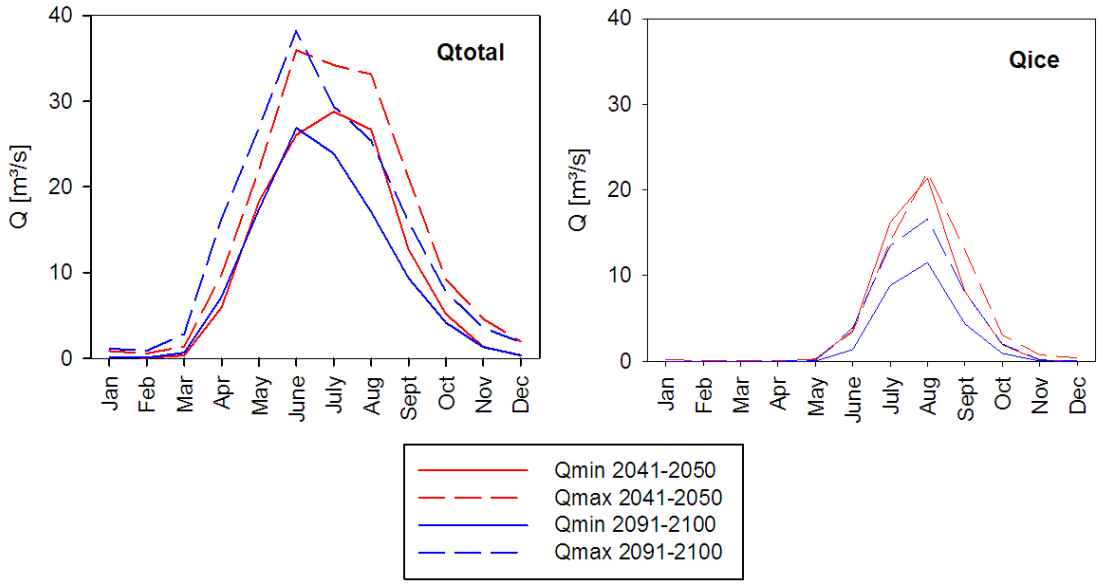

Figure 8.19: Example of uncertainty of simulated total discharge (left) and discharge resulting from icemelt (right) over time in the Canoe catchment.

Examining the minimum and maximum icemelt hydrographs of the decade 2041–2050, there is only a difference of 42 mm/a. The hydrographs differ only in September, during the other months the two graphs are very similar. In contrast, the minimum and maximum hydrographs of the decade 2091–2100 differ highly. There is a difference of about 148 mm/a. The difference between the minimum and maximum hydrograph increases over time considering discharge from icemelt. On the same time the volume of discharge decreases.

Altogether, the hydrographs show a high uncertainty in discharge. While the icemelt hydrographs show a higher uncertainty at the end of the century, there is no visible tendency in the total discharge hydrographs.

As the uncertainty in the input data plays an important part in the uncertainty of the simulated discharge as already discussed above the rainfall and snowfall data of the four different hydrographs are shown in the appendix (see appendix A.5). The uncertainty in rainfall is remarkable, especially in summer time during the period 2041–2050. During winter time between October and March the uncertainty in snowfall is for both decades

Table 8.4: Settings for the expected minimum and maximum discharge during the periods 2041-2050 and 2091-2100 in the Canoe catchment.

Decade	Global Climate Model	Scenario	Member	Parameterset
MIN 2041-2050	CM2.1	B1	4	13
MAX 2041-2050	CGCM3	A2	10	18
MIN 2091-2100	CM2.1	B1	2	13
MAX 2091-2100	CGCM3	A2	1	20

enormous

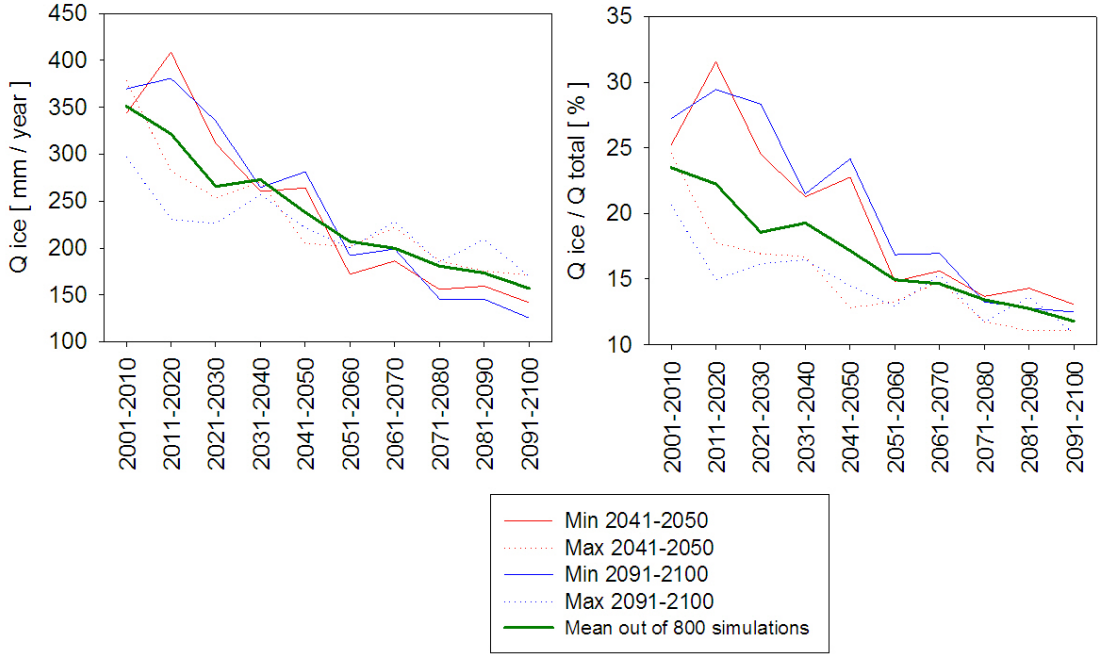

Figure 8.20: Development of icemelt and of the relation between icemelt and total runoff over time in the Canoe catchment.

The development of the discharge consisting of icemelt is illustrated in figure 8.20 on the left side. On the right side in figure 8.20 the relation of icemelt discharge to total discharge is illustrated. In each case the green line shows the mean values out of all 800 simulations resulting from different GCMs, downscaling results, scenarios and parameter sets used. The blue and red lines are four examples with parameter and input combinations which are expected to simulate a minimum or a maximum total discharge during the period 2041–2050 or 2091–2100, respectively.

The mean values of the icemelt show first a high decrease in icemelt and beyond 2050 a smaller decrease. The years around 2030 are an exception; there is a slight increase in icemelt. The four other time series illustrate that depending on the chosen parameter set and input combination the predicted icemelt can differ up to 91 mm/a. Parameter and input combinations, which simulate rather a smaller icemelt than the mean at the beginning of the century, simulate rather more icemelt than the mean beyond 2050 and vice versa. Showing a high uncertainty from decade to decade all four time series predict a decrease of icemelt over the decades.

The mean values of the relation between icemelt and total runoff show a similar pattern as the one of the icemelt. The percentage of icemelt on total runoff decreases at average from about 23 % to 12 % over the 21th century. The four other time series show a high variabilty from decade to decade and differ up to almost 10 % from the mean values. This time the solid lines show rather a higher percentage of icemelt over the whole 100 years, while the dotted lines show rather a smaller percentage. In summary, all four time series

predict a decrease of the percentage of icemelt on total runoff over the decades.

Illecillewaet catchment

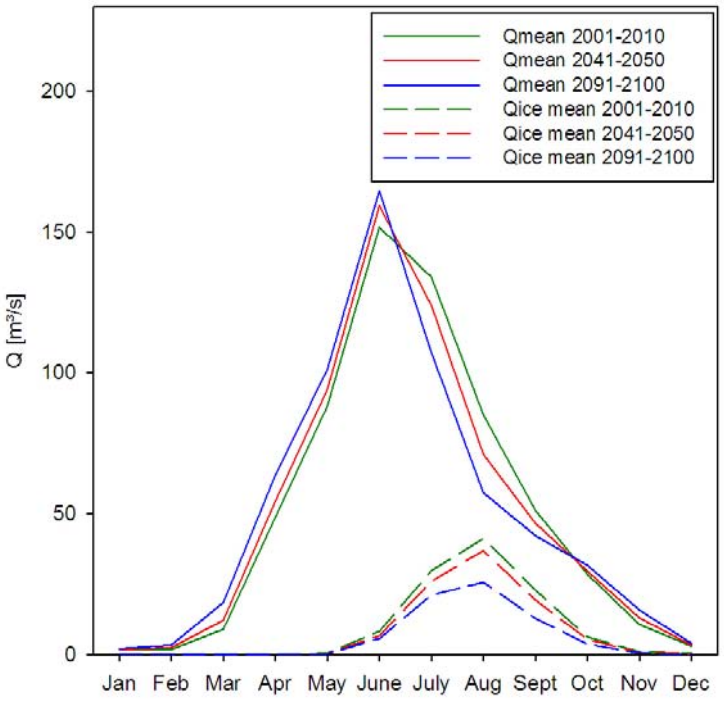

Figure 8.21: Development of simulated total discharge and discharge resulting from icemelt over time in the Illecillewaet catchment.

Figure 8.21 illustrates the simulated future total discharge and the discharge resulted from icemelt in the Illecillewaet catchment. The hypsographs show the mean values of the 800 simulations to identify the principal tendencies over the time.

Analyzing the icemelt there is a decrease over the years. During the decade 2001–2010 the volume of icemelt is about 251 mm/a; it decreases slightly to 218 mm/a during the decade 2041–2050 and finally to 159 mm/a during the decade 2091–2100. Between the period 2001-2010 and 2091-2100 there is a reduction of icemelt of almost 37 %. The peak of all hypsographs occurs in August.

The hypsographs of the total discharge show rather a shift to an earlier rising and declining of the graph than a reduction. During the decade 2001–2010 the total discharge is 1385 mm/a, during the decade 2041–2040 it is 1375 mm/a and during the decade 2091–2100 it is 1367 mm/a. The reduction between the first and the last decade of the century is not much more than 1 %. In the Illecillewaet catchment the tendency to earlier high discharge values is visible. The peak discharge remains in June; its value increases by about 9 % during the century. During July to October there is a decreasing streamflow over the decades.

Concerning future climate in the appendix there is a graphic illustrating the changes

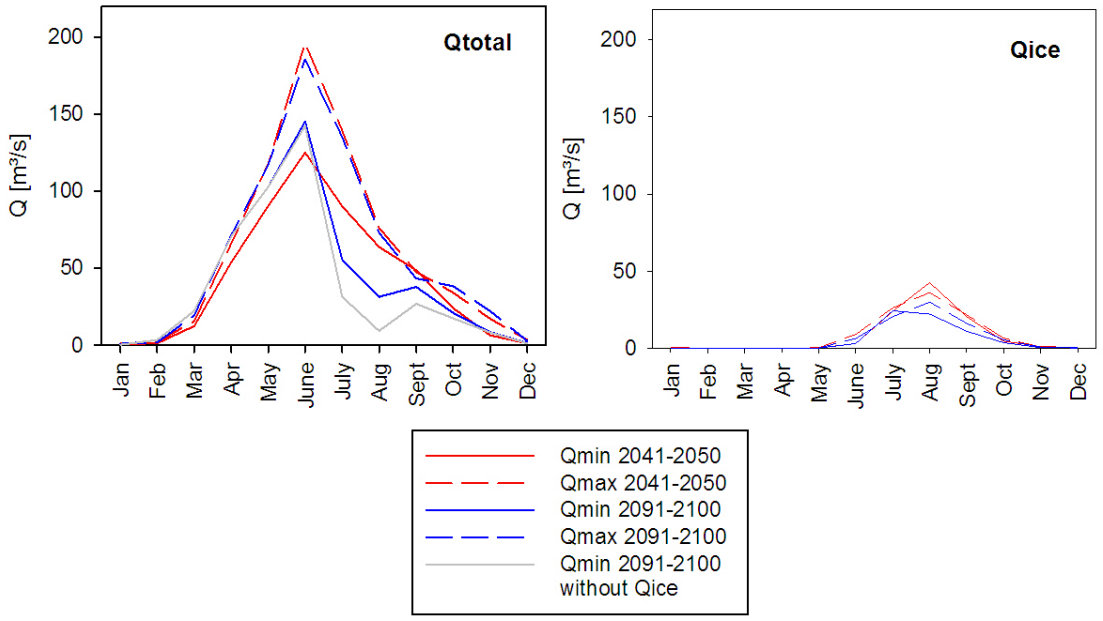

Figure 8.22: Example of uncertainty of simulated total discharge (left) and discharge resulting from icemelt (right) over time in the Illecillewaet catchment.

of rainfall, snowfall, and the resulting total precipitation over the decades (see fig A.6). Summarized the following changes are predicted:

Between the decades 2001–2010 and 2041–2050 there is a decrease in precipitation from June to August. The rainfall during the rest of the year is quite similar: There is only a little bit more rainfall in the winter months in the decade 2041–2050. Comparing the rainfall values of the decade 2041–2050 with the corresponding values of the decade 2091-2100, there is much less precipitation in summer time. Especially in July and August there is a high decrease in rainfall. In September there is a high increase of precipitation. During the other months in fall, as well as during the whole winter months until May there is more rain falling at the end of the century than during the decades before.

Analyzing the snowfall changes there is a more homogeneous pattern. Between 2001–2010 and 2041–2050 there is a higher decrease of snowfall during the whole year than the decrease between 2041–2050 and 2091–2100. The greatest reduction over the decades takes place during the winter months.

The air temperature is predicted to increase over the decades from 2.6 $\pm$ 0.3 °C during the period 2001–2010 to 4.3 $\pm$ 0.7 °C during the period 2091–2100. The CGCM3 model simulates at an average about 0.3 °C higher values than the CM2.1 model.

As shown above the uncertainty of discharge simulation is high. Figure 8.22 shows the hypsographs of total discharge on the left and of icemelt on the right side. There are two hypsographs for the decade 2041–2050 and two hypsographs for the decade 2091–2100 in each figure: One is based on a parameter set and an input combination, which are expected to produce a minimum discharge, the other one is based on a parameter set and an input combination, which are expected to produce a maximum discharge. The assumption about minimum and maximum discharge values are from figure 8.17. The

used settings are listed in table 8.5.

Comparing the hydrographs of total discharge for the period 2041–2050 there is a difference of 430 mm/a between the annual discharge of the minimum and maximum hypsograph. The greatest differences are in the high flow months between April and August. The difference between the minimum and maximum graph during the period 2091–2050 is a little bit higher with an annual discharge value of about 450 mm/a. The greatest difference is between the June and September. It is conspicuous that there is a high decrease at the minimum discharge graph in July and August. The gray graph illustrates the same graph without icemelt. Further the two maximum hydrographs are very similar; no shifting during the time is visible. The peak discharge occurs in all four graphs in the month June.

Analyzing the graphs illustrating icemelt, the minimum and maximum hydrographs of the decade 2041–2050 are very similar. The difference in annual discharge is only 9 mm/a. Just the peak of the minimum graph has a higher value than the peak of the maximum graph. The graphs of the period 2091–2100 shows that the peak of the minimum graph is in July whereas the peak of the maximum graph is in August. The two graphs differ by about 31 mm/a.

Altogether, the hydrographs show a high uncertainty in discharge. While the icemelt hydrographs show a higher uncertainty at the end of the century, there is no tendency visible in the total discharge hydrographs.

The rainfall and snowfall data of the four different hydrographs are shown in the appendix (see appendix A.7). In the rainfall curves there is a high uncertainty in summer between May and September for the decade 2041–2050 as well as for the decade 2091–2100. The difference in snowfall for the minimum and maximum settings are biggest during the winter months, especially in December.

Figure 8.23 illustrates the development of icemelt over time on the left side and the development of the relation between icemelt and total runoff over time on the right side. The green line shows the mean values of the 800 simulations, which are based on different parameter sets and different input combinations.

The mean icemelt time series show a slight decrease from about 95 mm/a to about 74 mm/a. Around the year 2010 and 2030 there are two periods of increasing icemelt predicted. The four other time series show a high uncertainty from decade to decade and differ considerable from the mean values in certain periods. There is one time series, which predicts more icemelt at the end of the century than at the beginning (blue dotted

Table 8.5: Settings for the expected minimum and maximum discharge during the periods 2041-2050 and 2091-2100 in the Illecillewaet catchment.

Decade	Global Climate Model	Scenario	Member	Parameterset
MIN 2041-2050	CM2.1	B1	4	7
MAX 2041-2050	CGCM3	A2	10	10
MIN 2091-2100	CM2.1	A2	4	7
MAX 2091-2100	CGCM3	B1	1	10

Figure 8.23: Development of icemelt and of the relation between icemelt and total runoff over time in the Illecillewaet catchment.

line), there is one time series which predicts rather an equal icemelt (red dotted line) and two time series predict a decrease in icemelt (red and blue solid lines).

The time series of the relationship between icemelt and total runoff show a very similar pattern to the time series of icemelt. The mean percentage decreases from 6.5 % at the beginning of the century to 5.1 % at the end of the century. While the red dotted line predicts rather an equal icemelt over the years, the other time series predict a decrease comparing the percentage of the beginning of the century with the one at the end of the century. However, the time series are highly variably and show partially a big difference to the mean values.

8.4.3 Future glacier area

Canoe catchment

Figure 8.24 shows the development of the glacier area in the Canoe catchment. The development is shown as a percentage of the area existing in the year 2000. The red line illustrates the median value, the green lines the 5 % and the 95 % quantile, respectively.

It is clearly visible that a decrease of glacier area with time is expected. But there is also a high uncertainty concerning the amount of decrease. This uncertainty increases with time. At the year 2100 the median indicates that 40 % of the glacier area of the year 2000 are left. The 95 % quantile predicts that 55 % are left, in contrast to the 5 % quantile, which predicts that only 25 % of the former area are left. There is a difference between the quantiles of 30 %, which equals an area of about 23 km^2.

The mean volume reduction over the century is 0.053 *pm* 0.010 km^3/a, the mean thinning rate over the century is 0.68 *pm* 0.14 m/a. The model calculated a mean equilibrium

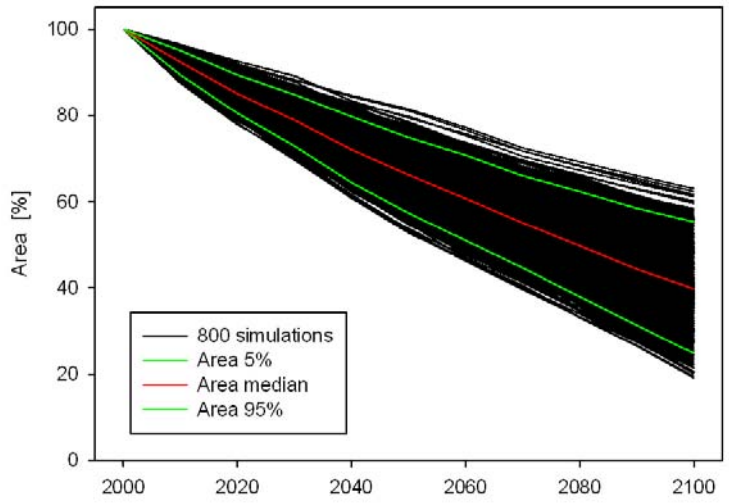

Figure 8.24: Development of glacier area in the Canoe catchment.

line for the year 2100 at an elevation of 2952 $\pm$ 120 m.a.s.l.

A randomly chosen example of the landuse change between 2010 and 2100 in the Canoe catchment is illustrated on the title page. Glaciers are painted in blue, open areas in brown and forest in green.

Illecillewaet catchment

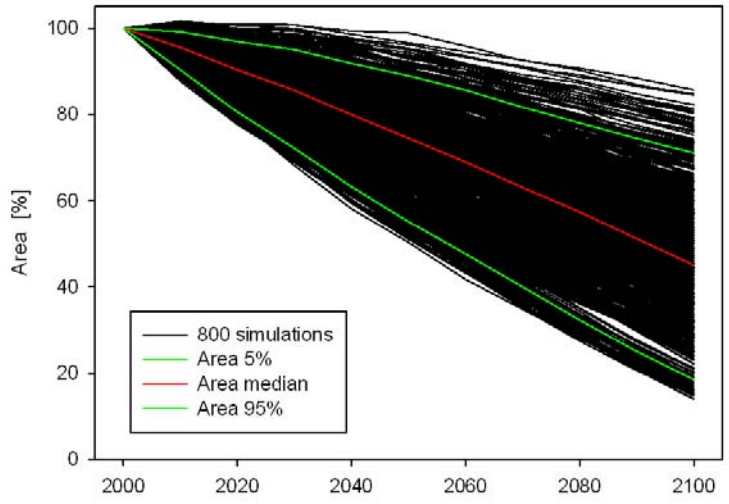

Figure 8.25: Development of glacier area in the Illecillewaet catchment.

Figure 8.25 illustrates the development of the glacier area in the Illecillewaet catchment. Based on different parameter sets and input combinations there are 800 different devel-

opments, which are shown. The red line shows the median, the green lines the 5 % and the 95 % quantile. The values indicate the remaining percentage of the area compared to the area existing in the year 2000.

The figure shows that the glacier area decreases in most cases with time. Only at the beginning of the century there are some simulations, which show an increase in the glacierized area. In the year 2100 the median indicates that about 45 % of the initial area is left. The 5 % quantile indicates that about 19 % of the glacierized area of 2000 is left; the 95 % quantil predicts an remaining glacierized area of about 71 %. The difference between the quantiles increases with time; in the year 2100 they differ in 52 %, which equals an area of about 57 km^2.

The mean volume reduction in the Illecillewaet catchment is 0.074 ± 0.028 km^3/a; the mean thinning rate over the century is 0.68 ± 0.26 m/a. The HBV-EC model predicted the equilibrium line of the year 2100 at an elevation of 2787 ± 130 m.a.s.l.

On the title page a randomly chosen example of the landuse change between 2010 and 2100 in the Illecillewaet catchment is illustrated. Glaciers are painted in blue, open areas in brown and forest in green.

8.4.4 Comparison of the catchments

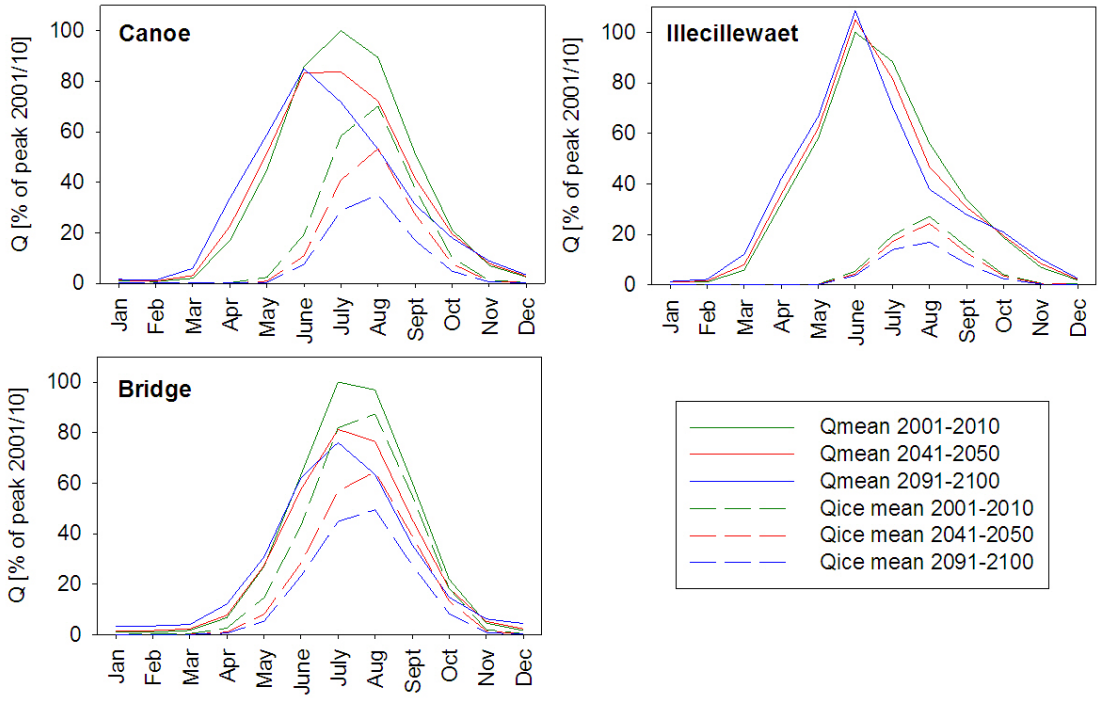

Figure 8.26: Comparison of the development of the total discharge and the icemelt over the time in the three considered catchments.

Figure 8.26 illustrates the total discharge and the discharge resulting from icemelt of the Canoe, the Illecillewaet and the Bridge catchment during the three different time periods. To compare the development of discharge, in each illustration the discharge values are

calculated as a percentage of the peak flow value during the period 2001–2010.

The hypsograph of the Bridge catchment is characterized by its high percentage of iceflow on the total discharge. In the Illecillewaet catchment only a small percentage of total discharge results from icemelt. In the Canoe catchment a big part of the total discharge results from icemelt, but not as much as in the Bridge catchment.

Comparing the regimes the hypsograph of the Bridge catchment shows a glacial regime with the peak in July at all periods, whereas the hypsograph of the Illecillewaet catchment can be classified as a nival regime with the peak in June. In the Canoe catchment there is a visible change in the regime: At the beginning of the century the peak is in July whereas at the end of the century it is in June; the glacial regime is expected to change into a nival regime.

Comparing the shift of discharge there is only a little shift visible in the Illecillewaet catchment. The peak discharge increases with time. In contrast, there is a big shift in the Canoe catchment with more discharge in spring and less discharge during summer and fall. The peak decreases. In the Bridge catchment the peak discharge decreases highly and there is less discharge in summer and in fall. However, the discharge in spring does not increase much over the time. In all three catchment the amount of discharge resulting from icemelt decreases over time.

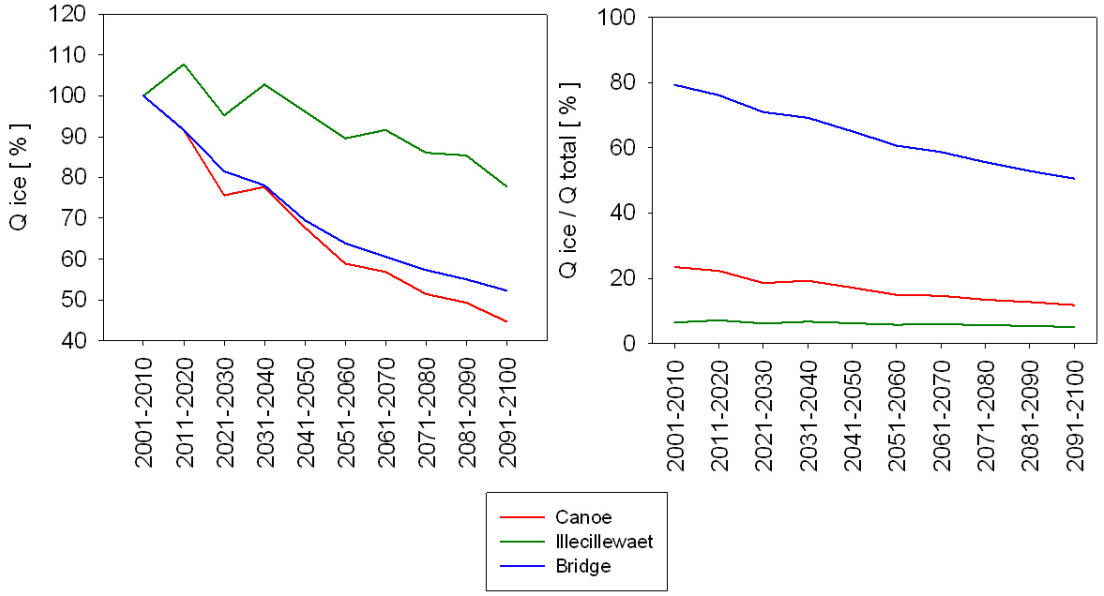

Figure 8.27: Comparison of the development of the icemelt and the relation of icemelt to total discharge over the time in the three considered catchments.

The decrease of icemelt can also be seen in figure 8.27 on the left side. The icemelt values indicate the percentage of icemelt related to the icemelt of the period 2001–2010.

The highest decrease in discharge resulting from icemelt between the period 2001–2010 and the period 2091–2100 is in the Canoe catchment; the lowest decrease in the Illecillewaet catchment. While the icemelt decreases constantly in the Bridge catchment,

there is one increase in the Canoe catchment. In the Illecillewaet catchment there are some up-and-downs in the time series visible.

On the right side of figure 8.27 the development of the relation between icemelt and total runoff over the time is illustrated.

Comparing the three catchments the highest percentage of icemelt on the total discharge is in the Bridge catchment. There is already an obvious smaller percentage in the Canoe catchment and the smallest percentage is in the Illecillewaet catchment.

Considering the temporal development there is a constant decrease from about 79 % to 51 % during the 21th century in the Bridge catchment. In the Canoe catchment there is also a decrease, but not as much as in the Bridge catchment (about 11 % during 100 years). Additionally, beyond the middle of the century there is a smaller decrease observable. In the Illecillewaet catchment there is a rather constant percentage of icemelt on total discharge during the whole century; during the 21th century the pecentage decreases by only 1 %.

Chapter 9

Discussion

9.1 Parameter sensitivity

As hydrologic models are in general non-linear systems, it is difficult to predict their behavior (TANG ET AL., 2007). UHLENBROOK ET AL. (1999) realized that it is in advance difficult to know which parameters are sensitive.

The following parameters were sensitive in studies, where the HBV model was applied: SFCF (HARLIN and KUNG, 1992), TT (UHLENBROOK ET AL., 1999; SEIBERT, 1997), FC (SEIBERT, 1997), KF (HARLIN and KUNG, 1992) and KS (HARLIN and KUNG, 1992).

As there have been different calibration schemes and in each case a different definitions of parameter sensitivity, no direct comparison between these results and the results of this thesis could be done. There was a tendency that the climate parameters as well as the runoff parameters are rather sensitive whereas forest, soil and glacier parameters were rather insensitive. The snow parameters did not show a tendency. Counterexamples for this hypothesis existed: TT e.g. was an insensitive parameter in the study of HARLIN and KUNG (1992), whereas this parameter was sensitive in the Canoe and Illecillewaet catchment and in the studies of UHLENBROOK ET AL. (1999) and SEIBERT (1997).

One could assume that the number of sensitive parameters decreases with an increasing size of the catchment. The Illecillewaet catchment has an area of about 1150 km^2 and four sensitive parameters, whereas the Canoe catchment has an area of about 300 km^2 and nine (very) sensitive parameters. However, SEIBERT ET AL. (2000) showed that the number of sensitive parameters of the HBV model does not depend on the catchment size and concluded that the variations come from other catchment characteristics. SEIBERT (1999) found for six parameters a relationship between the value of the parameters and some catchment characteristics as for example the percentage of forest or lake in a catchment. These relationships were not be confirmed in this thesis.

9.2 Calibration and validation

RANGO (1992) compared conceptual models and concluded a mean efficiency of 0.8 for the considered glacierized catchments.

With an efficiency between 0.83 and 0.87 at the Canoe catchment and between 0.80 and 0.84 at the Illecillewaet catchment during the calibration period the discharge of these catchments was consequently well simulated. During the validation period there was a slightly worse simulation. The efficiency at the Canoe catchment was between 0.79 and 0.85, the one at the Illecillewaet catchment between 0.77 and 0.85. The reason for the slightly decreased efficiency values of the validation period resulted perhaps from the assumed landuse of the mid 1990s. The validation period extended between 1976 and 1984 where a different landuse prevailed. Discharge simulation in snow- and glacierfed catch-

ments in other studies resulted often in an efficiency between 0.8 and 0.9 (e.g. BRAUN and AELLEN, 1990). HAGG ET AL. (2006) advised to be cautious to compare efficiencies, because they are heavily influenced by the variability of discharge. Also STAHL ET AL. (2008) noted that the efficiency is not an adequate objective function for catchments with a seasonal hydrograph and proposed to use benchmark efficiencies. Besides the study of SCHAEFLI and GUPTA (2007) no other study could be found to compare the calculated benchmark efficiencies. The benchmark efficiencies in this thesis decreased as in the study of SCHAEFLI and GUPTA (2007) in comparison with the commonly used efficiency. Due to the high uncertainty in the values a direct comparison of the values is difficult.

The dynamic of discharge considering the dynamic between the months as well as the dynamic between the years was in most cases well simulated. There are different possible reasons why the simulated discharge values did not always agree with the observed ones:

- **Insufficient measurement station coverage**: As there are strong climate gradients in the considered mountainous catchments, not enough climate stations exist to define the lapse rates of air temperature and precipitation adequately. Especially in the higher elevation zones, there is a lack of climate stations.

  Besides discharge data there are sometimes no other measurement data available for calibration and validation. In the Canoe catchment e.g. the HBV-EC model was calibrated with snow pillow and snow course measurements of neighboring catchments. Mass balance data were neither in the Canoe nor in the Illecillewaet catchment available.

- **Fall-winter storms**: It is possible that fall-winter storms causing heavy rainfalls are incorrectly simulated. As a consequence of a fixed lapse rate rainfall is miss interpreted as snowfall, especially if the climate station is situated in the valley. Discharge in winter time is consequently underestimated, discharge in the snow melt season of the following year overestimated (MOORE, 1993). This could be a reason for the underestimation of winter flow in the Canoe as well as in the Illecillewaet catchment.

- **Incorrectly discharge measurements in winter time**: As in winter time there is often a freezing of water, the discharge measurements are not credible. As a consequence of the greater volume of ice a higher river stage is observed and more discharge is calculated via the stage-runoff-relationship. In reality there is a decrease of discharge (MOORE ET AL., 2002; HAMILTON and MOORE, 1996; PROWSE, 1994). Another measurement problem is ice on the sensors, if they are not heated adequately or ice which damages sensors (e.g. HAMILTON ET AL., 2000).

- **Underprediction in spring**: The degree-day approach can not simulate an earlier melting at south facing slopes compared to north facing slopes. At south facing slopes snow and ice can melt even at subfreezing air temperatures (HAMILTON ET AL., 2000).

- **No inversions**: In winter time inversions are possible in the considered catchments KLOCK and MULLOCK (2001). However, inversions can not be simulated without

time varying lapse rates and without enough climate stations at higher elevation bands (BOON ET AL., 2009).

- **Constant lapse rates**: The HBV-EC model uses constant lapse rates. STAHL ET AL. (2006) showed that air temperature lapse rates are high variable during the year.
- **Linearity of QF**: In this thesis a linear outflow of the fast outflow was assumed. LINDSTRÖM ET AL. (1997) showed that an exponential outflow seems to be closer to reality. Changing the fast outflow equation can perhaps improve the simulations.
- **No routing delay**: No parameter was used to convert outflow into discharge. In small catchments with steep slopes like the Canoe catchment the delay between outflow and discharge is short and so there is no need for a delay parameter see also (SCHAEFLI ET AL., 2005). At larger catchments like the Illecillewaet catchment a delay parameter could be introduced. As no shift in the discharge data can be seen in the Illecillewaet catchment, the introduction of a delay parameter would perhaps not improve the simulation. Additionally, HUSS ET AL. (2008) confirmed a quick response of discharge in glacierized catchments as there are in general shallow soils, sparse vegetation and a low retention capacity of the prevailing ice and rock.

The use of snow data for calibration meant to calibrate with a highly variable value. JONSDOTTIR ET AL. (2006) emphasized the non-linear dynamics concerning snow. This could be the reason for a Mean Error up to 728 mm in the Canoe and up to 490 mm in the Illecillewaet catchment during the calibration period considering the simulation of snow courses. Considering that the used snow course stations for the Canoe catchment are situated in the neighboring Thompson basin and downstream of the catchment, can surely also explain the high Mean Error. The assumed constant gradient for air temperature during the year could be a reason for the increasing Mean Error between April and June. STAHL ET AL. (2006) showed that there is a high variation of the gradient during the year with higher gradients during the summer months. This means that after STAHL ET AL. (2006) there are lower air temperatures in the higher elevation zones and higher air temperatures in the lower elevation zones – in comparison with the climate reference station – than assumed in this thesis. The differences are higher in summer which could explain the rather bad simulation in June in comparison with the one in April. The constant air temperature gradient could also be a reason for the rather underestimation of the snow water equivalent at the higher situated snow courses and the rather overestimation at the lower situated snow courses.

Comparing the measured snow water equivalent at the snow pillow stations with the simulated snow water equivalent in the Illecillewaet, there was a quite well simulation with a MAE range of 69–96 mm at the 2A06P station and a MAE range of 84–140 mm at the 217P station. In contrast, there was a worse simulation in the Canoe catchment resulting in a MAE range of 315–333 mm due to a shift between the measured and simulated SWE values from the third considered year on. The reason for this shift could not be found. As there was no shifting in the Illecillewaet catchment it is assumed that there is no error in the IDL-code. A shifting as a consequence of gaps in the input time series and

a poor regression can also be excluded. However, a measurement error could have been occurred. Additionally, it should be kept in mind, that the snow pillow station is situated in the neighboring Thompson catchment. That the model was often not able to simulate the peaks of the snow water equivalent adequately, could also be a consequence of an assumed constant temperature gradient over the year. For th time between March and June, the time of the highest snow accumulation, STAHL ET AL. (2006) assumed a higher gradient for air temperature than the one used for this thesis. Consequently, in this thesis there are higher air temperature values in the higher elevation zones and there the snow accumulation is underestimated.

The snow line data should be interpreted with caution as there are high uncertainties in simulation as well as in measurement. As the snow line value in the Illecillewaet catchment is a mean value for its whole valley, this value is more representative for the catchment than the snow line value in the Canoe catchment. The used snow line values for the Canoe catchment resulted from flights along the Columbia River in the proximity of the Canoe catchment.

In general the following problems concerning model calibration have to be considered (UHLENBROOK ET AL., 1999; HARLIN, 1991; PERRIN ET AL., 2001):

- **Overparameterization**: With 30 parameters which have to be calibrated the HBV-EC model has more parameters than many other conceptual models e.g. the GSM-SOCONT model used by SCHAEFLI ET AL. (2005). To find the best parameter sets by a Monte-Carlo simulation more than 2^{30} simulation runs should be done assuming only two possible values of each parameter. As the range of each parameter allows more values even more simulation runs should be done. 2500 runs are not enough to find the best parameter combinations.

- **Interdependence**: Often there is an interdependence between model parameters: UHLENBROOK ET AL. (1999) showed that the parameter FC is sensitive if only this parameter is varied over its range and all the other parameters are kept constant. By varying all parameters the parameter is not sensitive any more. This behavior was confirmed in this thesis; e.g. the parameters CMIN or AM behaved in a similar manner. To reduce the problem of interdependence ZHANG and LINDSTRÖM (1997) and HARLIN (1991) proposed to split the year into subperiods where only some of the parameters are relevant.

- **Local optima**: Often there are local optima on the response surface and the best parameter sets can not be found. SOROOSHIAN and GUPTA (1995) stated that it is difficult, quasi not possible to obtain an unique optimal parameter set. YAPO ET AL. (1998) confirmed that it is not possible to decide which solution is the best one: If a solution results in a good objective function 'A', an other objective function, function 'B', has a worse result. A second solution has a good objective function 'B', but a bad function 'A'. There is no 'best' solution. Parameter sets with similar good solutions are called Pareto solutions. Considering this problem the results of the 20 best parameter sets were analyzed.

- **Initial values**: Often the values of the best parameter sets depend on the initial values of storage terms. In this thesis the storage terms got the value zero at the beginning of simulation. For the discharge simulation there was one year of initialization.

- **Problem of scale**: Other data than discharge are measured at the hillslope scale and not at the catchment scale. To overcome this problem as many snow courses and snow pillows as possible should be used for calibration.

Additionally, the criterion to select the best parameter sets was relatively subjectively chosen (weights, order of considered objective functions). In many studies there is not a sequentially filtering of the best parameter sets using different objective functions as in this thesis, but one criterion which combines different objective functions (see MADSEN, 2000, GUPTA ET AL., 1998). These functions must also be weighted what has also a certain subjectivity as consequence GUPTA ET AL. (1998).

9.3 Projection into future

9.3.1 Uncertainty in the future discharge

It could be shown that there is a high uncertainty in future discharge in the Canoe catchment as well as in the Illecillewaet catchment and that this uncertainty resulted from the different parameter sets as well as from the input combinations. While in the Canoe catchment in the middle of the century the parameter sets had still a higher influence on the uncertainty than the input combinations, in the Illecillewaet catchment the influence of the input combinations was already at the middle of the century higher than the one of the parameter sets. In general there was a tendency that the uncertainty resulting from the input combinations became more important over time. This resulted from the increased uncertainty in the prediction of air temperature and precipitation with time as can be seen in MOTE ET AL. (2005). This increased uncertainty in the predicted climate variables resulted from a high uncertainty in the evolution of population, technology, emissions and CO_2 concentration (HUSS ET AL., 2008).

Analyzing the uncertainty of the input combinations the greatest uncertainty resulted from the chosen Global Climate Models. The decadal mean discharge varied highly depending on the choice of the GCM, and also the difference between the scenarios depended highly on this choice. It must kept in mind that only two different GCMs were used. To approach at the best the possible climate evolutions in future other GCMs should be used. For example four GCMs could be used which predict extreme evolutions: a hot-dry, a hot-wet, a cold-wet and a cold-dry climate (see for differences in GCMs MOTE ET AL., 2005). The CGCM3 model can be classified as a model which predicts a wet climate with a mean temperature increase; the CM2.1 model simulates a drier and a little bit colder climate than the CGCM3 model.

In most cases using the A2 scenario resulted in higher discharge. Only in the Illecillewaet catchment using the CM2.1 model the B1 scenario produced more discharge than the A2 scenario. In STAHL ET AL. (2008) the A2 scenario tended toward more discharge

in August than the B1 scenario. The prediction of the relative quantity of discharge depending on the scenario is ambiguous.

9.3.2 Future discharge

STAHL and MOORE (2006) suggested that in BC most glaciers have passed the initial phase of increased discharge. Considering the discharge of the Canoe and Illecillewaet catchment one can ask if the total discharge of the catchment has passed the initial phase of increased discharge and if the main reason for this reduction is a reduction in icemelt.

Canoe catchment

In the Canoe catchment this suggestion could be confirmed. Total discharge decreased about 13 % during the 100 years of simulation. The total reduction in discharge resulted from a high reduction during the summer months June to September and a smaller increase during spring from March to June. The main reason for the high reduction in summer discharge was the reduction in icemelt. Icemelt decreased about 53 % over the century. Additionally, the Global Climate Models predicted less precipitation during summer. The increase in spring discharge resulted from an earlier onset of snowmelt. In addition due to higher temperatures more rain fell during these months.

The ablation area decreased over time with the consequence of a decrease of icemelt. There is no or not enough increase in ablation area at higher elevation zones which could compensate the decrease in ice area at the glacier tongue. The equilibrium line was predicted at an elevation of 2952 $\pm$ 120 m.a.s.l. for the year 2100. At best the highest 3% of the catchement area are glacierized at the end of the century.

In summary the simulations predicted for the Canoe catchment a shift of discharge and a decreased quantity of discharge. Considering however the uncertainty in the simulation results an exactly prediction of water quantity was not possible.

The examples illustrated in a good way the high uncertainty in the input data. Already before the discharge generation by the model there were high uncertainties e.g. between the possible rainfall during the period 2041–2050. The differences in rainfall and snowfall were – besides the uncertainty due to different parameter sets and air temperatures – the reason for the high uncertainty in discharge.

As expected the icemelt decreased over time and also the percentage of discharge resulting from icemelt on total discharge. Again high uncertainty was visible.

Illecillewaet catchment

In the Illecillewaet catchment there was almost no reduction in discharge. The decrease of discharge in summer could be compensated by the increase in spring. The decrease resulted from the reduction in icemelt and a reduction of rainfall during the summer months. The increase resulted from increased rainfall in spring, but especially from snowmelt, which started earlier in the year because of higher air temperature.

The predicted equilibrium line for the year 2100 was predicted at an elevation of 2787 $\pm$ 130 m.a.s.l. Consequently, at best about 1 % of the catchment area was glacierized at

the end of the century. As a consequence of a smaller ablation area the icemelt decreased over the years.

In summary a shifting of discharge was visible. Considering the decreasing icemelt the statement of STAHL and MOORE (2006) was also in the Illecillewaet catchment confirmed. However, there is no reduction of total discharge as a consequence of the reduction in icemelt, because there is only a glaciation of about 10 % in the catchment. Processes like snowmelt play a more important role in this catchment than the icemelt.

Considering the examples in the Illecillewaet catchment there was a high uncertainty in rainfall, snowfall and the resulting discharge. The minimum hydrograph of the period 2091–2100 in figure 8.22 showed a high decrease in discharge during the months July and August. Reducing the total discharge by icemelt resulted in the grey line which showed that the reduction in total discharge did not result from a decreased icemelt. Figure A.7 illustrated that there was especially in August extremely less rainfall in comparison with the other examples. This could be the reason for this high reduction in total discharge.

As expected a small decrease in icemelt as well as in the relation of icemelt to total discharge was found out (figure 8.23). However, the differences between the mean time series and the four examples were enormous. One reason could be the heterogeneity of the Illecillewaet catchment. The concept of the HBV-EC model to simulate discharge using different HRUs and to summarize the resulting discharge to total discharge does not consider interactions between the different HRUs. If the HBV-EC model is limited by a certain degree of heterogeneity should be further tested. Other reasons for the high uncertainty as well as limitations of the model are now discussed.

General remarks

It could be seen that there were high uncertainties in discharge simulations. Besides the uncertainties from the parameter sets and the input combinations there were some limitations of the model which should be kept in mind when evaluating the results. Some general remarks about the simulation of future discharge follow:

- The values of the 20 best parameter sets were kept constant over time. In reality the parameter values will change over time e.g. the melt factor.
- As mentioned in STAHL ET AL. (2008) glaciers thin before they retreat. However, the thinning of the glacier was not integrated in the model.
- Firn is an important short-time storage and influences discharge (JANSSON ET AL., 2003). However, also firn was not integrated in the model.
- Under a changing climate also the vegetation will change. The change in vegetation was not considered in the model. STAHL ET AL. (2008) assigned this factor a small effect on discharge.
- Debris cover was not taken into consideration in the HBV-EC model. HUSS ET AL. (2007) showed how glacier retreat was reduced because of debris cover. There were no information about debris cover in the considered catchments.

- Concerning the volume area scaling method the constant and exponent were based on a literature value. They should be verified as proposed by STAHL ET AL. (2008) with maps and airphotos. Additionally, it should be kept in mind that they were kept constant over time.
- RADIC ET AL. (2007) showed that the V-A scaling model diverged from an iceflow model beyond 100 years of simulation. The amount of divergence depended on the mass-balance and the initial size of the glacier.
- Concerning the Global Climate Models they smooth the terrain for their calculations. As British Columbia is a mountainous region it could be problematic to smooth the topography (LOUKAS and QUICK, 1996)
- MOTE ET AL. (2005) realized that most models simulate a too cold climate. This could also be the case for the used GCMs.

9.3.3 Future glacier area

As illustrated in the figures 8.24 and 8.25 the HBV-EC model simulated a decrease in glacier area and so in glacier volume in the Canoe as well as in the Illecillewaet catchment during the 21th century.

SCHIEFER ET AL. (2007) calculated a volume reduction of 1.23 ± 0.31 km^3/a and a mean thinning rate of 0.53 ± 0.13 m/a for the period 1985–1999 considering all glaciers in the Columbia Mountains. Comparing this mean thinning rate with the ones in the Canoe and Illecillewaet catchment, which were calculated for the period 2001–2100, a higher thinning during the 21th century than at the end of the 20th century could be seen.

LOUKAS and QUICK (1996) used the UBC Watershed Model to calculate a reduction of glacier area in the Illecillewaet catchment. They calculated a reduction of 33 % based on a doupling of CO_2 concentration in the atmosphere. IPCC (2007) predicted a doubling of the CO_2 concentration – in reference to the CO_2 concentration in the year 2000 – under the A2 scenario in approximately 2090; under the B1 scenario the doubling of CO_2 concentration will not be reached before 2100.

Comparing the glacier area reduction at the years 2080 and 2090 with the results of LOUKAS and QUICK (1996) the HBV-EC model simulated in average even a higher reduction. However, considering the high uncertainty at the end of the century a clear comparison is not possible. The high dependence of the area reduction on the predicted scenario is also visible in the study of HUSS ET AL. (2008). They predicted a reduction between 51 and 100 % for the area of three glaciers in Switzerland during the period 2006–2100.

9.3.4 Comparison of the catchments

As could be shown the discharge of the Canoe,the Illecillewaet and the Bridge catchment was sensitive to climate change, but in each case in a different way. While discharge of the Bridge and also of the Canoe catchment was highly influenced by icemelt and consequently by changes in icemelt, discharge from glaciers played an inferior role in the Illecillewaet catchment.

The reason for this behavior are in the most part certainly the different percentages on glaciation: While about 60 % of the Bridge catchment are covered with glaciers, in the Canoe catchment about 26 % of the area are glaciers. In the Illecillewaet catchement only about 10 % of the area are covered with glacier.

The study of REES and COLLINS (2006) could confirm that glacier change has an higher influence on discharge if the catchment has a higher percentage of glacier landuse.

The differences in heterogeneity have surely also influence on the behavior of discharge. In the Illecillewaet catchment there is a high heterogeneous landuse. Interactions between the different HRUs exist, but can not be simulated. In the Canoe catchment there are rather large connected HRUs and in the Bridge catchment there is a very homogeneous landuse where glacier is the main HRU.

Concerning the reduction in glaciermelt the Illecillewaet catchment showed a quite different behavior than the Canoe and Bridge catchment (see figure 8.27). The reason could be that in the Canoe and Bridge catchment the percentage of high laying glacierized areas is bigger than in the Illecillewaet catchment (see hypsographic curve figure 4.2). Considering an increased equilibrium line over the time a higher part of surface is affected by icemelting in the Canoe and Bridge catchment than in the Illecillewaet catchment. The higher reduction in icemelt in the Canoe catchment in comparison with the one in the Bridge catchment could also be explained by a bigger part of high laying surface areas of the Canoe catchment.

The high percentage of icemelt on total discharge in the Bridge catchment depends on the high glaciation of this catchment. As there is a smaller glaciation in the Canoe catchment also the percentage of icemelt on total discharge is lower. In the Illecillewaet, the catchment with the lowest glaciation, there is the smallest percentage of icemelt on total discharge. The different behavior of the three catchments concerning the relationship between icemelt and total discharge over time is assumed to result from the combination of the hypsographic curve and the total glaciation of the catchments. In the Illecillewaet the total discharge was predicted to remain rather constant over time and icemelt decreased slightly which results in a slight decrease of the percentage of icemelt on total discharge over the years. In the Bridge catchment the total discharge decreased more than the corresponding icemelt which has as consequence a high reduction in the relationship of icemelt on total discharge. In the Canoe catchment a reduction in icemelt and a corresponding smaller reduction of total discharge results in a decrease of the relationship of icemelt on total discharge which lays in between the one of the Bridge and the one of the Illecillewaet catchment.

As in all three catchments the icemelt and the annual discharge decreased over the century, this thesis confirms the results of STAHL and MOORE (2006) that the initial state of increased discharge as consequence of increased icemelt is over in British Columbia. In contrast the Swiss glaciers in the study of HUSS ET AL. (2008) and the synthetic glaciers in the study of REES and COLLINS (2006) showed an increase in discharge until the middle of the century and beyond a decrease. It could also be confirmed that discharge in August will decline as in the study of STAHL and MOORE (2006).

Chapter 10

Conclusion

The discharge of the Canoe and Illecillewaet catchment in British Columbia was simulated over the period 2001–2100 using the HBV-EC model. Climate change and the consequently change in glacier area were considered by scaling up the glacier area after each decade using calculated mass balance data and the empirical volume-area method. The obtained results were compared with the results of the Bridge catchment in British Columbia.

The study showed that it is in principal possible to simulate discharge using the outlined approach in glacierized data sparse catchments. Tendencies in future discharge and glacier area were pointed out as well as the different behavior of the considered catchments on climate change.

The study also confirms that there are high uncertainties when predicting discharge. On the one hand, it must be kept in mind that the model is a simple representation of the environment and can not simulate all the complex processes in a catchment. Especially conceptual models as the used HBV-EC are limited in calculating discharge in very heterogeneous catchments. Also the high uncertainty in parameter values and their change with time, which is not known and not integrated into the model, plays an important role. There are only sparse data available to calibrate and validate the model. On the other hand, there are high uncertainties resulting from the input data. There are limited climate stations in glacierized catchments. Time series are sometimes incomplete and an interpolation in mountainous catchments with high gradients is problematical. Concerning the generated input data to simulate future discharge, it was shown that there is a high variability in these generated precipitation and temperature data, especially due to the different Global Climate Models used.

In order to improve discharge predictions many different measurement data are necessary to be able to calibrate and validate a model in an adequate way. Additionally, scientists should go on to improve predictions of Global Climate Models.

Progress in modeling hydrological processes depends on a much closer cooperation between modelers and field scientists, "the Cains and Abels of hydrology" (DUNNE, 1983).

Bibliography

Ambroise B., Perrin J.L., Reutenauer D. (1995). Multicriterion validation of a semidistributed conceptual model of the water cycle in the Fecht Catchment (Vosges Massif, France), Water Resources Research, vol. 31 (6), pp. 1467–1481.

Bahr D., Meier M., Peckham S. (1997). The physical basis of glacier volume-area scaling, J. Geophys. Res., vol. 102 (No. B9), pp. 20.355 – 20.362.

Bahr D.B. (1997). Global distributions of glacier properties: a stochastic scaling paradigm, Water Resources Research, vol. 33 (7), pp. 1669–1679.

Barnett T., Adam J., Lettenmaier D. (2005). Potential impacts of a warming climate on water availability in snow-dominated regions, Nature, vol. 438 (7066), pp. 303–309.

Barry R. (2006). The status of research on glaciers and global glacier recession: a review, Progress in Physical Geography, vol. 30 (3), pp. 285–306.

Bergström S. (1995). In: Computer models of watershed hydrology, Water Resources Publications, Higland Ranch, Colorado, USA, pp. 443–476.

Bergström S., Lindstrom G., Pettersson A. (2002). Multi-variable parameter estimation to increase confidence in hydrological modelling, Hydrological Processes, vol. 16 (2), pp. 413–421.

Boon S., Flowers G., Munro D. (2009). Canadian Glacier Hydrology, 2003-2007, Canadian Water Resources Journal, vol. 34 (2), pp. 195–204.

Braun L., Aellen M. (1990). Modelling discharge of glacierized basins assisted by direct measurements of glacier mass balance, IAHS Publ., vol. 193, pp. 99–106.

Braun L., Grabs W., Rana B. (1993). Application of a Conceptual Precipitation-Runoff Model in the Langtang Kfaola Basin, Nepal Himalaya, Snow and Glacier Hydrology, IAHS Publ., vol. 218, pp. 221–237.

Braun L.N., Weber M., Schulz M. (2000). Consequences of climate change for runoff from Alpine regions, Annals of Glaciology, vol. 31 (1), pp. 19–25.

CCCma (2008).
URL `http://www.cccma.ec.gc.ca/eng_index.shtml(10.12.2009)`

CHC (2007). Ensim Hydrologic Reference Manual, Canadian Hydraulisc Centre, National Research Council, Ottawa, Ontario, Canda, 306 p.

Chen J., Ohmura A. (1990a). On the influence of Alpine glaciers on runoff, IAHS Publ., vol. 193, pp. 117–125.

Chen J., Ohmura A. (1990b). Estimation of alpine glacier water resources and their change since the 1870s, IAHS Publ., vol. 193, pp. 127–135.

Collins D. (2006). Climatic variation and runoff in mountain basins with differing proportions of glacier cover, Hydrology Research, vol. 37 (4-5), pp. 315–326.

Collins D.N., Taylor D.P. (1990). Variability of runoff from partially-glacierised Alpine basins, IAHS Publ., vol. 193, pp. 365–372.

Delworth T., Broccoli A., Rosati A., Stouffer R., Balaji V., Beesley J., Cooke W., Dixon K., Dunne J., Dunne K., Durachta J., Findell K., Ginoux P., Gnanadesikan A., Gordon C., Grieffies S., Gudgel R., Harisson M., Held I., Hemler R., LARRY W. Horowitz L., Klein S., Knutson T., Kushner P., Langenhorst A., Lee H., Lin S., Lu J., Malyshev S., Milly P., Ramaswamy V., Russell J., Schwarzkopf M., Sheliakova E., Sirutis J., Spelman M., Stern W., Winton M., Wittenberg A., Wyman B., Zeng F., Zhang R. (2006). GFDL's CM2 global coupled climate models - Part 1: Formulation and simulation characteristics, Journal of Climate, vol. 19 (5), pp. 643–674.

Dingman S.L. (2002). Physical Hydrology, 2nd edition, Waveland press, Inc., 646p.

Dunne T. (1983). Relation of field studies and modeling in the prediction of storm runoff, Journal of Hydrology, vol. 65, pp. 25–48.

Dyurgerov M., Meier M. (1997). Year-to-year fluctuations of global mass balance of small glaciers and their contribution to sea-level changes, Arctic and Alpine Research, pp. 392–402.

Eaton B., Moore R. (2007). Chapter 4 - Regional Hydrology, In: Pike, R.G., Compendium of Forest Hydrology and Geomorphology in British Columbia. BC Ministry of Forests and Range Research Branch, Victoria, BC and FORREX Forest Research Extension Partnership, Kamloops, BC, pp. 1–41.
URL `http://www.forrex.org/program/water/compendium.asp(12.12.2009)`

Escher-Vetter H. (2001). Zum Gletscherverhalten in den Alpen im zwanzigsten Jahrhundert, Klimastatusbericht 2001, DWD, pp. 51–57.

Flato G., Boer G., Lee W., McFarlane N., Ramsden D., Reader M., Weaver A. (2000). The Canadian Centre for Climate Modelling and Analysis global coupled model and its climate, Climate Dynamics, vol. 16 (6), pp. 451–467.

Flowers G., Marshall S., Björnsson H., Clarke G. (2005). Sensitivity of Vatnajökull ice cap hydrology and dynamics to climate warming over the next 2 centuries, J. Geophys. Res, vol. 110, F02011, doi:10.1029/2004JF000200, 19p.

Fountain A., Tangborn W. (1985). The effect of glaciers on streamflow variations, Water Resources Research, vol. 21 (4), pp. 579–586.

Gupta H., Sorooshian S., Yapo P. (1998). Toward improved calibration of hydrologic models: Multiple and noncommensurable measures of information, Water Resources Research, vol. 34 (4), pp. 751–763.

Hagg W., Braun L., Weber M., Becht M. (2006). Runoff modelling in glacierized Central Asian catchments for present-day and future climate, Nordic hydrology, vol. 37 (2), pp. 93–105.

Haith D., Shoemaker L. (1987). Gerneralized Watershed Loading Functions For Stream Flow Nutrients, Journal of the American Water Resources Association, vol. 23 (3), pp. 471–478.

Hamilton A., Hutchinson D., Moore R. (2000). Estimating winter streamflow using conceptual streamflow model, Journal of Cold Regions Engineering, vol. 14, pp. 158–175.

Hamilton A.S., Moore R.D. (1996). Winter streamflow variability in two groundwater-fed sub-Arctic rivers, Yukon Territory, Canada, Canadian journal of civil engineering, vol. 23 (6), pp. 1249–1259.

Hamon W. (1961). Estimating potential evapotranspiration, Journal of the Hydraulics Division, vol. 87 (HY3), pp. 107–120.

Harlin J. (1991). Development of a process oriented calibration scheme for the HBV hydrological model, Nordic Hydrology, vol. 22 (1), pp. 15–36.

Harlin J., Kung C.S. (1992). Parameter uncertainty and simulation of design floods in Sweden, Journal of Hydrology(Amsterdam), vol. 137 (1), pp. 209–230.

Hock R. (2003). Temperature index melt modelling in mountain areas, Journal of Hydrology, vol. 282 (1-4), pp. 104–115.

Hock R. (2005). Glacier melt: a review of processes and their modelling, Progress in Physical Geography, vol. 29 (3), pp. 362–391.

Hock R., Jansson P., Braun L. (2005). Modelling the response of mountain glacier discharge to climate warming, In: U. M. Huber, H. K. M. Bugmann, and M. A. Reasoner, 2005: Global Change and Mountain Regions (A State of Knowledge Overview), Springer, Dordrecht, pp. 243–252.

Hornberger G., Wiberg P. (2005). Numerical Methods in the Hydrological Sciences, Special Publications Series 57, American Geophysical Union.

Horton P., Schaefli B., Mezghani A., Hingray B., Musy A. (2006). Assessment of climate-change impacts on alpine discharge regimes with climate model uncertainty, Hydrological Processes, vol. 20 (10), pp. 2091–2109.

Huss M., Farinotti D., Bauder A., Funk M. (2008). Modelling runoff from highly glacierized alpine drainage basins in a changing climate, Hydrological Processes, vol. 22 (19), pp. 3888–3902.

Huss M., Sugiyama S., Bauder A., Funk M. (2007). Retreat scenarios of Unteraargletscher, Switzerland, using a combined ice-flow mass-balance model, Arctic, Antarctic, and Alpine Research, vol. 39 (3), pp. 422–431.

IPCC (2000). Emission Scenarios, A Special Report of Working Group III of the Intergovernmental Panel on Climate Change. Cambridge University Press, Cambridge, UK and New York, USA, 570 pp.
URL http://www.ipcc.ch/ipccreports/sres/emission/index.php?idp=0(10.12.2009)

IPCC (2007). Climate Change 2007: The Physical Science Basis, Technical report, WMO/UNEP, Cambridge University Press.

Jansson P., Hock R., Schneider T. (2003). The concept of glacier storage: a review, Journal of Hydrology, vol. 282 (1-4), pp. 116–129.

Johannesson T., Raymond C., Waddington E. (1989). Time-scale for adjustment of glaciers to changes in mass balance, Journal of Glaciology, vol. 35, pp. 355–369.

Jonsdottir H., Madsen H., Palsson O. (2006). Parameter estimation in stochastic rainfall-runoff models, Journal of Hydrology, vol. 326 (1-4), pp. 379–393.

Klemes V. (1986). Operational testing of hydrological simulation models., Hydrological Sciences Journal, vol. 31 (1), pp. 13–24.

Klock R., Mullock J. (2001). The Weather of British Columbia, NAV Canada.
URL http://www.navcanada.ca/ContentDefinitionFiles/publications/lak/bc/BC31E-W.PDF

Kotlyakov V., Rototaeva O., Nosenko G. (2004). The September 2002 Kolka glacier catastrophe in North Ossetia, Russian Federation: evidence and analysis, Mountain Research and Development, vol. 24 (1), pp. 78–83.

Lindström G. (1997). A simple automatic calibration routine for the HBV model, Nordic hydrology, vol. 28 (3), pp. 153–168.

Lindström G., Johansson B., Persson M., Gardelin M., Bergström S. (1997). Development and test of the distributed HBV-96 hydrological model, Journal of Hydrology, vol. 201 (1-4), pp. 272–288.

Loukas A., Quick M. (1996). Effect of climate change on hydrologic regime of two climatically different watersheds, Journal of Hydrologic Engineering, vol. 1 (2), pp. 77–88.

Madsen H. (2000). Automatic calibration of a conceptual rainfall-runoff model using multiple objectives, Journal of Hydrology, vol. 235 (3-4), pp. 276–288.

Madsen H. (2003). Parameter estimation in distributed hydrological catchment modelling using automatic calibration with multiple objectives, Advances in Water Resources, vol. 26 (2), pp. 205–216.

Martinec J., Rango A. (1989). Effects of climate change on snowmelt runoff patterns, Proc. Third International Assembly on Remote Sensing and Large-Scale Global Processes, vol. 186, pp. 31–38.

McCarthy D. (2003). Estimating lichenometric ages by direct and indirect measurement of radial growth: a case study of Rhizocarpon agg. at the Illecillewaet Glacier, British Columbia, Arctic, Antarctic, and Alpine Research, vol. 35 (2), pp. 203–213.

MOE (2007a). Ministry of Environment: Lord,T.M. and Valentine, K.W.G.
URL http://www.env.gov.bc.ca/soils/landscape/3.2soilmap.html(01.11.2009)

MOE (2007b). Ministry of Environment: Lavkulich, L.M. and Valentine, K.W.G.,.
URL http://www.env.gov.bc.ca/soils/landscape/2.3system.html#fig231(01.11.2009)

MOE (2007c). Ministry of Environment: Schaefer, D.G.
URL http://www.env.gov.bc.ca/soils/landscape/1.2climate.html(01.11.2009)

Moore R. (1993). Application of a conceptual streamflow model in a glacierized drainage basin, Journal of hydrology, vol. 150, pp. 151–168.

Moore R., Demuth M. (2001). Mass balance and streamflow variability at Place Glacier, Canada, in relation to recent climate fluctuations, Hydrological Processes, vol. 15 (18), pp. 3473–3486.

Moore R.D., Hamilton A.S., Scibek J. (2002). Winter streamflow variability, Yukon Territory, Canada, Hydrological Processes, vol. 16 (4), pp. 763–778.

Mote P., Salathe E., Peacock C. (2005). Scenarios of future climate for the Pacific Northwest, Report, Climate Impacts Group, University of Washington, 11p.

Nash J.E., Sutcliffe J.V. (1970). River flow forecasting through conceptual models, part I - A discussion of principles, Journal of Hydrology, vol. 10 (3), pp. 282–290.

NRCAN (2008). Natural Resources Canada.
URL http://gsc.nrcan.gc.ca/map/1880a/index_e.php(01.11.2009)

Oerlemans J. (1988). Simulation of historic glacier variations with a simple climate-glacier model, Journal of Glaciology, vol. 34 (118), pp. 333–341.

Oerlemans J., Anderson B., Hubbard A., Huybrechts P., Johannesson T., Knap W., Schmeits M., Stroeven A., Van de Wal R., Wallinga J. (1998). Modelling the response of glaciers to climate warming, Climate Dynamics, vol. 14 (4), pp. 267–274.

Osborn G., Luckman B. (1988). Holocene glacier fluctuations in the Canadian Cordillera (Alberta and British Columbia), Quaternary Science Reviews, vol. 7, pp. 115–128.

Parde M. (1947). Fleuves et Rivières, sec. Edn. Colin, Paris.

Perrin C., Michel C., Andreassian V. (2001). Does a large number of parameters enhance model performance? Comparative assessment of common catchment model structures on 429 catchments, Journal of hydrology, vol. 242 (3-4), pp. 275–301.

Prowse T. (1994). Environmental significance of ice to streamflow in cold regions, Freshwater Biology, vol. 32 (2), pp. 241–259.

Radic V., Hock R., Oerlemans J. (2007). Volume-area scaling vs flowline modelling in glacier volume projections, Annals of Glaciology, vol. 46, pp. 234–240.

Radic V., Hock R., Oerlemans J. (2008). Analysis of scaling methods in deriving future volume evolutions of valley glaciers, Journal of Glaciology, vol. 54 (187), pp. 1–12.

Rango A. (1992). Worldwide Testing of the Snowmelt Runoff Model with Applications for Predicting the Effects of Climate Change, Nordic Hydrology, vol. 23, pp. 155–172.

Rees H., Collins D. (2006). Regional differences in response of flow in glacier-fed Himalayan rivers to climatic warming, Hydrological Processes, vol. 20 (10), pp. 2157–2169.

Rodenhuis D., Bennett K., Werner A., Murdock T., Bronaugh D. (2007). Hydroclimatology and future climate impacts in British Columbia., Pacific Climate Impacts Consortium, University of Victoria, Victoria BC, 131 p.

Ryder J., Thomson B. (1986). Neoglaciation in the southern Coast Mountains of British Columbia: chronology prior to the late Neoglacial maximum, Canadian Journal of Earth Sciences, vol. 23 (3), pp. 273–287.

Schaefli B., Gupta H. (2007). Do Nash values have value?, Hydrological Processes, vol. 21 (15), pp. 2075–2080.

Schaefli B., Hingray B., Niggli M., Musy A. (2005). A conceptual glacio-hydrological model for high mountainous catchments, Hydrology and Earth System Sciences, vol. 9 (1-2), pp. 95–109.

Schiefer E., Menounos B., Wheate R. (2007). Recent volume loss of British Columbian glaciers, Canada, Geophysical Research Letters, vol. 34, L16503, doi:10.1029/2007GL030780, 6p.

Seibert J. (1997). Estimation of parameter uncertainty in the HBV model, Nordic hydrology, vol. 28 (4), pp. 247–262.

Seibert J. (1999). Regionalisation of parameters for a conceptual rainfall-runoff model, Agricultural and Forest Meteorology, vol. 98 (1), pp. 279–293.

Seibert J. (2005). HBV light version 2 Users manual.
URL `http://people.su.se/~jseib/HBV/HBV_manual_2005.pdf(15.12.2009)`

Seibert J., Uhlenbrook S., Leibundgut C., Halldin S. (2000). Multiscale calibration and validation of a conceptual rainfall-runoff model, Physics and Chemistry of the Earth, Part B, vol. 25 (1), pp. 59–64.

Sidjak R., Wheate R. (1999). Glacier mapping of the Illecillewaet icefield, British Columbia, Canada, using Landsat TM and digital elevation data, International Journal of Remote Sensing, vol. 20 (2), pp. 273–284.

Singh P., Bengtsson L. (2005). Impact of warmer climate on melt and evaporation for the rainfed, snowfed and glacierfed basins in the Himalayan region, Journal of Hydrology, vol. 300 (1-4), pp. 140–154.

Sorooshian S., Gupta V.K. (1995). Model Calibration, in: Singh, V. P. : Computer models for watershed hydrology. Water Resources Publications, Highland Ranch, Colorado, USA, pp. 23–68.

Stahl (2009). personal communication via mail (12.11.2009).

Stahl K., Moore R., Floyer J., Asplin M., McKendry I. (2006). Comparison of approaches for spatial interpolation of daily air temperature in a large region with complex topography and highly variable station density, Agricultural and Forest Meteorology, vol. 139 (3-4), pp. 224–236.

Stahl K., Moore R., Shea J., Hutchinson D., Cannon A. (2008). Coupled modelling of glacier and streamflow response to future climate scenarios, Water Resources Research, vol. 44, W02422, doi:10.1029/2007WR005956, 13p.

Stahl K., Moore R.D. (2006). Influence of watershed glacier coverage on summer streamflow in British Columbia, Canada, Water Resources Research, vol. 42, W06201, doi:10.1029/2006WR005022, (6), 6p.

Tang Y., Reed P., Wagener T., van Werkhoven K. (2007). Comparing sensitivity analysis methods to advance lumped watershed model identification and evaluation, Hydrology and Earth System Sciences, vol. 11 (2), pp. 793–817.

Uhlenbrook S., Seibert J., Leibundgut C., Rodhe A. (1999). Prediction uncertainty of conceptual rainfall-runoff models caused by problems to identify model parameters and structure, Hydrol. Sci. J, vol. 44 (5), pp. 279–299.

Van de Wal R., Wild M. (2001). Modelling the response of glaciers to climate change by applying volume-area scaling in combination with a high resolution GCM, Climate Dynamics, vol. 18 (3), pp. 359–366.

Watson R., Zinyowera M., Moss R., Dokken D. (1996). Climate Change 1995. Impacts, Adaptation and Mitigation of Climate Change: Scientific and Technical Analyses., Cambridge University Press. GB.

Weber F. (2009). personal communication via mail (28.04.2009).

Yapo P., Gupta H., Sorooshian S. (1998). Multi-objective global optimization for hydrologic models, Journal of Hydrology, vol. 204 (1-4), pp. 83–97.

Zappa M., Badoux A., Gurtz J. (2000). The application of a complex distributed hydrological model in a highly glaciated alpine river catchment, Int. Assoc. Danube Res., Limnological Reports, vol. 33, pp. 23–28.

Zhang X., Lindström G. (1997). Development of an automatic calibration scheme for the HBV hydrological model, Hydrological Processes, vol. 11 (12), pp. 1671–1682.

A Appendix

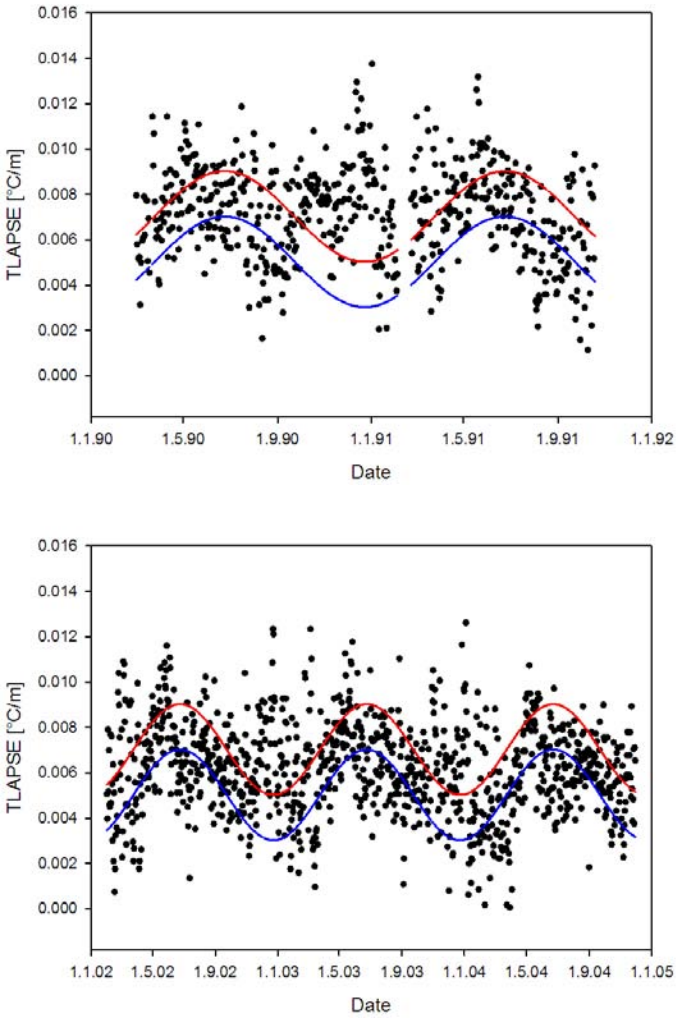

Figure A.1: Lapse rate for temperature between the climate station Revelstoke (1176749) and Glacier NP Rogers pass (1173191) between 1st Jan, 1990 and 31th Dec, 1991 (top) and between 1st Jan, 2001 and 31th Dec, 2004 (bottom). Blue line: Minimum lapse rate after calibration; Red line: Maximum lapse rate after calibration.

```
; IDL-script to compute Potential Evaporation (mm/day) based on daily
; mean air temperature. Adapted from Hornberger and Wiberg (2006)
; MatLab code$

PRO evp_hamon, out_path, hamon_output, latitude,dur, input, day, month,
    year, climate

climate = { DOY: lonarr(dur), temperature: fltarr(dur) ,delta:fltarr(dur),
            omega:fltarr(dur) , hpd:fltarr(dur) , svp:fltarr(dur), pet:fltarr(dur)}

climate.temperature=input[0,0:dur-1] ; daily mean temperature
climate.DOY[0] = 1                   ; first day = 1

; creates real day of the years

for k=1, dur-1 do begin
  if (climate.DOY[k] le 365) then
    climate.DOY[k] = climate.DOY[k-1] +1 ; no leap years considered
  if (climate.doy[k] eq 366) then
    climate.doy[k] =1
endfor

; parameters for saturation vapor pressure relation

a = 0.6108
b = 17.27
c = 237.3

; solar declination
climate.delta = 0.4093 * sin((2*!pi/365) * climate.DOY - 1.405)

; sunset hour angle
climate.omega = acos(-tan(2*!pi*latitude/360) * tan(climate.delta))

; sunlight hours per day
climate.hpd   = 24 * climate.omega/!pi

; saturated vapor pressure
climate.svp   = a * exp(b * climate.temperature / (climate.temperature + c))

; potential evaporation [mm/day]
climate.pet   = (2.1 * (climate.hpd^2) * climate.svp) / (climate.temperature + 273.3)



; creates output

openw, lun, out_path+hamon_output , /get_lun
printf, lun, 'DOY, day, month, year, PET_Hamon'
for f=0, dur-1 do begin
  printf, lun, climate.doy[f], day[f], month[f], year[f], climate.pet[f],
          format= '(i10, i10, i10, i10, f13.4)'
endfor

free_lun, lun

end
```

Figure A.2: Procedure to calculate potential evaporation based on HAMON (1961)

Table A.1: Information about the measurement stations in the Illecillewaet catchment. Numbers in brackets indicate the quantity of gaps in the time series (m=month, y=year).

Kind of station	Name of station	Number	Elevation [m.a.s.l.]	Latitude	Longitude	Measurement time	Operator
Hydrometric station	Illecillewaet River at Greeley	08ND013	507	51.012	-118.082	Nov 15th, 1963 to Dec 31th, 2005	HYDAT
Climate station	Glacier NP Rogers Pass	1173191	1323	51.301	-117.516	June 14th, 1965 to Dec 31th, 2004	BC Hydro
Snow pillow	Mount Revelstoke	2A06P	1830	51.033	-118.15	Dec 13th, 1992 to Sept 30th, 2006 (11m)	WSD
Snow pillow	Fidelity Mountain	2A17P	1870	51.233	-117.7	Oct 23th, 1987 to Dec 31th, 1988	WSD
Snow course	Glacier	2A02	1250	51.25	117.5	April 2nd, 1937 to 2005	WSD
						Mai 1st, 1946 to 2005	WSD
						June 1st, 1948 to 1955(2y)	WSD
Snow course	Mount Revelstoke	2A06	1830	51.033	-118.15	April 2nd, 1947 to 1997(2y)	WSD
						Mai 1st, 1947 to 2005	WSD
						June 1st, 1948 to 1997(1y)	WSD
Snow course	Mount Abbot	2A14	1980	51.267	-117.5	April 2nd, 1959 to 2005	WSD
						Mai 1st, 1959 to 2006(3y)	WSD
						June 1st, 1959 to 1995	WSD
Snow course	Fidelity Mountain	2A17	1870	51.233	-117.7	April 2nd, 1963 to 1997	WSD
						Mai 1st, 1963 to 2005	WSD
Snow line	Along Illecillewaet basin					At 7 days, mid Mai to mid June, 1994 to 2000	

Table A.2: Information about the measurement stations in the Canoe and the Bridge catchment. Numbers in brackets indicate the quantity of gaps in the time series (m=month, y=year).

Kind of station	Name of station	Number	Elevation [m.a.s.l.]	Latitude	Longitude	Measurement time	Operator
Hydrometric station	Canoe River below Kimmel Creek	08NC004	965	52.732	-119.408	July 20th, 1971 to Dec 31th, 2005 (24m)	HYDAT
Climate station	Cariboo Lodge	1171393	1128	52.7194	-119.4717	many gaps between Jan 1st, 1976 to Dec 31th, 2004	BC Hydro
Snow pillow	Azure River (N. Thompson basin)	1E08P	1620	52.617	-119.717	Sept 11th, 1996 to Sept 30th, 2006	WSD
Snow course	Azure River (N. Thompson basin)	1E08	1620	52.617	-119.717	April 2nd, 1970 to 2005	WSD
						May 1st, 1970 to 1999	WDD
						June 1st, 1970 to 1996	WDS
Snow course	Canoe River	2A01A	910	52.783	-119.283	April 2nd, 1941 to 2005	WSD
						May 1st, 1956 to 2004 (25y)	WSD
Snow line	Section: Mica to Donald					At 7 days, mid May to mid June,1994 to 2000	
Hydrometric station	Bridge River below Bridge Glacier	08ME023	1375	50.856	-123.45	Oct 21th, 1978 to Dec 31th, 2005 (7m)	HYDAT
Climate station	Upper La Joie DCP	LJU	1829	50.860	-123.184	Feb 10th, 1985 to Dec 31th, 2004	BC Hydro

Table A.3: Information about the climate stations situated in about 100 km of the Canoe River station. Table top: Data sorted after R^2 considering precipitation. Table bottom: Data sorted after R^2 considering temperature.

Name of Station	Number	Elevation (m)	Latitude	Longitude	Operated from	Operated to	Common years	R^2	Used data
Valemount South	117HCL9	930	52.75	-119.3	1994	1996	2	0.7816	
Albreda	1170237	873	52.67	-119.2	1973	1977	1	0.6332	
Mica Dam	1175122	579	52.05	-118.59	1951	2004	28	0.5943	1
Valemount North	1178CL9	892	52.85	-119.25	1971	1989	13	0.5073	
Blue River North	1160900	689	52.15	-119.28	1946	1985	9	0.4529	
Dunster	1092578	725	53.13	-119.85	1974	1995	19	0.4469	
Tete Jaune	1098138	777	52.92	-119.38	1981	1985	4	0.4236	
Tete Jaune (A)	109QJ3G	731	53.00	-119.54	1989	2004	15	0.3990	2
Blue River A	1160899	683	52.13	-119.29	1969	2004	28	0.3794	
Valemount East	11783L9	808	52.83	-119.25	1970	2004	28	0.3357	
McBride Elder Creek	1094948	707	53.42	-120.35	1992	2004	12	0.1537	
Valemount South	117HCL9	930	52.75	-119.3	1994	1996	2	0.9838	
Valemount North	1178CL9	892	52.85	-119.25	1971	1989	13	0.9738	1
Albreda	1170237	873	52.67	-119.2	1973	1977	1	0.9710	
Tete Jaune	1098138	777	52.92	-119.38	1981	1985	4	0.9653	
Valemount East	11783L9	808	52.83	-119.25	1970	2004	28	0.9638	4
Dunster	1092578	725	53.13	-119.85	1974	1995	19	0.9571	2
Mc Bride Elder Creek	1094948	707	53.42	-120.35	1992	2004	12	0.9534	3
Blue River A	1160899	683	52.13	-119.29	1969	2004	28	0.9512	
Blue River North	1160900	689	52.15	-119.28	1946	1985	9	0.9479	
Mica Dam	1175122	579	52.05	-118.59	1951	2004	28	0.9362	
Tete Jaune (A)	109QJ3G	731	53.00	-119.53	1989	2004	15	0.7018	

Table A.4: Information about mean errors at the 5 % and 95 % quantile of the snow courses at the Illecillewaet catchment during the validation period.

Number of snow course	Month	ME_5	ME_{95}
2A02	April	-285	-131
	May	54	235
	June	246	298
2A06	April	-38	80
	May	75	176
	June	119	320
2A14	April	-21	111
	May	44	167
	June	5	131
2A17	April	-64	55
	May	49	151

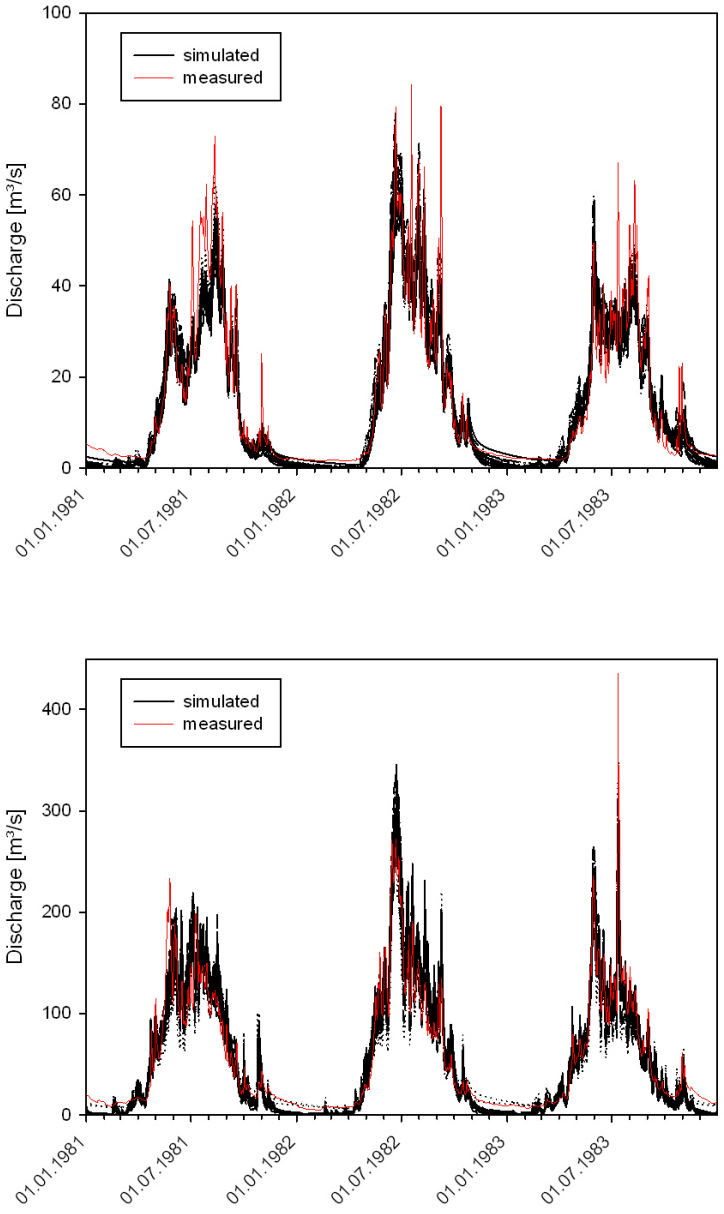

Figure A.3: Top: Simulated and observed discharge between 1st Jan, 1981 and 31th Dec, 1983 at the Canoe catchement. Bottom: Simulated and observed discharge between 1st Jan, 1981 and 31th Dec, 1983 at the Illecillewaet catchment.

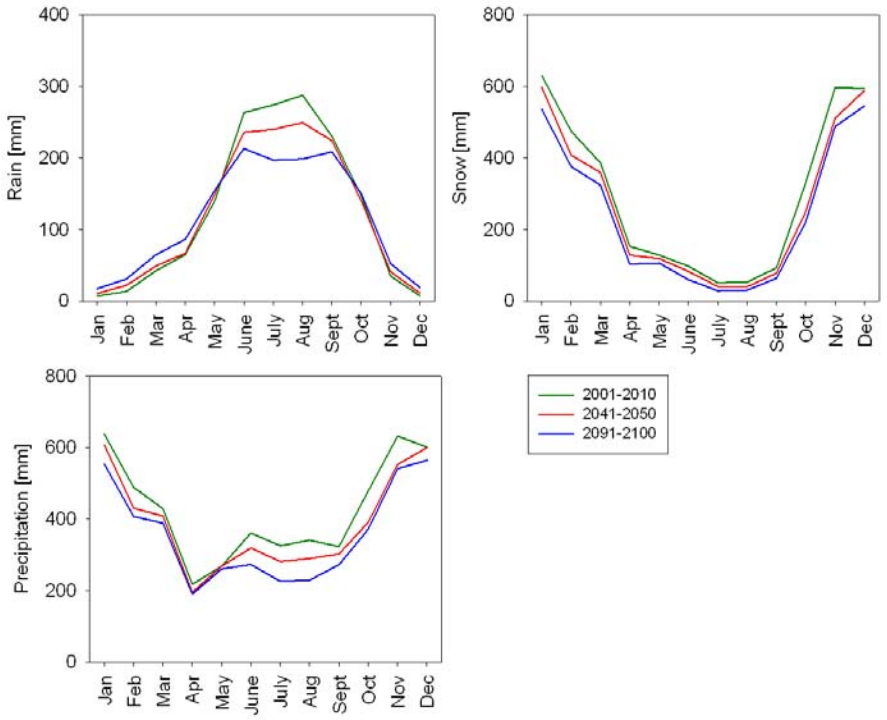

Figure A.4: Development of mean rainfall, snowfall and precipitation in the Canoe catchment.

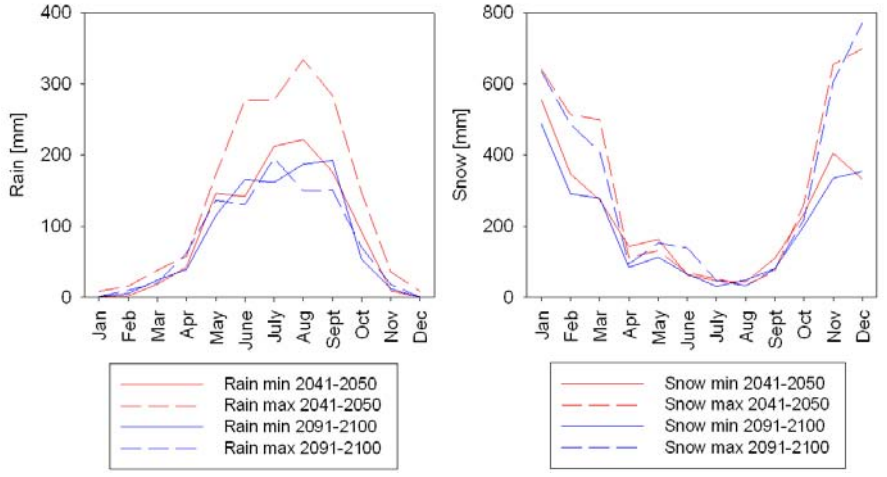

Figure A.5: Four examples of development of rainfall and snowfall in the Canoe catchment.

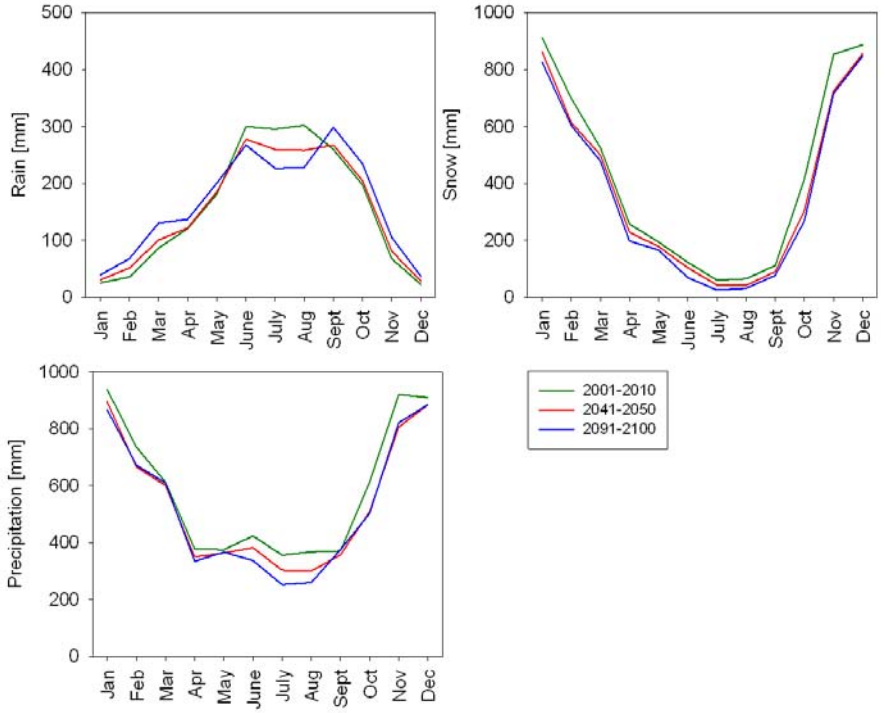

Figure A.6: Development of mean rainfall, snowfall and precipitation in the Illecillewaet catchment.

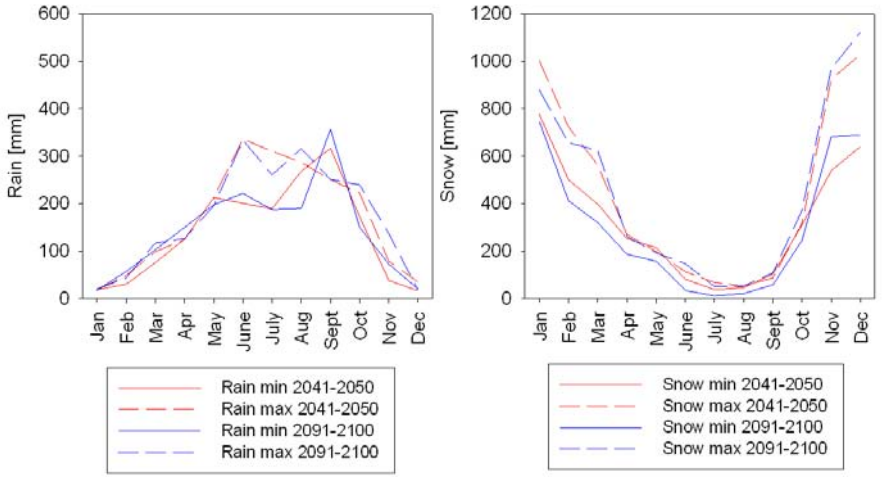

Figure A.7: Four examples of development of rainfall and snowfall in the Canoe catchment.

Ehrenwörtliche Erklärung

Hiermit erkläre ich, dass die Arbeit selbständig und nur unter Verwendung der angegebenen Hilfsmittel angefertigt wurde.

Ort, Datum Unterschrift